DYNAMIC ANALYSIS AND DESIGN OPTIMIZATION OF A VEHICLE SUSPENSION SYSTEM

A THESIS SUBMITTED TO
THE GRADUATE SCHOOL OF SCIENCE AND ENGINEERING
OF
KOÇ UNIVERSITY

BY

EMRE ÖLÇEROĞLU

IN PARTIAL FULFILLMENT OF THE REQUIREMENTS
FOR
THE DEGREE OF MASTER OF SCIENCE
IN
MECHANICAL ENGINEERING

JANUARY 2011

SIGNATURE PAGE

I hereby declare that all information in this document has been obtained and presented in accordance with academic rules and ethical conduct. I also declare that, as required by these rules and conduct, I have fully cited and referenced all material and results that are not original to this work.

Name, Last Name: Emre Ölçeroğlu

Signature:

ABSTRACT

DYNAMIC ANALYSIS AND DESIGN OPTIMIZATION OF A VEHICLE SUSPENSION SYSTEM

Suspension system of a vehicle plays an important role in maintaining the comfort of the passengers by isolating and absorbing road shock from the passenger compartment. For that reason, it is critical to understand the dynamics of the suspension system components and more importantly, the way they interact with each other. In this thesis, the effect of the dynamic, material and dimensional properties of the system components on the performance of the suspension system is analyzed and a general approach is developed to understand the relationship between the design parameters and the suspension vibration isolation performance.

The Frequency Response Function (FRF) of the suspension system is obtained through a Finite Element Model (FEM) by using the commercial FE analysis software NASTRAN®. The FEM is used to study the effect of the design parameters of the system components such that the vibration isolation performance of the suspension system can be improved. For this purpose, a structured parametric study, based on techniques from the field of industrial design of experiments is employed to understand the relationship between the design parameters and the suspension vibration isolation performance. A screening study is performed to identify the components that have the highest contribution to the suspension system vibration isolation performance. For each run, the dynamic analysis of the suspension system is performed, the FRFs are constructed and the vibration isolation performance is quantified using several metrics that consider the amount of vibration transmitted through the suspension system. The highest contributors to the vibration isolation performance are identified and preliminary optimization runs are performed to find the optimum values for the critical design parameters. A stochastic approach is also implemented to the above study to consider the variations and uncertainties that arise from a variety of sources like manufacturing processes, external disturbances, and operating conditions.

In addition to the above study, material and dimensional properties of particular components of the suspension system are selected as design parameters. A similar procedure is followed to determine an optimum configuration for a better vibration isolation performance. The results are compared using various configurations for sample studies. The results show that the presented approaches can be effectively used to improve the suspension performance by modifying the design parameters of the suspension system.

ÖZ

ARAÇ SÜSPANSİYON SİSTEMLERİNİN DİNAMİK İNCELENMESİ VE TASARIM İYİLEŞTİRİLMESİ

Araçlarda yolcu konforunun sağlanmasında yoldan gelen darbeleri emip bunların şiddetini azaltan süspansiyon sistemi önemli rol oynar. Bu sebepten dolayı bu sistemler özenli bir şekilde dizayn edilmelidirler. Bu dizaynı başarılı bir şekilde yapabilmek için süspansiyon sisteminin tüm bileşenlerinin ve bunların birbirleriyle olan etkileşimlerinin dinamik davranışları anlaşılmalıdır. Bu tezde sistem bileşenlerinin dinamik, malzeme ve boyutsal özelliklerinin süspansiyon performansı üzerine olan etkileri analiz edilmiştir.

NASTRAN® isimli ticari sonlu eleman analiz yazılımı aracılığıyla sonlu eleman modelimizin frekans cevap fonksiyonları elde edilip, kritik titreşim yolları açığa çıkarılmıştır. Bu kritik öğeler incelenerek sonlu eleman modeli gerçek aracı temsil edecek şekilde dikkatlice düzenlenmiştir. Sonlu eleman modeli son haline geldikten sonar, model, süspansiyon sisteminin performansı artırmak üzere optimizasyon çalışmalarında kullanılmıştır. Dizayn parametreleri ve süspansiyon sistem performansı arasındaki ilişkiyi anlamak için temeli endüstriyel deney tasarlama tekniklerine dayanan düzenli ve parametrik bir çalışma yapılmıştır. Bu çalışmalar süspansiyon performansına en çok etkisi olan bileşenleri belirlemek için yapılan bir tarama işlem ile başlatılmıştır. Her seferinde dizayn parametreleri değiştirilerek sistemin frekans cevap fonksiyonları elde edilmiş ve buna göre çeşitli performans ölçütleri ile değerlendirmeler yapılmıştır. En etkili bileşenler ortaya çıktıktan sonra en uygun konfigurasyonu bulmak uzere optimizasyon işlemi gerçekleştirilmiştir.

Bahsedilen bu çalışmaya ek olarak, parametrizasyon ve optimizasyon işlemleri yay, damper ve kütle gibi dinamik özelliklerin dışında malzeme ve boyutsal özellikler kullanılarak tekrarlanmıştır. Takip edilen yöntem ve elde edilen sonuçlar gösterdi ki bu metotla araç

süspansiyonlarının performansları etkili bir şekilde en uygun performanslı hale getirilebilir ve merak edilen değişikliklerin sonuçları hakkında hızlı bir şekilde fikir sahibi olunabilir.

ACKNOWLEDGEMENTS

Beyond everyone, I would like to express my sincere gratitude to my supervisor Asst. Dr. İpek Başdoğan for her deep guidance and interest throughout this study.

I am also grateful to Can Durukal who helped me in my studies at the point where I was stuck clueless. He shared his knowledge without any hesitation and gave haste to the progress.

I am thankful to Cumhur Pıçak, who was in charge of the project at TOFAŞ side, for his efforts to make things easier for us and being a friend more than just an inspector.

I especially wish to thank one person, Ender Koç from Ex-En Mühendislik, who always helped me in overcoming the technical difficulties I encountered in software applications. He always prioritized my issues among his other jobs and responded very quickly.

I want to thank Asst. Dr. Sibel Salman for her guidance whenever we needed help in statistical fields.

I would also like to show my appreciation to other authorized people at TOFAŞ, namely, Halil Bilal, Cenk Gebeceli, Mehdi Yıldız, Aytekin Özkan and Mustafa Özer. Without their suggestions I would encounter too much hard time.

I would like to express my intimate thanks to Ezgi Köker for always being with me and helping me overcome the hard times. Without her endless motivation and encouragement the difficulties I encountered would be unbearable.

I want to appreciate my office and leisure mate Can Gökgöl for being more than a friend to me and turning the hard times into joy times during the last 2 years.

Financial support provided by TOFAŞ Inc. and Koç University are gratefully acknowledged.

Above all, I would like to present my deepest thanks to my father, my mother, my elder sister and his husband and many other people from my family for always supporting, encouraging and watching over me through my all life.

Table of Contents

List of Tables

TABLE

List of Figures

FIGURE

CHAPTER 1

INTRODUCTION

Suspension system of a road vehicle plays an important role in maintaining the comfort of the passengers by isolating them from the ground vibrations and absorbing the road shocks. For that purpose, it is critical to understand the dynamics of the suspension system components and more importantly, how they interact with each other.

In this thesis, a comprehensive general theory is introduced by deriving a methodology for defining the optimal relationship among the vehicle suspension parameters and the suspension performance metrics. The performance metrics used in this thesis are "Discomfort", "Working Space" and "Road Holding" measures of the vehicle. The suspension design parameters are selected from the general dynamic properties like mass, stiffness, damping and also, material and dimensional properties.

The finite element model of the front suspension system and two randomly profiled road models are used to reach the performance metrics through the frequency response functions (FRFs) that are obtained by the commercial finite element software NASTRAN®.

A structured parametric study, based on techniques from the field of industrial design of experiments (DOE) is employed to understand the relationship between the design parameters and the suspension performance metrics. For each configuration of the parameters, after acquiring the FRFs and the DOEs, a screening study is performed to identify the contribution of each parameter and their interaction to the performance metrics. Design Expert StatEase® software is used in these studies. After the highest contributors to the performance metrics are identified, regression models that form a relationship between the suspension response and the system are created. This regression models are obtained by using a methodology called "Response Surface Methodology (RSM)". Then these models are utilized to perform optimization studies to determine the best configuration of the suspension parameters to improve the suspension system performance. In the end, it was observed that the suspension performance of the vehicle is improved significantly.

The same steps are repeated with a more realistic approach. Normally a designer cannot change the coefficients of the suspension springs or dampers, directly as we did in our

previous studies. Those studies helped us in determining the significant system components for obtaining a better suspension performance. However, instead of changing the coefficients of system components he can change the material properties and thicknesses of the suspension components which can be done during the design process. Similar preparation and optimization procedure is followed for a material based optimization study as well.

In literature, we have found a lot of studies that employ optimization methods in the suspension analysis and these studies were noteworthy, relevant and helpful to our work. M. Gobbi and G. Mastinu [1] used a simple quarter car model to derive a number of analytical formulae describing the dynamic behavior of passively and actively suspended vehicles. They applied multi-objective programming (MOP) approach and also conducted a monotonicity analysis on the performance metrics. In the end, response surfaces of the performance metrics are plotted with respect to the design variables to let them be able to select optimal parameters. In another study, again by Gobbi et al., they used the multi-objective programming together with the theory of robust design. They calculated the optimal trade-off solutions (Pareto-optimal solutions) in a stochastic framework in a non-dimensional analytical form.

In the literature, there are many other studies those try to estimate the vehicle's behavior when interacting with different road irregularities [2-7]. In these works, the dynamic response of the vehicle is modeled by exposing them to random excitations which are used to present the road irregularity. Giving the random excitation by using power spectral density functions is very common in the literature and makes further processing easier as all of the surveyed works approve this [14-17].

As mentioned above, while preparing this thesis, DOE methodology covered a great and important portion of the preparation steps. There are many sources in the literature to benefit from and of these sources; Box, Wilson and Montgomery's basics helped us in building a strong theoretical foundation to reach further steps [18-21, 26].

Sutherland, Jain and Bank's applications with examples aided in understanding how DOE works practically and the way the theory is applied [23-27].

Liang et al. followed a similar approach for material and dimensional optimization studies. However their work was based on applied acoustics and we adapted the idea to our

suspension optimization [28, 29]. Their study also reveals many things explicitly that are happening in the background of the softwares used in our studies.

When the parameters of interest are not interacting with each other, single objective optimization works well. In literature [5, 8-13], conducted works show that if there are interactions between these parameters, one needs to apply multi-objective optimization to get more realistic results. In the light of this information, both single and multi objective optimization are used and the differences between the results are examined in this thesis.

In Chapter 2, the finite element model used in our work is described in detail. The performance metrics to be optimized are introduced in Chapter 3. Chapter 4 includes the validation of our finite element model by comparing it with a high fidelity model. In Chapter 5 and Chapter 6, after giving a brief history and theory about DOE, all the details of optimization procedure is presented. Chapter 7 includes another optimization study from a different point of view. Main goal presented in Chapter 7 is to minimize the magnitude of maximum peak in a/F transfer function. The results presented can be useful for academic purposes or industry that may want to use the simple and general theory described.

CHAPTER 2

FINITE ELEMENT MODEL OF THE FRONT SUSPENSION SYSTEM

2.1 CONSTRUCTION OF THE NASTRAN MODEL

In this thesis, we analyzed the effect of the dynamic properties (eg: spring and damping coefficients) of the suspension system components on the frequency response of the suspension system. This section outlines the steps and also gives the details of the converting the readily provided TOFAŞ ABAQUS model to a NASTRAN model.

The standard extension for an input file in ABAQUS is ".inp". The first step in the conversion process was to convert the ".inp" format to ".hm" format in HYPERMESH which was done by TOFAŞ. Then the ".hm" file was converted to NASTRAN input format ".bdf" in HYPERMESH. After the ".bdf" format is obtained, the file can be manipulated in PATRAN which is the user interface for NASTRAN. When the ".bdf" file was first opened in PATRAN, there were many errors (Figure 2.1), as expected. The reason for these errors was the wrong formatting of force/displacement tables (4 tables, used twice, resulting in 8 errors) and a few wrong properties IDs (2 wrong IDs) adding up to 10 errors. Wrong IDs were traced from the .ses file (session file) which is readable after closing the PATRAN, and it gives the detailed information about that PATRAN session. At this step, main focus was on clearing these errors/warnings. After eliminating all the error messages, all the "geometrical characteristics" of the ABAQUS elements were imported successfully. However, during the conversion process, the dynamic properties of the elements were not imported correctly since many of the ABAQUS elements do not have corresponding elements in NASTRAN. After this step, the properties of the elements were corrected one by one, by checking the original ABAQUS model and comparing it to the one present in NASTRAN format.

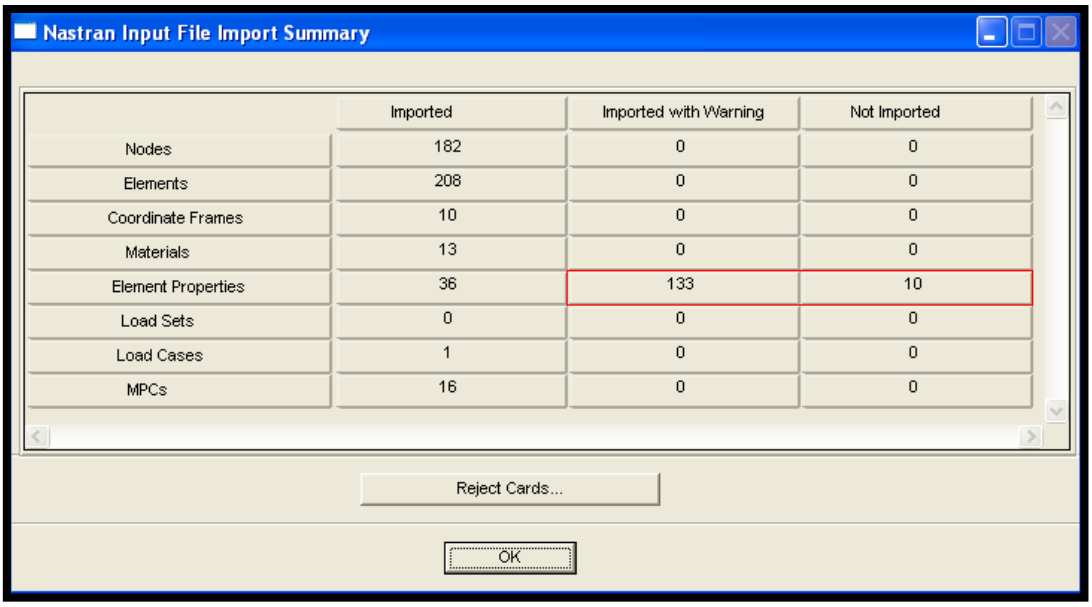

Figure 2.1: Finite element model status after the first import

2.2 CONVERSION OF THE ELEMENTS

2.2.1 BEAM ELEMENTS

HYPERMESH converted all the properties of the "Beam Elements" from ABAQUS to NASTRAN correctly. We also made sure that the directional cosine values (DirCos values) of these elements were converted with no errors (Figure 2.2)

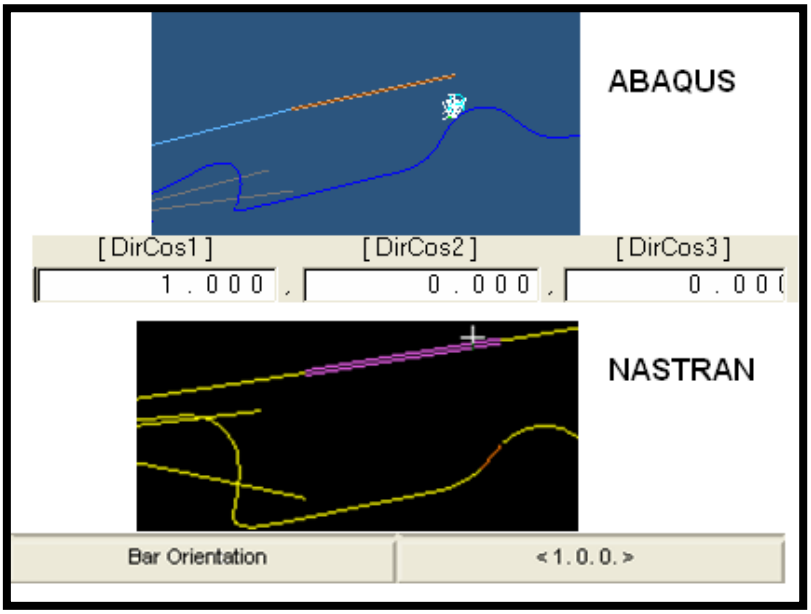

Figure 2.2: Directional Cosine values of beam elements

2.2.2 SPRING ELEMENTS

There are 3 kinds of spring elements available in ABAQUS (SPRING1, SPRING2 and SPRINGA) whereas there is only one type of spring element in NASTRAN (CELAS). CBUSH in NASTRAN is a very appropriate element to modify and use as a spring so that it can represent the spring properties in ABAQUS. When the CBUSH element is used without damping, it simply behaves as a spring element. For instance, when "TSUPDX" spring element group in ABAQUS model is considered, SPRING2 type element is used and it has 6 different characteristics at each direction. In NASTRAN, CBUSH elements allow defining spring properties in 6 directions. To make the conversion, the first 3 directions the force/displacement fields are defined and for the last 3, constant stiffness values are entered. The spring stiffness properties are shown below (Figure 2.3).

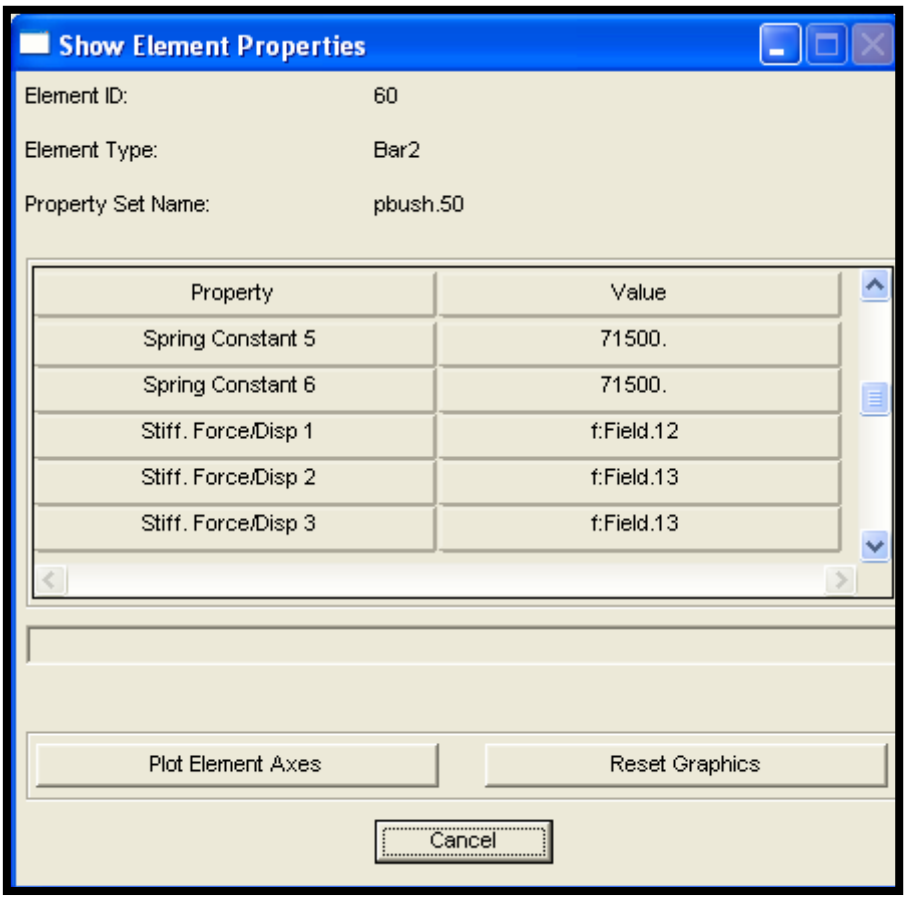

Figure 2.3: Constant and non-linear stiffness values of TSUPDX element

The other concern for spring elements was the orientations of the spring elements. TSUPDX group is considered again:

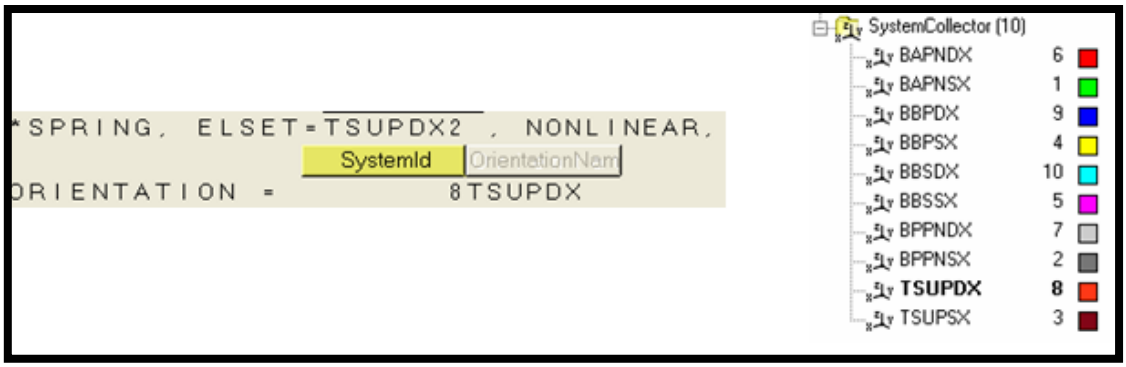

Figure 2.4: TSUPDX Spring orientation

As it can be observed in Figure 2.4 (HYPERMESH Interface), TSUPDX spring group uses coordinate number 8 to define its orientation. HYPERMESH converted the coordinate systems with no errors from ABAQUS to NASTRAN. So in .bdf file, while defining the CBUSH elements, it is possible to define the orientations of springs at the end of the command line:

*"CBUSH,60,50,49,66,,,**8**"*

Number "8" shows the id number of the coordinate system. The information at the end of the command line shows that the spring is oriented with respect to this coordinate system "8" (See Figure 2.5).

The other concern about the spring elements is some of them have one of their nodes fixed at the ground (eg: SPRING1 elements). There is no direct way to do this in PATRAN using CBUSH properties and it had to be done manually. We used the SPC (Single Point Constraint) command to create this effect. While applying SPC's, the node which has no connection with other elements is chosen so that only the spring is grounded not other elements. As it can be seen from Figure 2.6, it may be tricky to choose these elements when the spring is defined between two nodes that are located at the same coordinate. Node 134 is only associated with element 11 which is the spring itself. However Node 133 has connections with other elements too so it is the connecting node between the spring and other elements. Thus, the SPC is applied on node 134 in order not to affect the elements other than the spring.

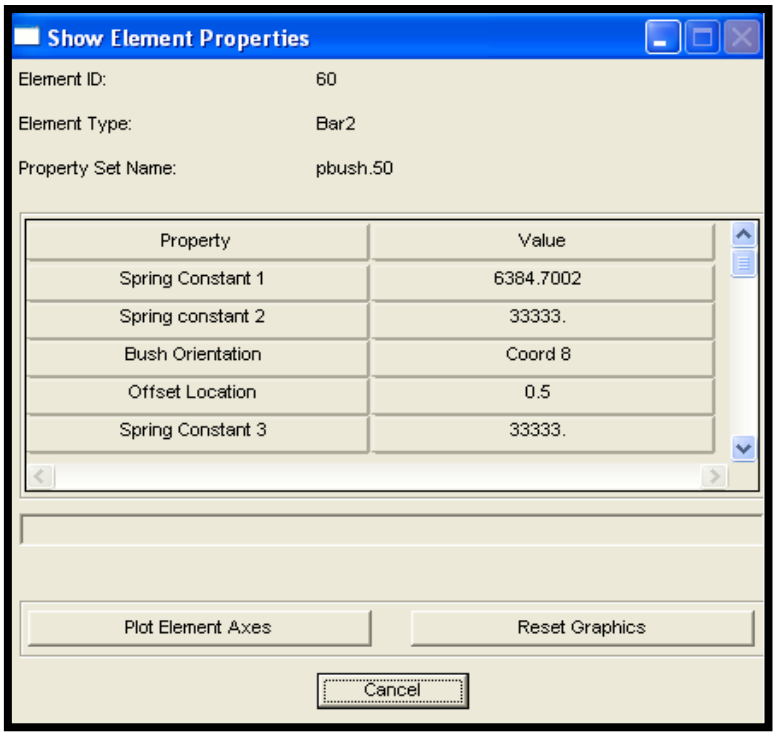

Figure 2.5: Orientation (Coord 8) of TSUPDX in PATRAN

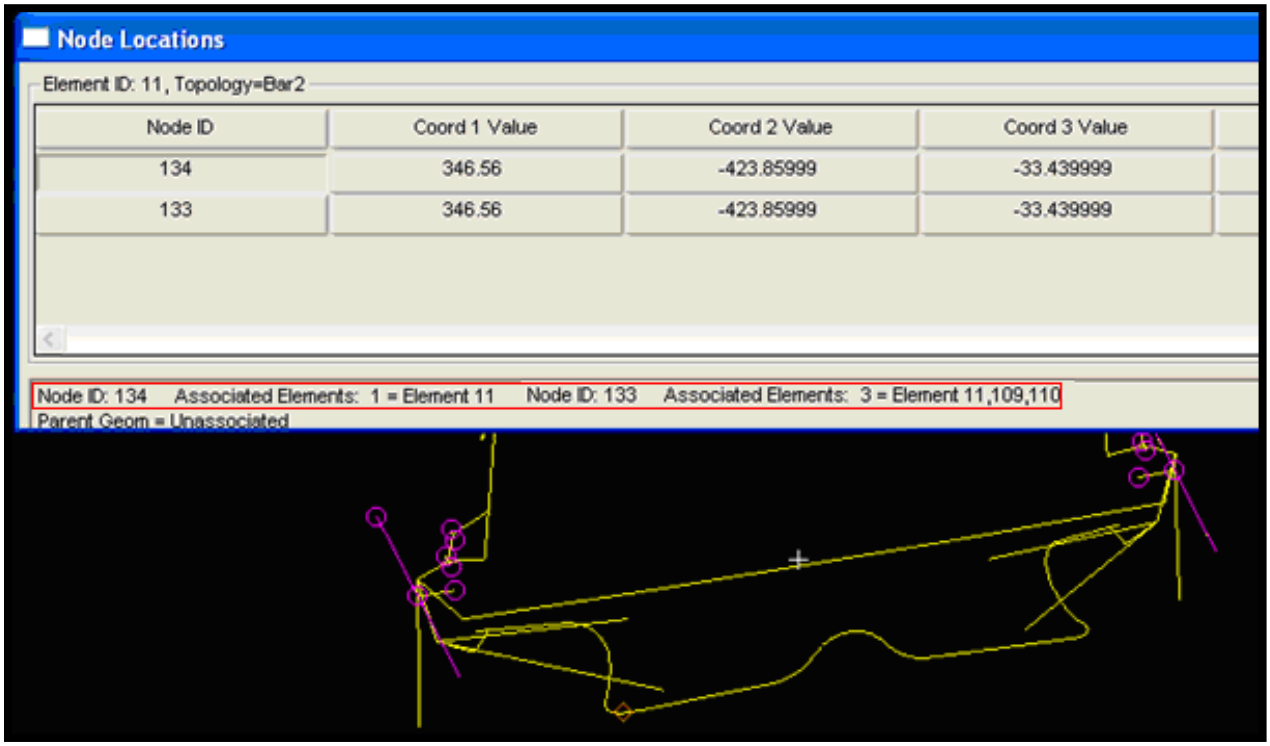

Figure 2.6: Connectivity data of two different nodes located on the same coordinates

2.3 OTHER ELEMENTS AND OTHER CHECKS

Other elements such as PIN and EQUATION elements in ABAQUS are translated as rigid body elements (RBE2), causing no serious problems.

The sliding effect of the dashpot is given with the command "SLIDER" in ABAQUS. The way it is defined in ABAQUS is like this:

SLIDER, 21, 10, 100

SLIDER, 4, 10, 100

However there is no direct way of defining this motion in NASTRAN. The corresponding nodes are found in NASTRAN .bdf code and then SPCs are defined for those nodes, while allowing the movement in the desired degree of freedom.

Also as a final check, we performed the modal analysis of the suspension system and observed the mode shapes. We found out that some of the nodes were not properly fixed to the ground so that we made the required modifications accordingly.

2.4 A FINAL OVERVIEW OF THE FINITE ELEMENT MODEL

The linear NASTRAN Finite Element Model (FEM) of the front suspension system is shown in Figure 2.7.

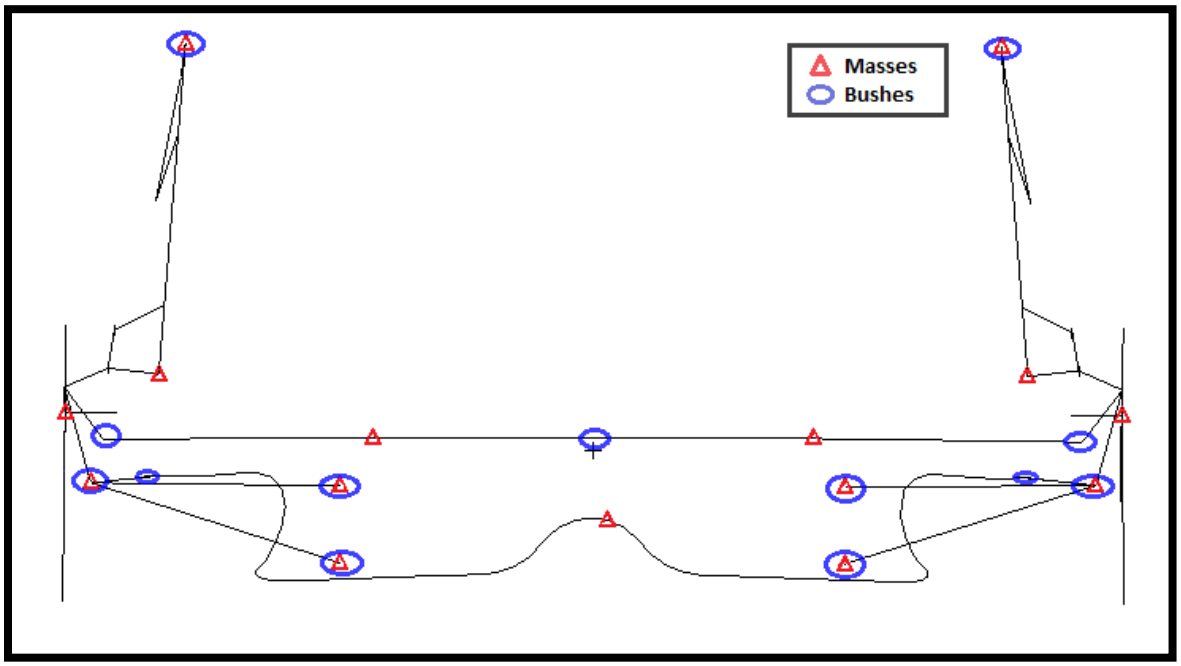

Figure 2.7: (Stick) Finite element model of the front suspension system

The spring/damping elements (k_1, k_2, k_2`, k_3, c) that connects the suspension tower and the vehicle chassis and the tire are considered as the important components of this suspension system (See Figure 2.8) and they are selected as the design parameters for this study. The vehicle and tire masses are also represented in the model as m_1 and m_2, respectively. There are also bushes that connect the suspension system to the vehicle body at different locations (See blue circles in Figure 2.7). A visual explanation of the stick finite element model is shown in Figure 2.8.

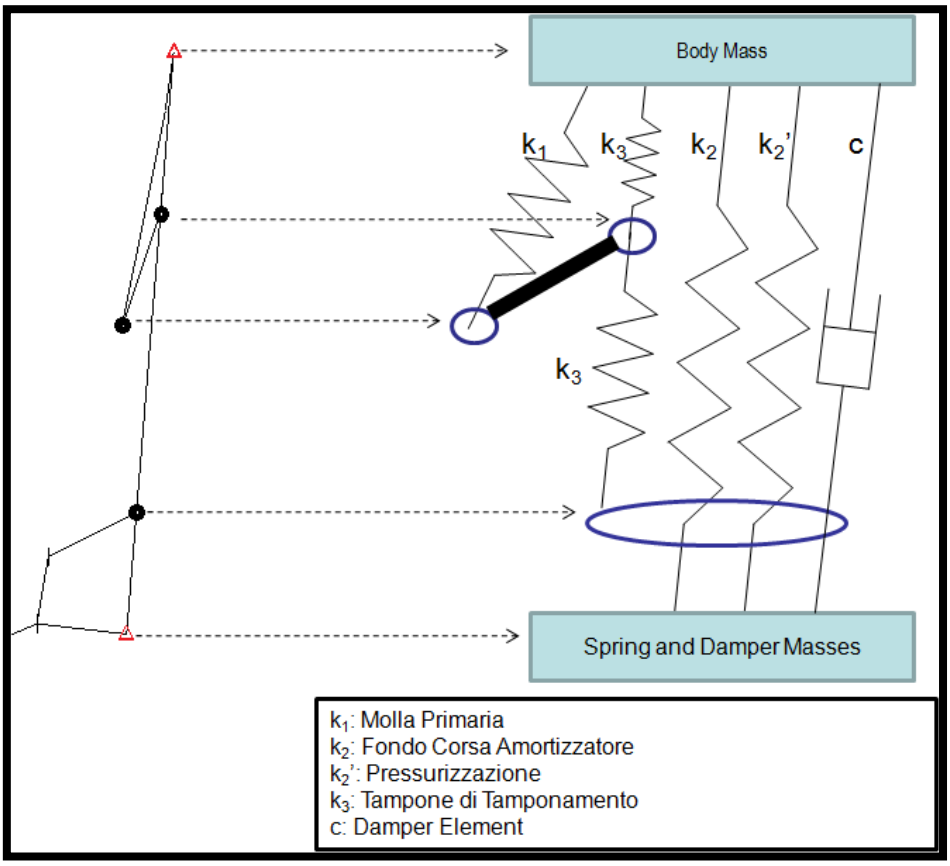

Figure 2.8: Upper Side of the suspension system

The frequency response function (FRF) of the suspension system can be obtained through a linearized finite element model. For that purpose, we converted the nonlinear ABAQUS model to a linearized NASTRAN model such that the frequency response analysis can be performed. An example of the nonlinear spring data used in the linearization procedure is shown in Figure 2.9 and Table 2.1. The spring coefficient is obtained by taking the most general slope of the displacement vs. force diagram such that a constant spring coefficient can be obtained for the linear springs used in the NASTRAN model.

TOFAŞ also provided a high fidelity finite element model for our use. However, due to the detailed structure of this model, simulations took too much time and computer source so, this model was not preferred to use. To distinguish the two models, the one we used in our studies will often be called as the “stick” finite element model.

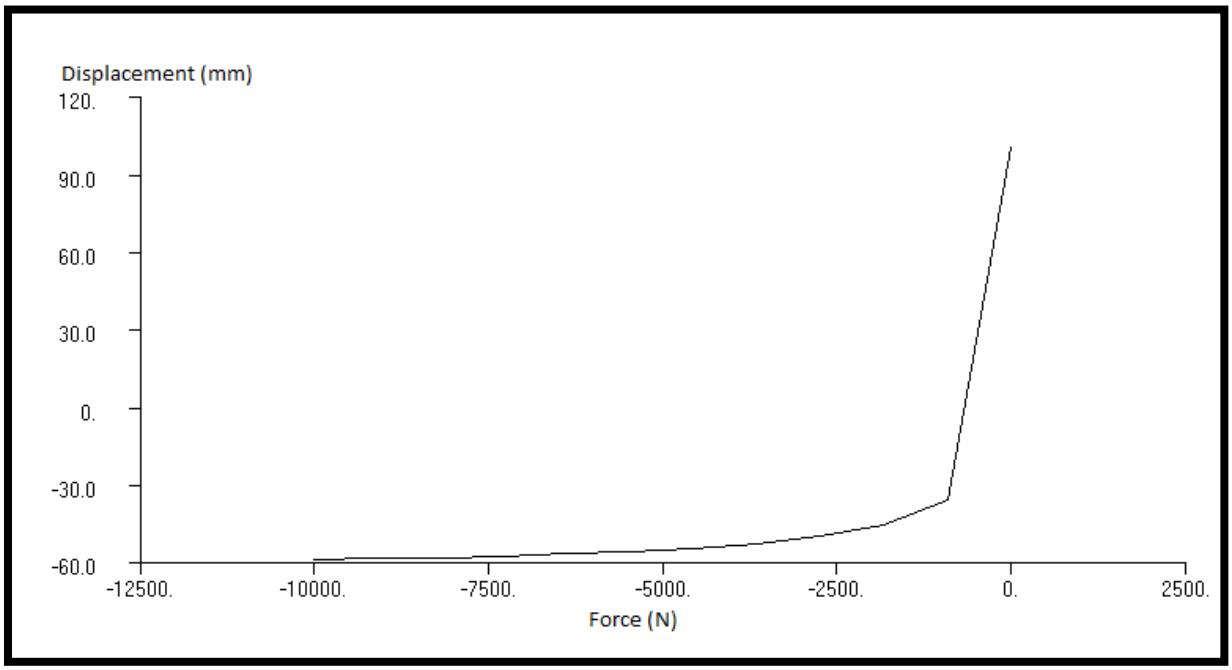

Figure 2.9: Non-Linear Force vs. Displacement curve of TAMTDX spring

f	Value
-10010.2	-59.200001
-9100.0908	-58.757172
-8189.9814	-58.314346
-7279.8721	-57.684807
-6369.7627	-56.880112
-5459.6533	-56.075413
-4549.5439	-54.620056
-3639.4348	-53.097416
-2729.3257	-50.136627
-1819.2166	-45.484074
-909.10742	-36.07019
1.001709	100.18867

Table 2.1: Force (N) vs. Displacement (mm) values of TAMTDX spring

CHAPTER 3

PERFORMANCE METRICS

As mentioned in the above paragraphs, vehicle's performance will be studied according to some performance metrics for each configuration. The responses of the vehicle model are, respectively, the vertical body acceleration $\ddot{x_1}$, the force applied between the road and the wheel (F_z), the relative displacement between the wheel and the vehicle body (x_1-x_2) according to Figure 3.1.

The three performance metrics associated with these responses are as follows:

1) The "Discomfort" is found out by calculating the standard deviation of the vertical body acceleration $\sigma_{\ddot{x}}$. As this standard deviation gets higher, discomfort also goes higher.

2) "Road Holding" can be related to the computation of the standard derivation of the tire radial force σ_{F_z}. The variation of this force means a loss of contact and thus leads to poor road holding.

3) The standard deviation of the relative displacement between the vehicle body and the wheel σ_{x1-x2} is related to design constraints and related to "Working Space".

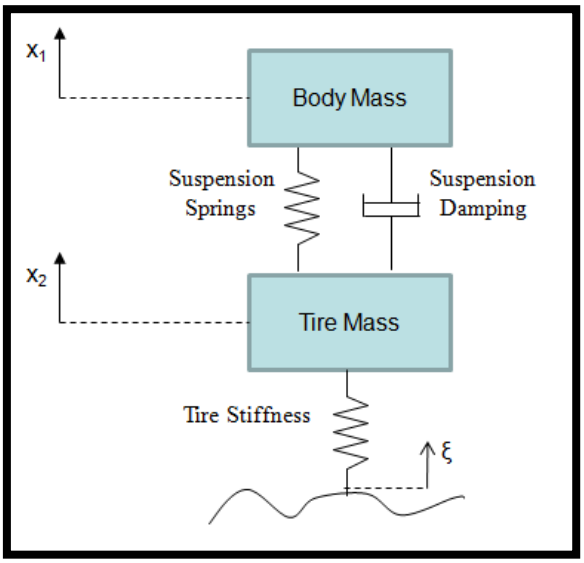

Figure 3.1: Quarter car vehicle model in correspondence with the finite element model

In order to excite the system, a unit displacement (1 millimeter) is given to the tire. This helps us define the road irregularity (ξ) which will be mentioned in the next sections. The transfer functions that are going to be used in the calculation of performance metrics are shown in Figures 3.2, 3.3 and 3.4. Figure 3.2, shows the transfer function between the displacement ξ (road irregularity) and the vertical body acceleration, $\ddot{x}$. Figure 3.3, shows the transfer function between the displacement ξ (road irregularity) and the vertical body force applied between the road and the tire (F_z). Figure 3.4, shows the transfer function between the displacement ξ (road irregularity) and the relative displacement between the tire and the vehicle body (x_1-x_2). All these transfer functions are obtained using the stick FEM.

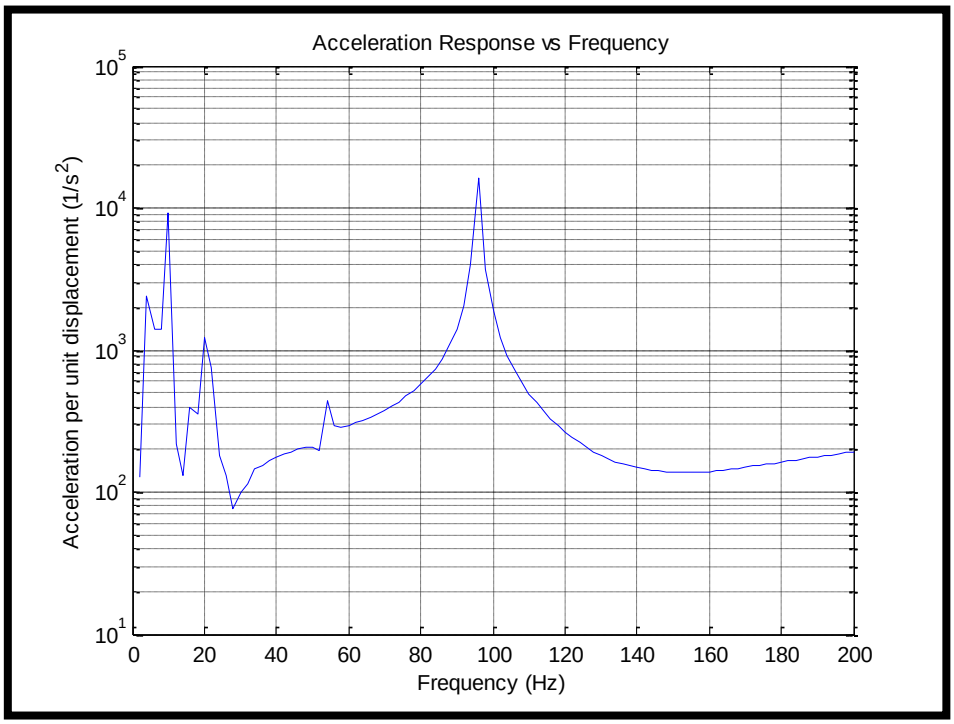

Figure 3.2: Transfer function between the displacement (ξ) and the vertical body acceleration $\ddot{x}$

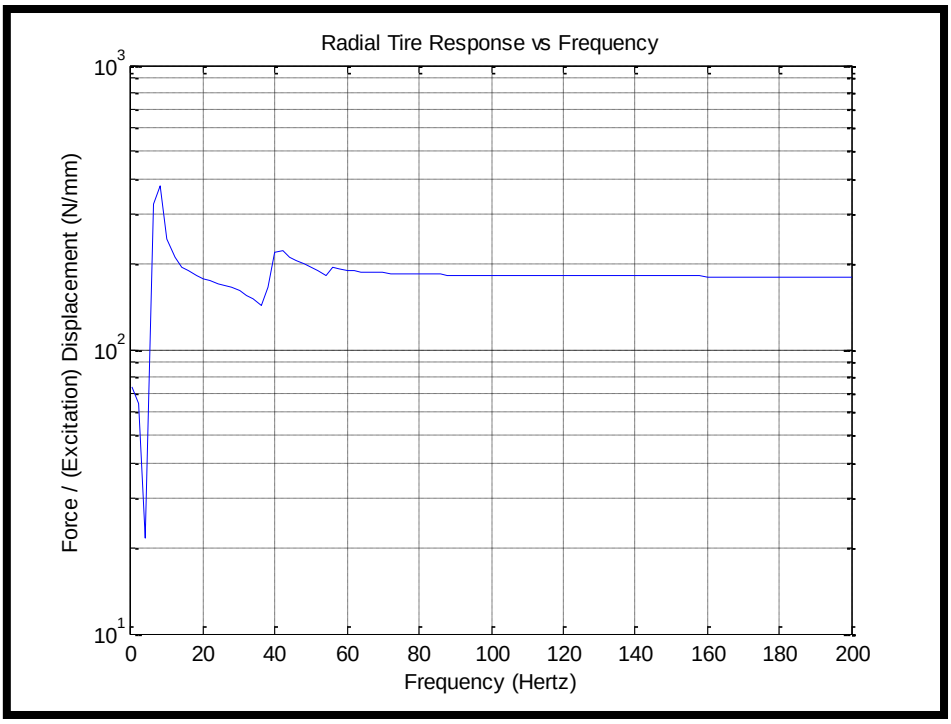

Figure 3.3: Transfer function between the displacement (ξ) and the force applied between the road and the tire (F_z)

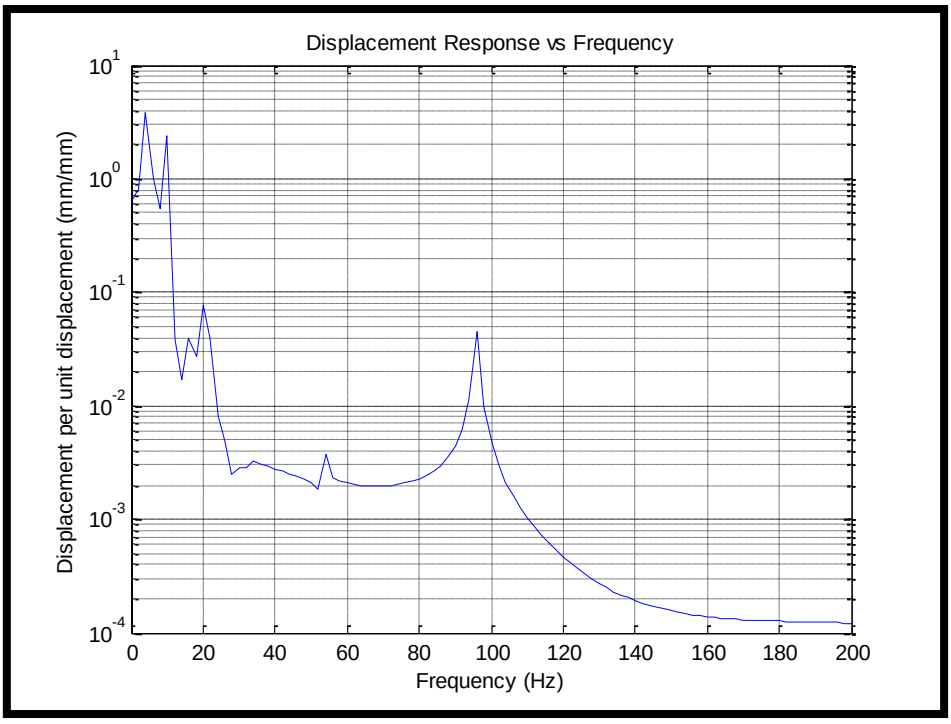

Figure 3.4: Transfer function between the displacement (ξ) and the displacement between the tire and the vehicle body (x_1-x_2)

3.1 CALCULATION OF PERFORMANCE METRICS

In order to calculate the performance metrics, the transfer functions should be processed simultaneously with the road profile to add the road irregularity effect as well. For this purpose the concept of power spectral density (PSD) is employed. The road profile functions (signal generators) that we have used, when multiplied by an appropriate factor (transfer functions in our case), will give the power transmitted by the signals per unit frequency and this is called the power spectral density of the signal. The spectral density, in definition, describes the average frequency content of a random process at any time [14].

So, in our case the power spectral density of the vehicle output performance can be calculated as follows:

$$S_l(\omega) = |H_l(j\omega)|^2 S_{\varepsilon q}(\omega) \qquad l = 1\,, 2, 3 \qquad q = 1, 2 \tag{3.1}$$

In this equation index l stands for the 3 performance metrics (discomfort, road holding, and working space) and q stands for the 2 kinds of road profiles that we use in our studies which will be explained in the next section. To be mode clear; for l = 1, S_l represents the PSD of the *vertical acceleration of the vehicle body*, for l = 2, S_l represents the PSD of the vertical force at the wheel-road interface, and for l = 3, S_l represents the PSD of the relative displacement between chassis and wheel (suspension stroke). $S_{\varepsilon q}$ is the input spectra (road input) and H is the transfer function between the disturbance and the corresponding vehicle response calculated using the finite element model. The index q=1 refers to the road input PSD1 and the index q=2 refers to the road input PSD2 (see next section).

As the PSD of the output performances (S_l) are calculated, the variance of the performance can be calculated as follows:

$${\sigma_l}^2 = \frac{1}{2\pi} \int_{-\infty}^{+\infty} S_l(\omega) d\omega \qquad l = 1, 2, 3 \tag{3.2}$$

Where σ_l (standard deviation) in the above equation refer, respectively to $\sigma_{\ddot{x}}$, σ_{Fz}, σ_{x1-x2}. In this way it is possible to calculate the values of the three performance metrics for the suspension system. For our studies, we developed a MATLAB code to calculate the standard deviation values. This procedure is repeated for all experiments. The MATLAB code handles the post-processing of the inputs and outputs of the FEM and also prepares the experiments required for the DOE analysis.

3.2 ROAD IRREGULARITY MODEL (INPUT SPECTRUM)

The displacement (road irregularity) may be represented by a random variable defined by a stationary and ergodic process with zero mean value [15, 16]. The definition of an ergodic process comes out to be like this: If almost every member of the ensemble shows the same statistical behavior as the whole ensemble, then it is possible to determine the statistical behavior by examining only one typical sample function and the process including this ensemble is called an ergodic process. The zero mean value as well indicates that the observed samples show a very stable (stationary) behavior that their average is constant.

The Power Spectral Density (PSD) of the process may be determined on the basis of experimental measurements and in the literature there are many different formulations for road irregularity representations [16, 17].

In this study, two spectrums are used to represent the road irregularities. Corresponding expressions are shown in (3.3) and (3.4).

$$S_{\varepsilon 1}(\omega) = \frac{A_b v}{\omega^2} \tag{3.3}$$

$$S_{\varepsilon 2}(\omega) = \frac{A_v s_c}{{s_c}^2 + \omega^2} \tag{3.4}$$

Parameter	Unit	Reference Value
A_b	m	1.4e-5
$\alpha = s_c/v$	rad/m	0.4
A_v	m	3.5e-5

Table 3.2: Road irregularity parameters

The value *a* (rad/m) depends on the shape of the road irregularity spectrum. The "*v*" variable in both equations represents the vehicle speed. In DOE analysis, the performance metrics are calculated based on three different vehicle speeds since the PSD of the road irregularity changes as the vehicle speed changes. In a log-log scaled plot (abscissa being ω), the spectrum of equation (3.3) takes the shape of a line with gradient -2. Because of this reason expression (3.3) is simply called the one slope power spectral density (PSD1). The one-slope PSD approximates various roads with different degrees of accuracy. It generally overestimates the amplitudes of the irregularity at low frequency [16, 17]. A better correlation can be obtained by using a more complex spectrum like the one in equation (3.4) as suggested in [16]. In a log-log scaled plot (abscissa being ω), the tendency of this equation takes the

shape of a two-slope curve so this spectra is simply called the two slope power spectral density (PSD2).

Figure 3.5 summarizes the procedure followed up to now for calculating the performance metrics. As it can be observed from the figure, the transfer functions of the vehicle responses are obtained from the FEM. Then the output performance spectral density is calculated by multiplying the input power spectral densities (road irregularity) with the square of the transfer functions. In the end, the standard deviation of the output performance is calculated using equation 3.2.

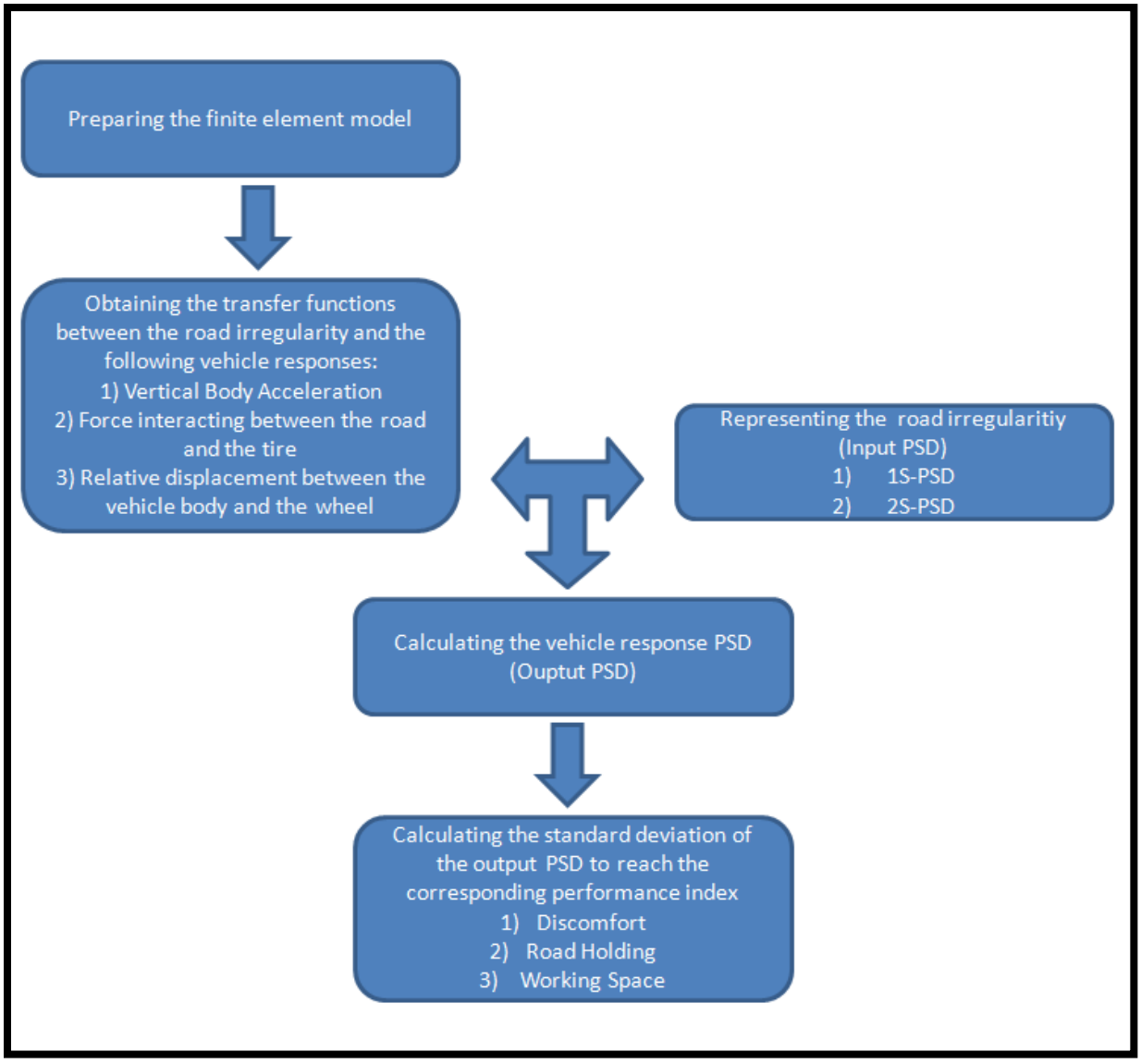

Figure 3.5: Flow chart showing the procedure for performance metric calculation

CHAPTER 4

VALIDATION OF THE STICK FINITE ELEMENT MODEL

As it was mentioned in the overview section of the finite element model (Section 2.4), apart from the stick finite element model, there is also a detailed, high fidelity finite element model available for our use. However, a single run for our purposes with the detailed model (Figure 4.1) takes about 2 hours to complete. The computational time becomes a critical issue especially when we perform the DOE studies (more than 500 runs are required). For that reason, we concluded that the stick model was more suitable to use for DOE analysis. However, the stick model had to be validated such that the results obtained from the stick model should be comparable with the ones obtained from the detailed model. The following section presents sample comparison studies made between the stick model and the detailed model.

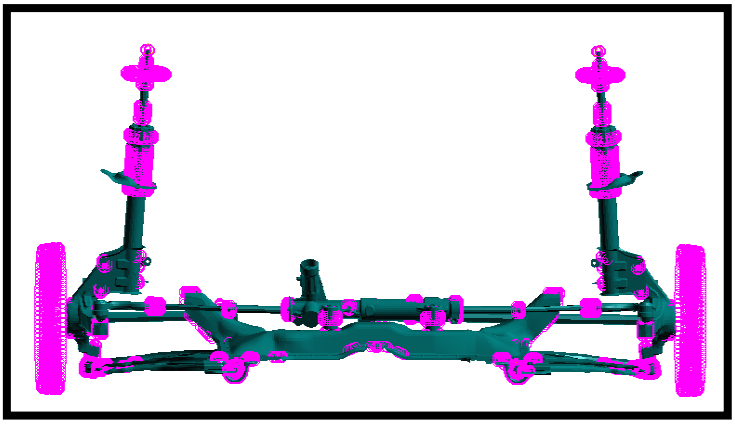

Figure 4.1: Detailed front suspension finite element model

4.1 COMPARISON OF THE DETAILED FE MODEL AND THE STICK MODEL RESPONSES (DAMPED / UNDAMPED)

In the detailed FE model and the ABAQUS version of the stick model, there was no damping element defined. Only a general structural damping was given. We introduced a damper element into the suspension system, so that we can consider the damping as a design factor for our optimization studies since it carries a great importance in suspension performance.

In the comparison, we used the same response/excitation model for our studies; i.e., response is the suspension tower vertical acceleration and its displacement; while the excitation is one millimeter of vertical displacement to the tire.

If Figures 4.2 and 4.3 are observed, the comparison of the stick model with / without damping and the detailed FEM model can be seen. As it can be observed from the figure, the stick model represents the system dynamics very accurately although the peaks at the high frequencies cannot be captured with this model. Those peaks correspond to some components which are not present in the stick model.

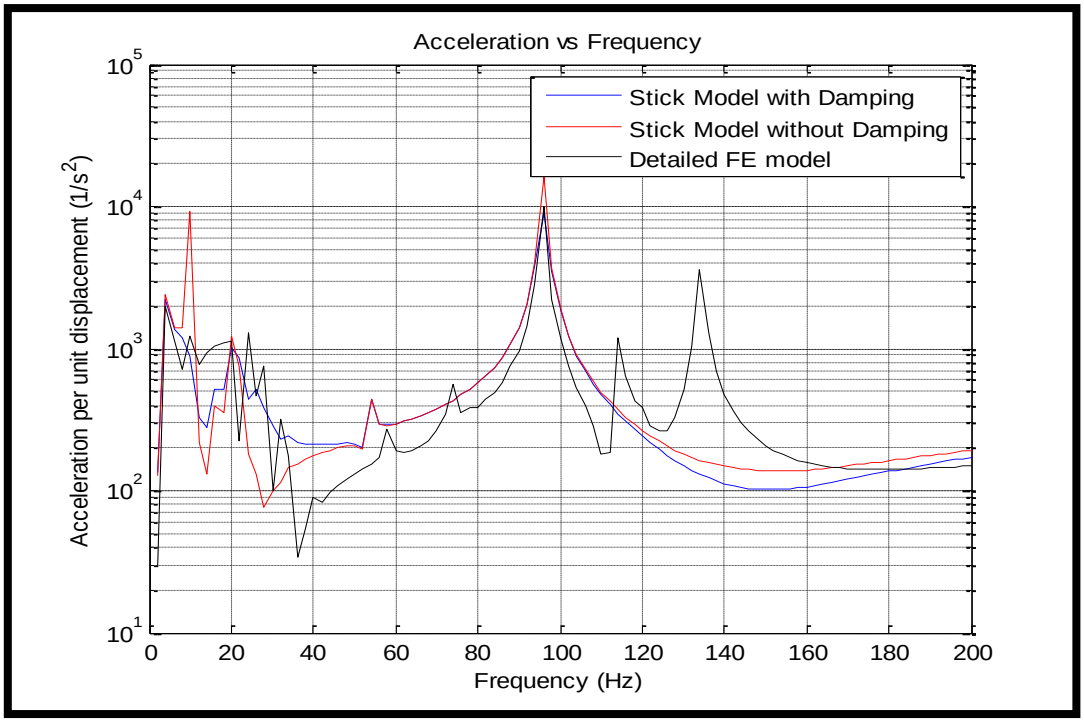

Figure 4.2: (a/F) Response compared for damped/undamped stick model and the detailed model

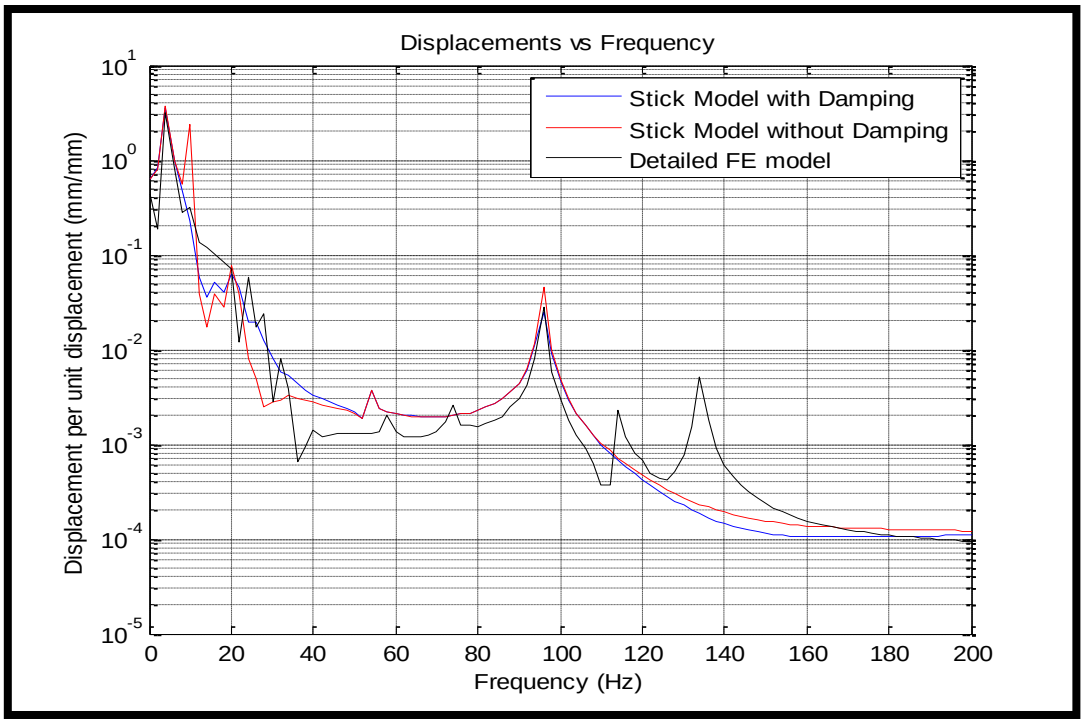

Figure 4.3: (Displacement / F) Response compared for damped/undamped stick model and the detailed model

4.2 COMPARISON OF THE PERFORMANCE METRIC "DISCOMFORT" BETWEEN THE DETAILED FINITE ELEMENT MODEL AND THE STICK MODEL

In this section, the effect of the discrepancies of the two models on the performance metric will be examined to justify the use of the stick model in our studies. Figures 4.4 and 4.5 show the discomfort response obtained for PSD1 and PSD2 road profiles, velocities changing between 0-150 m/s.

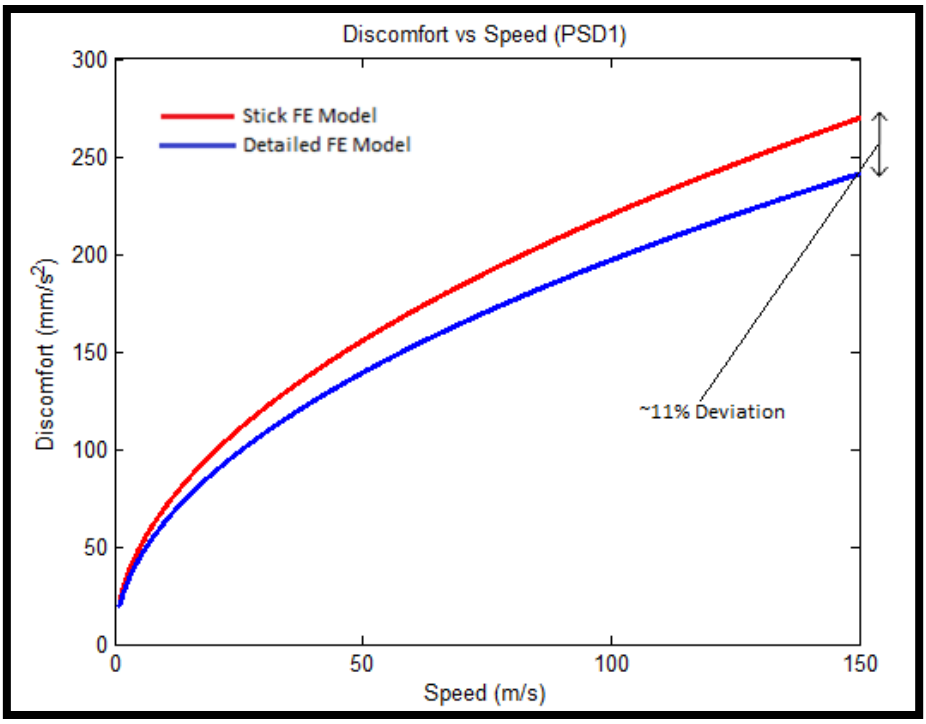

Figure 4.4: Discomfort in PSD1

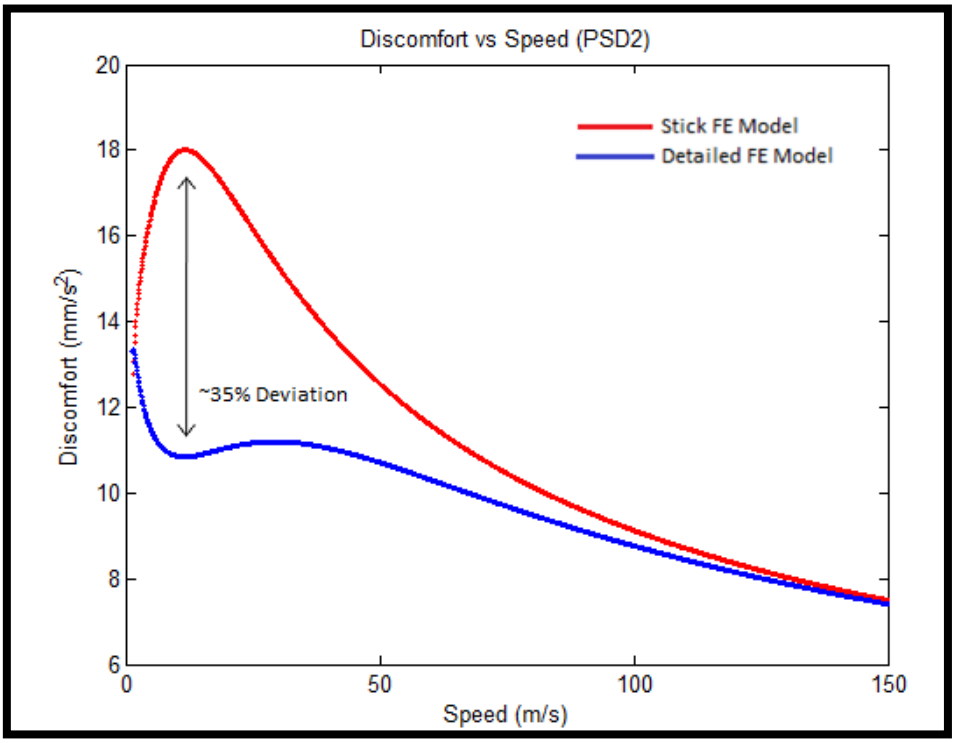

Figure 4.5: Discomfort in PSD2

As it can be observed from the figures above, the detailed model and the stick model results match very well with each other for PSD 1 road profile (11% Deviation at most). Although the curves in PSD2 do not seem to match with each other at low speeds at first glance (35% Deviation at most), considering the general trend, they actually match fine as well. For PSD2

even a better match is observed at higher speeds. These plots verify that using the stick model instead of the detailed model will not lead to significant differences in the performance metric calculations.

4.3 (a/F) RESPONSE COMPARISON FROM THE WISHBONE

Learning from TOFAŞ feedback, in automotive industry, the response of the vehicle suspension system is tested using some points on the wishbone. Those three points (e.g. 1, 2, 3) are shown in Figure 4.6. The force is applied at point 1 and the responses are measured at points 1, 2 and 3. The figures 4.7, 4.8 and 4.9 show the comparisons of these transfer functions obtained by the stick model and the detailed model. When these tests are conducted for the damped stick model and the detailed model, we observe results that are close enough for the purposes of our studies except some extra peaks in the detailed model.

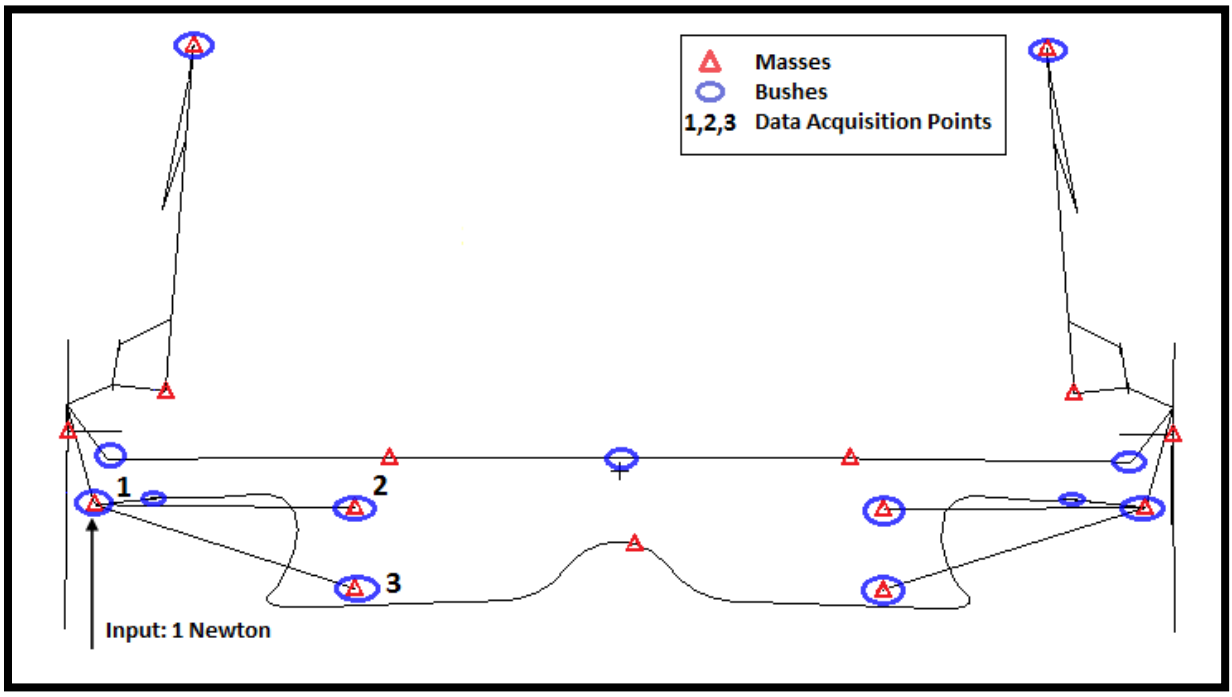

Figure 4.6: Stick Model showing the force input point and the response acquisition points

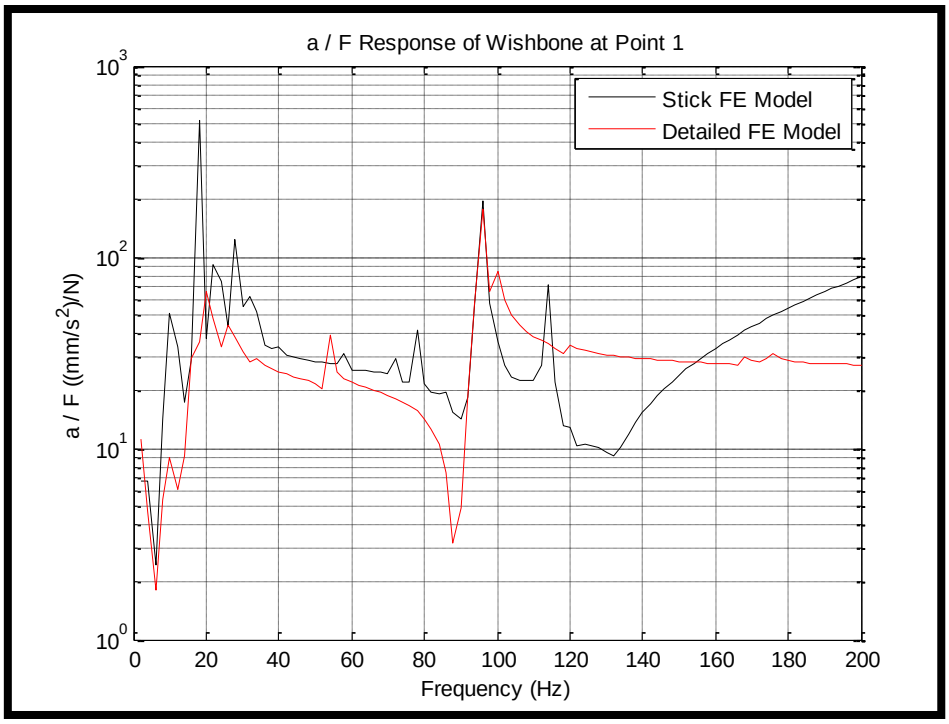

Figure 4.7: (a / F) response of the suspension system @ point 1 comparing the stick model and the detailed model

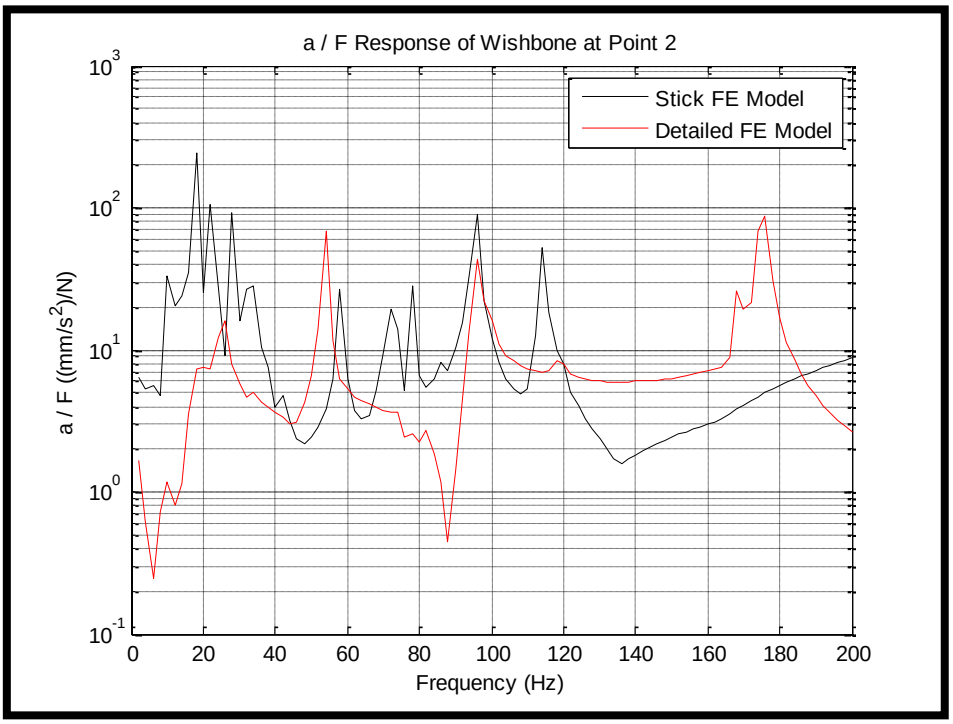

Figure 4.8: (a / F) response of the suspension system @ point 2 comparing the stick model and the detailed model

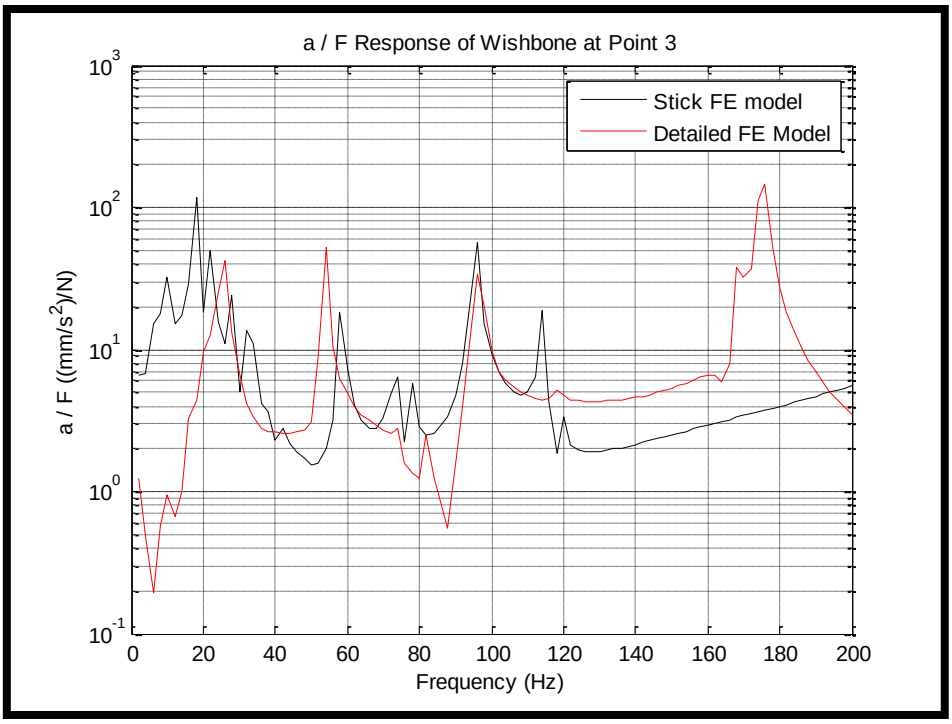

Figure 4.9: (a / F) response of the suspension system @ point 3 comparing the stick model and the detailed model

CHAPTER 5

DESIGN OF EXPERIMENTS METHODOLOGY, RESPONSE SURFACE MODELING AND OPTIMIZATION

In our studies, Design of Experiments (DOE) and Response Surface Method (RSM) techniques are employed in collaboration to find the optimal relationship between the suspension design parameters and the performance metrics. To do so, the regression models obtained from the DOE and RSM methods are used in single and multi objective optimization studies to find the optimum solutions by the minimization of the three different objective functions (e.g. performance metrics). In these studies, NASTRAN, MATLAB and StatEase Design Expert software are used for different purposes. The details of the DOE, RSM and optimization procedure are described in the following sections.

5.1 BACKGROUND ON DOE & RSM

DOE is a statistical methodology that came out from the idea of developing an effective and efficient experimentation plan. Roots of DOE extend back to 1920s when R.A Fisher had an idea to point out agricultural experimentation problems [18]. In our day, DOE methodology evolved so much that its theory and application tools are widely used in natural sciences and in any kind of engineering discipline because of its effectiveness and benefits [19]. While the majority of applications of RSM were in chemical and process industries prior to 1970s, application of RSM has since spread to many other areas and industries such as physical sciences and engineering, food sciences, social sciences, and biological sciences. Myers et al., (2004) [20] reviewed the progress of RSM in the general areas of experimental design and analysis, and indicate how advances in other fields of applied sciences have affected its role. The authors show many examples to the use of RSM in various applications such as manufacturing process improvement and control. For further references on RSM methodology and applications, the reader is referred to Myers and Montgomery, 2002 [21]. Basically, DOE aims to determine an appropriate set of experiments that are sufficient to obtain an adequate (not much than that) level of information by varying the main design factors of interest over an operating range in a structured manner by using statistical tools. To become more precise, DOE decides how many experiments are sufficient to reach a satisfying and reliable level of

information, how and in what range the design variables should be altered while doing these experiments and how to obtain acceptable models that describe the relationship between the variables and objective outputs (response variables). In scientific studies, the aim is to show that the statistical evidence is related to the effect of some factors on response. On the other hand, for the industrial purposes, the aim is to decrease the cost of the projects while trying to reach the required information for the relationship between the main factors and the responses. To find this relationship, regression models based on RSM are utilized to approximate the responses of the main parameters and find functions of them that are defined in the range that those parameters are varied.

Foundations of RSM go back to Box and Wilson (1951) which has since been an important tool for industrial statistics [18]. RSM became an indispensable element of industrial experimentation according to many, working in this field. In fact, RSM is nothing but a collection of statistical and mathematical tools useful for developing, improving, and optimizing products and/or processes. The fundamental goal of RSM is to obtain an approximate functional relationship between the input variable(s) and the output objective function(s) to construct a comprehensive model over an entire domain of interest. A well known method to obtain this model is to employ regression, which relates controllable variables to responses. The regression equations provide information about the properties of the system from which the data (generally obtained through a set of designed experiments) is taken, and can be used to improve/optimize processes through appropriate deterministic optimization procedures. These regression equations also give us the chance to see the theoretical responses which unless otherwise can never be obtained in real life due to the restriction on the input variables. This can force to create new ideas about altering constrains if desired and unusual responses are obtained.

The increased use and availability of computational models to evaluate performance of different product designs has allowed the use of RSM for computer experiments (rather than physical experiments for which RSM has been initially developed). The use of RSM presents two fundamental advantages over other optimization schemes (e.g., random search schemes such as genetic algorithms) [20]:

-First, RSM yields a functional relationship between the factors (i.e., various components and parameters of the product design) and response variables (i.e., some performance metric for the design) of interest over the search space. This provides a better understanding of the

system behavior, and complements the product designer's expertise with the system. The step-by-step nature of the technique also allows interaction of the designer with the optimization scheme.

-Secondly, such functional relationships (obtained through regression analysis, in general) allows for much faster search of the design space compared to random search schemes. This is particularly important for computer models that require significant amount of computational time to run. According to the use of main factors and the creation of the DOE, there are several approaches available. In this thesis, full factorial and fractional factorial designs will be introduced.

5.2 FULL FACTORIAL DESIGN

In full factorial design approach, all of the main factors are included with all the levels and possibilities of those factors. To calculate the number of experiments in full factorial design approach, the below formula is used:

$$N = \prod_{i}^{k} n_i \quad i = 1, \dots, k \tag{5.1}$$

where k is the number of factors, n_i is the number of levels for the factor i and N is the total number of the experiments required.

Under the full factorial classification, there are several choices related to the number of levels regarding the main factors. In this section, two level factorials are introduced and used. Related information can be found in the next section.

5.2.1 TWO-LEVEL FULL FACTORIAL DESIGN

In two-level full factorial design, the main factors have two levels which are mentioned as either 'high' and 'low' or '+1' and '-1' in the literature. If the design uses all the possible combinations of those two levels of all the factors, it is called a "two level full factorial design". In this design approach the number of the experiments required is simply equal to 2^k where k represents the number of the factors used. For instance, when 7 main factors exist in the model with two levels for each factor, $2^7 = 128$ experiments will be conducted for DOE purposes when the two-level full factorial approach is to be used [22].

5.3 TWO-LEVEL FRACTIONAL FACTORIAL DESIGN

In fractional factorial designs, the main idea is to decrease the number of experiments needed for the analysis. For this purpose the number of experiments is equal to $2^{(k-p)}$ where k represents the number of design factors and p is smaller number than k [22]. Before moving to the DOE applied for our purposes, a little theoretical background on fractional factorial design is needed [23-25].

A numerical example for 4 design variables will be used.

If a full-factorial design is to be conducted, a total of $2^4 = 16$ experiments should be organized (Table 5.1)

Experiment Nr.	Parameter 1	Parameter 2	Parameter 3	Parameter 4
1	—	—	—	—
2	+	—	—	—
3	—	+	—	—
4	+	+	—	—
5	—	—	+	—
6	+	—	+	—
7	—	+	+	—
8	+	+	+	—
9	—	—	—	+
10	+	—	—	+
11	—	+	—	+
12	+	+	—	+
13	—	—	+	+
14	+	—	+	+
15	—	+	+	+
16	+	+	+	+

Table 5.1: 2-Level full factorial standard order for 4 parameters

Assuming our sources are inadequate for a full-factorial design. (time constraint, computational limitations etc.) In a case where 8 experiments are affordable instead of 16, a fractional factorial experiment can be set.

$$2^{k-p} = 2^{4-1} = 8 \qquad (5.2)$$

k = Number of Design Parameters

p = Number of parameters introduced through confounding with other parameters.

For this case, parameter 4 will be introduced into design through the interactions of parameters 1, 2 and 3. (Confounded with parameters 1, 2 and 3)

(Parameter 4 = Parameter 123)

Experiment Nr.	I	1	2	3	12	13	23	123
1	+	—	—	—	+	+	+	—
2	+	+	—	—	—	—	+	+
3	+	—	+	—	—	+	—	+
4	+	+	+	—	+	—	—	—
5	+	—	—	+	+	—	—	+
6	+	+	—	+	—	+	—	—
7	+	—	+	+	—	—	+	—
8	+	+	+	+	+	+	+	+

Table 5.2: Introduction of parameter 4, through interactions of 123

Through Table 5.2, we can reach to the recipe matrix in which 123 is shown as parameter 4.

Experiment Nr.	1	2	3	4
1	—	—	—	—
2	+	—	—	+
3	—	+	—	+
4	+	+	—	—
5	—	—	+	+
6	+	—	+	—
7	—	+	+	—
8	+	+	+	+

Table 5.3: The recipe matrix in which the number of required experiments is lowered

From Table 5.3, we can also reach the interactions of each variable. In this procedure, parameter 4 is deliberately confounded with the interactions of parameters 1, 2, 3 i.e. 4 = 123. This 4 = 123 term is defined as the "generator" of the design. If the interactions are investigated carefully, one can see that I=1234; 3=124; 23=14; 1=234; 12=34; 123=4; 2=134 and 13=24 are also confounded due to the nature of the table. Term "I" is called identity and it consists of a column of "+"s. Any column multiplied by I results in itself.

I = 1234 is the alternative form of the generator.

Instead of confounding one parameter to others, it is possible to apply confounding in multiple parameters as well. This confounding procedure is what defines the quality and accuracy of the design of experiments. More specifically the term "Design Resolution" is used for the grading of the relationship between the main effects and the confounded terms. A clear illustration of how the design resolution is decided on is given in appendix section (Appendix B) in the end.

5.4 RESPONSE SURFACE MODELING

Response surface is a surface which is useful to explain the correlation between the main factors of the design and the response of the models. Usually response surface method is applied after DOE approach for determination of the coefficients of the main factors in an equation related to the response of the model.

The response surface model is usually expressed with a constant term, a linear term and a second-order quadratic term, which can be written for n_v design variables below:

$$y^{(p)} = c_o + \sum_i c_i x_i + \sum_{1 \le i \le j \le n_v} c_{ij} x_i x_j \qquad p = 1, \dots, n_s \qquad (5.3)$$

where $y^{(p)}$ is the dependent variable of the response surface model (underlying equation), c_o, c_i, c_j are the regression coefficients, x_i is the design variable, and n_s is the number of observations. In our studies for response surface method, central composite design approach [26] is used to determine the experimental combinations.

After the DOE analysis is completed, StatEase Design Expert software is used to prepare the response surface models of the performance metrics.

5.5 DOE AND RSM RESULTS

In this section, before starting to list the experiments, their results and moving to the optimization part; indicating how the experiments are conducted and how they are organized will be mentioned shortly. In Figure 5.1; input to the model, data acquisition points are shown and the locations of the bushes are made known once again.

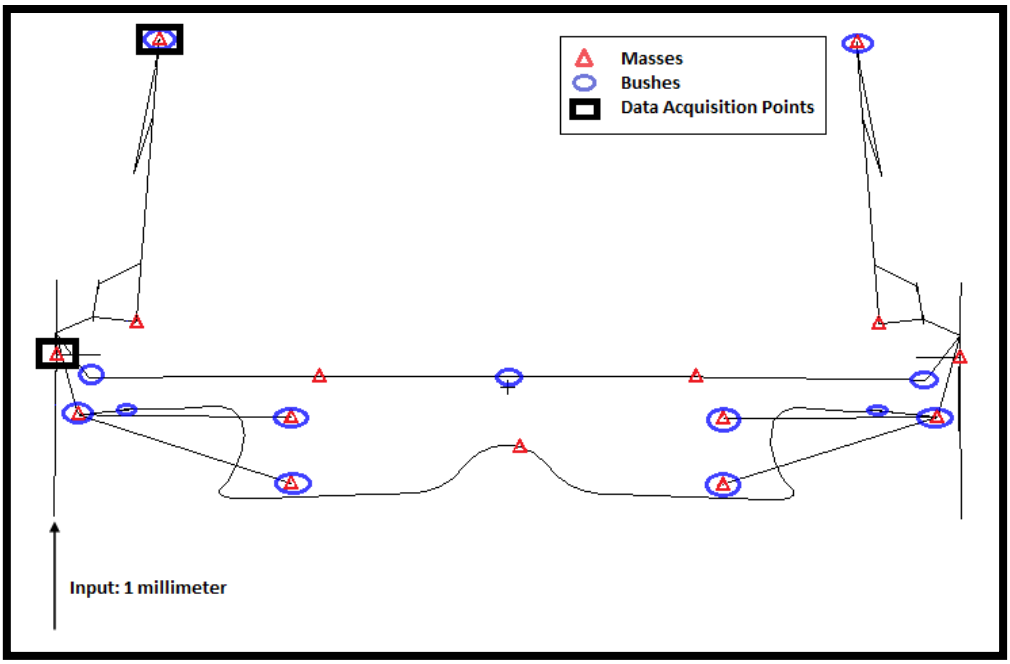

Figure 5.1: Stick finite element model with data acquisition and input points shown

The above rectangle is used for body mass calculations while the below rectangle is used for representing the tire location when acquiring data.

5.5.1 BUSH STUDY

We applied the DOE methodology in two stages. First, single point springs (bushes in FEM) are studied. There are a series of bushes that connect the suspension system to the vehicle body. These bushes were modeled as nonlinear springs in the ABAQUS model. These nonlinear springs are linearized, while the ABAQUS model was transformed into NASTRAN model.

Spring coefficients of the bushes (mostly vertical components) are selected and a DOE analysis is performed with 9 factors using the discomfort, road holding and the working space as the performance metrics (See Table 5.4 for the list of the bushes used in this study). The Design Expert software is used in the analysis. The high and low levels for each stiffness values were determined by increasing and decreasing the baseline values of the factors by 20%, respectively. A full-factorial experiment would have required 2^9 (=512) runs, which is not very practical considering our sources. Hence, a fractional factorial experimentation, which only required $2^{(9-4)}$ (= 32) runs for IV resolution design, is prepared. An additional run was added to test the factors at their baseline values, which was also used to check for curvature in the DOE analysis.

Factor Name	Factor Code	Nominal Value (N/m)	Low Value (N/m)	High Value (N/m)
PBUSH 50/2 (Translational Z)	A	2350	1880	2820
PBUSH 5/15 (Translational Z)	B	9800	7840	11760
PBUSH 7/21 (Translational Z)	C	3567	2853.6	4280.4
PBUSH 14/44 (Translational Z)	D	500	400	600
PBUSH 14/44 (Rotational Y)	E	33000	26400	39600
PBUSH 53/27 (Translational Z)	F	1000000	800000	1200000
PBUSH 12/45 (Translational Z)	G	6000	4800	7200
PBUSH 51/3 (Translational Y)	H	100	80	120
PBUSH 46 (Translational Y)	J	2000	1600	2400

Table 5.4: List of the bushes included in the DOE and their low & high values

DOE approach is applied for three performance metrics (Discomfort, Road Holding, and Working Space), for three different speeds (v = 1 m/s, v = 10 m/s, and v = 50 m/s) and two different road profiles (PSD1 and PSD2). 33 experiments are performed for each road and velocity variable. That makes a total of 33x3x3x2 experiments (See Table 5.5 for clarification) when all of these factors are considered.

Performance Metric	v = 1 m/s	v = 10 m/s	v = 50 m/s
		PSD1	
Discomfort	33 Experiments	33 Experiments	33 Experiments
Road Holding	33 Experiments	33 Experiments	33 Experiments
Working Space	33 Experiments	33 Experiments	33 Experiments
		PSD2	
Discomfort	33 Experiments	33 Experiments	33 Experiments
Road Holding	33 Experiments	33 Experiments	33 Experiments
Working Space	33 Experiments	33 Experiments	33 Experiments

Table 5.5: Clarification for the number of experiments conducted for each criterion

Table 5.6 lists the results of the DOE for bushes on discomfort performance at 50 m/s for PSD2 road profile. Rest of the table for this analysis can be found in the Appendix.

Run	PSD2
	v = 50 m/s
	Discomfort
1	12.59944548
2	12.58514778
3	12.57859592
4	12.56458731
5	12.58296863
6	12.59726613
7	12.56243686
8	12.57644466
9	12.54911201
10	12.56337620
11	12.52833715
12	12.54249278
13	12.56124878
14	12.54698566
15	12.54039528
16	12.52623989
17	12.58520827
18	12.59926274
19	12.56436201
20	12.57869627
21	12.59708317
22	12.58303036
23	12.57654957
24	12.56220822
25	12.55936488
26	12.54903646
27	12.54245449
28	12.52815181
29	12.54690964
30	12.56110667
31	12.52605280
32	12.54036048
Centroid	12.54201368

Table 5.6: DOE Results of bushes for discomfort @50 m/s in PSD2 road profile

In the analysis section of the design, the half normal plot is used to select the most significant design factors. As it can be seen in the figure below, the factors falling right of the others are more important. Figure 5.2 is representing the case where “discomfort” performance metric is investigated for the PSD2 and v = 50 m/s configuration.

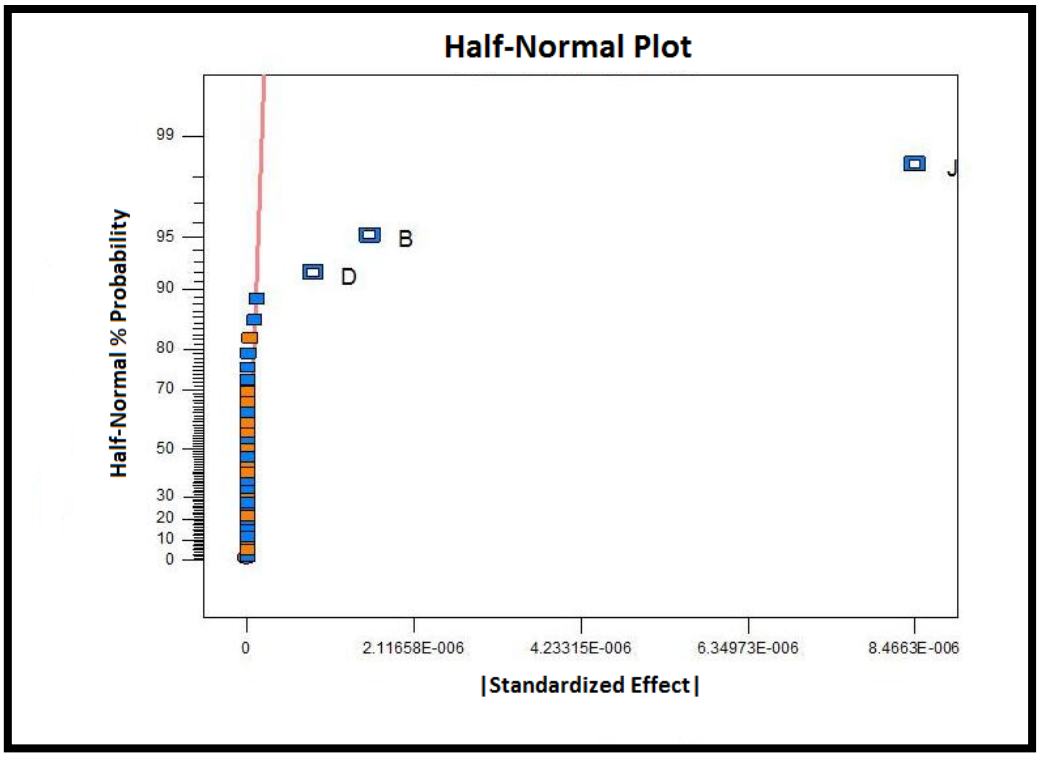

Figure 5.2: Half-Normal Plot of bushes for discomfort @ 50 m/s in PSD2 road profile

In this configuration, the most significant factors appeared to be as B (PBUSH 5/15 (Translational Z)), D (PBUSH 14/44 (Translational Z)) and J (PBUSH 46 (Translational Y)). Table 5.7 tabulates the ANOVA table showing the significance of the design factors and regression model for the selected configuration.

Source	Sum of Squares	df	Mean Square	F Value	p-Value (Prob > F)
Model	5.988e-10	3	1.996e-10	15335.45	< 0.0001
B-PBUSH 5/15	1.961e-11	1	1.961e-11	1506.73	< 0.0001
D-PBUSH 14/44	5.762e-12	1	5.762e-12	442.67	< 0.0001
J-PBUSH 46	5.734e-10	1	5.734e-10	44056.93	< 0.0001

Table 5.7: Analysis of Variance (ANOVA) Table of bushes for discomfort @ 50 m/s in PSD2 road profile

As it can be observed from the ANOVA Table, all the factors chosen in the half normal plot are significant according to p-values that are smaller than 0.0001 [26]. An additional step is required for the confirmation of the analysis results. Normal plot of residuals is used to verify the significant design parameters chosen for the analysis. This graph shows internally studentized residuals vs normal % probability. The experiments should fit to the line of expected results. This fit can be easily observed from Figure 5.3.

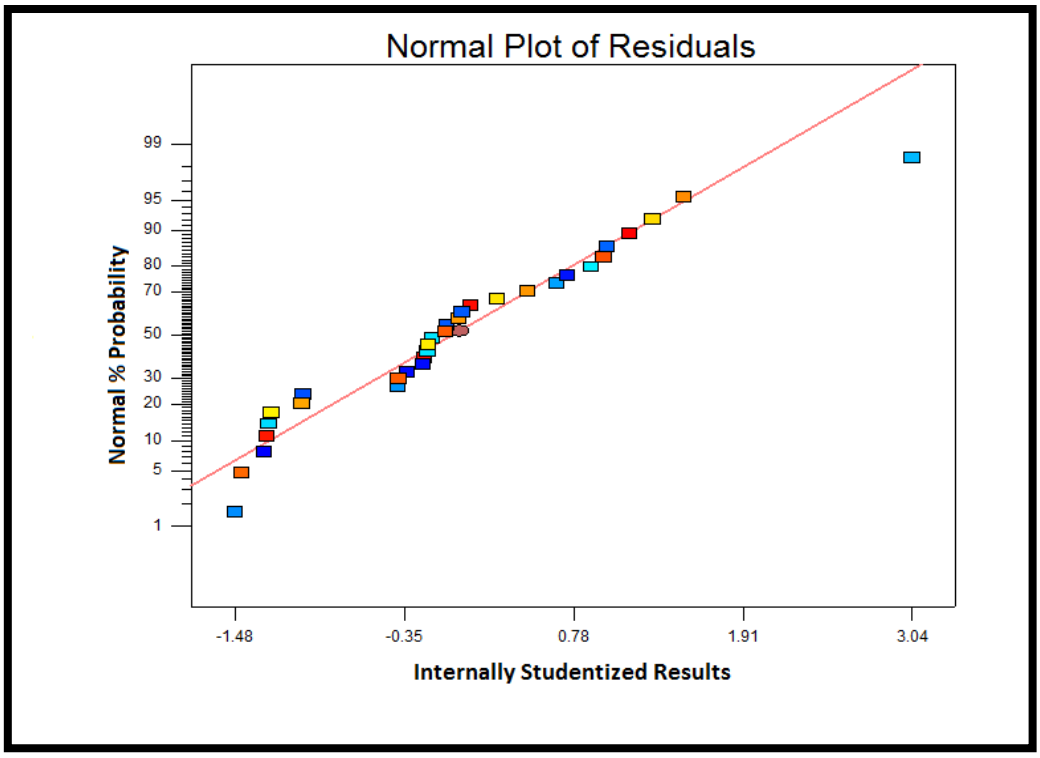

Figure 5.3: Internally studentized regression plot of bushes for working space @50 m/s in PSD2 profile

Corresponding regression equation is shown in (5.4):

$$
\begin{aligned}
&Discomfort = \\
&+12.66992 \\
&-5.23258E-006 * \boldsymbol{PBUSH(5-15)\ Translational\ Z} \\
&-1.81771E-004 * \boldsymbol{PBUSH(14-44)\ Translational\ Z} \\
&+1.74507E-005 * \boldsymbol{PBUSH46\ Translational\ Y}
\end{aligned}
\tag{5.4}
$$

Similar procedure is applied to every 33 experiments and the most significant factors are selected for each performance metric. According to the results of the experiments, the most significant bushes are B (PBUSH 5/15 (Translational Z)), C (PBUSH 7/21 (Translational Z)), D (PBUSH 14/44 (Translational Z)), E (PBUSH 14/44 (Rotational Y)) and J (PBUSH 46 (Translational Y)). The results are summarized in Table 5.8. The results of DOE show that the bushes do not change any of the performance metrics at significant levels (see Appendix 10.D). So for the rest of this study, the bush stiffness coefficients are not being considered as the design variables.

Performance Metric	v = 1 m/s	v = 10 m/s	v = 50 m/s
		PSD1	
Discomfort	J (R^2 = 0.9976)	J (R^2 = 0.9976)	J (R^2 = 0.9976)
Road Holding	J (R^2 = 0.9997)	J (R^2 = 0.9997)	J (R^2 = 0.9997)
Working Space	J (R^2 = 0.9932)	J (R^2 = 0.9932)	J (R^2 = 0.9932)
		PSD2	
Discomfort	D, J (R^2 = 0.9992)	B, D, J (R^2 = 0.9986)	B, D, J (R^2 = 0.9973)
Road Holding	J (R^2 = 0.9997)	B, D, E, J (R^2 = 0.9993)	B, C, D, E, J (R^2 = 0.9994)
Working Space	J (R^2 = 0.9995)	B, D, E, J (R^2 = 0.9997)	B, C, D, E, J (R^2 = 0.9998)

Table 5.8: Significant Factors for bush study at all speeds and in all road profiles

5.5.2 MAIN DESIGN FACTORS STUDY

Spring coefficients of the main components in the suspension system, the body and the tire masses, the damping coefficient of the damper element and the tire stiffness are selected as the design variables and a DOE analysis is performed with 8 factors using the discomfort, road holding and the working space as the performance metrics. The high and low levels for the design variables were determined by increasing and decreasing the baseline values of the factors by 20%, respectively. A full-factorial experiment would have required 2^8 (=256) runs, which is not very practical to simulate in a source-wise limited computer. Hence, a fractional factorial experimentation, which only required $2^{(8-3)}$ (= 32) runs for a resolution IV design, is prepared. An additional run was added to test the factors at their baseline values, which was also used to check for curvature in the DOE analysis (Appendix 10.B). In Table 5.9, the main design factors are listed with the corresponding low and high values used in the DOE analysis.

Factor Name	Factor Code	Nominal Value	Low Value	High Value
k_1	A	1500 N/mm	1200 N/mm	1800 N/mm
k_2	B	2666 N/mm	2132.8 N/mm	3199.2 N/mm
k_2`	C	0.33 N/mm	0.264 N/mm	0.396 N/mm
k_3	D	2055 N/mm	1644 N/mm	2466 N/mm
Damping	E	1 Ns/mm	0.8 Ns/mm	1.2 Ns/mm
m_1	F	0.579 ton	0.4632 ton	0.6948 ton
m_2	G	0.016 ton	0.0128 ton	0.0192 ton
Tire stiffness	H	180 N/mm	144 N/mm	216 N/mm

Table 5.9: List of the main design factors included in the DOE and their low & high values

A similar procedure is followed for the determination of the significant factors. The half normal plot and normal residuals are shown in Figures 5.4 and 5.5 respectively for discomfort in PSD2 and at *v*=10 m/s configuration together with the ANOVA chart in table 5.10.

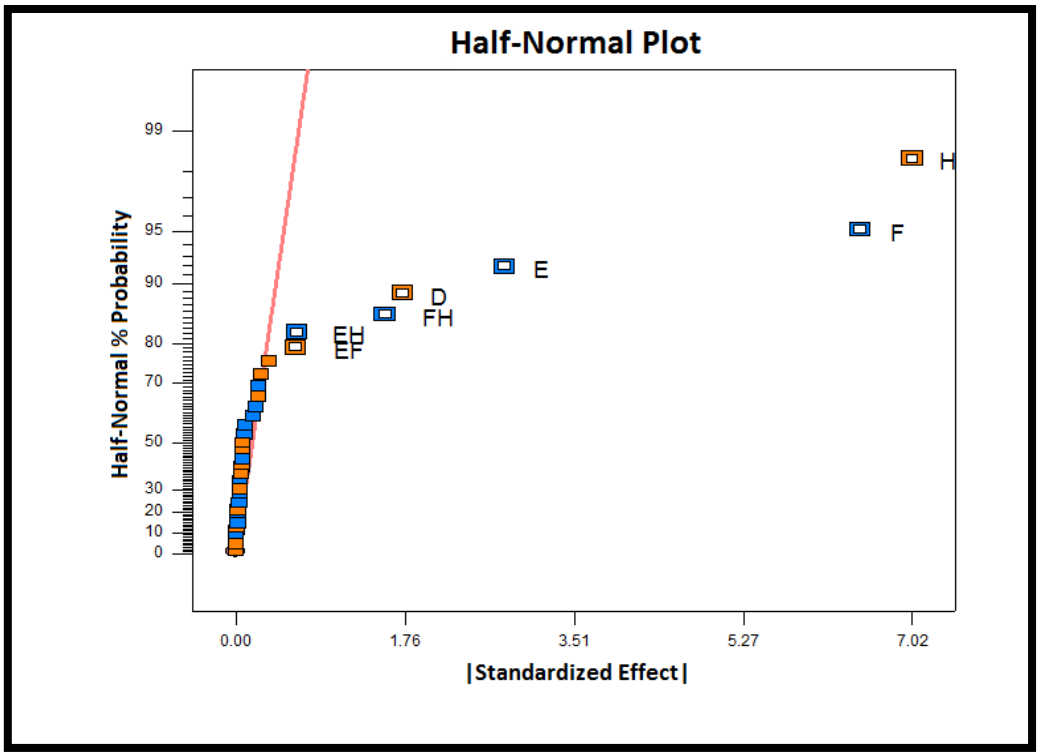

Figure 5.4: Half-Normal Plot of main design factors for discomfort @ 10 m/s in PSD2 road profile

As it can be observed from Figure 5.4, the significant factors are chosen as D (k_3), E (Damping), F (m_1), H (Tire stiffness) from main factors and the interactions EF (Damping x m_1), EH (Damping x Tire stiffness), and FH (m_1 x Tire stiffness). During this study, it is seen that these factors have significant effect on results of the experiments and the results are changing in significant percentages.

In the ANOVA table (Table 5.10), the significance of the model and the selected model terms are shown. As it can be observed from the ANOVA Table, all the factors chosen in the half normal plot are significant according to p-values that are smaller than 0.0001 [26].

Source	Sum of Squares	df	Mean Square	F Value	p-Value (Prob > F)
Model	842.56	7	120.37	854.83	< 0.0001
D (k_3)	24.03	1	24.03	170.63	< 0.0001
E (Damping)	62.21	1	62.21	441.85	< 0.0001
F (m_1)	336.25	1	336.25	2388.02	< 0.0001
H (Tire Stiffness)	394.58	1	394.58	2802.28	< 0.0001
EF	3.10	1	3.10	21.99	< 0.0001
EH	3.21	1	3.21	22.83	< 0.0001
FH	19.18	1	19.18	136.21	< 0.0001

Table 5.10: Analysis of Variance (ANOVA) Table of main design factors for discomfort @ 10 m/s in PSD2 road profile

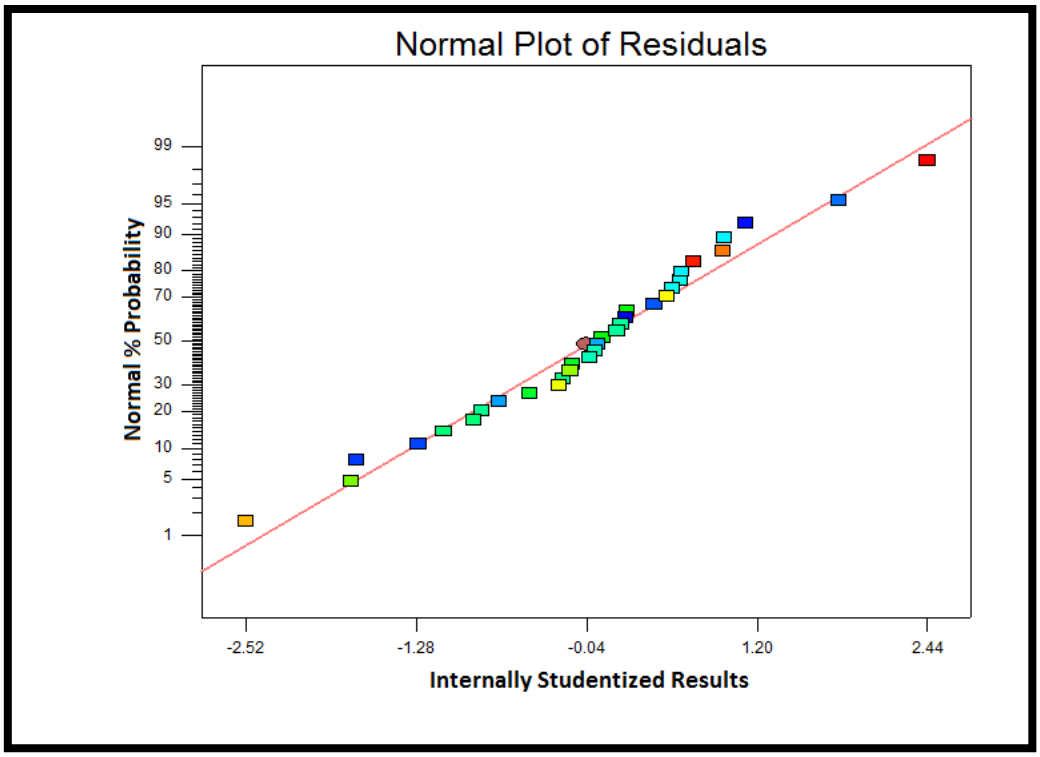

Figure 5.5: Internally studentized regression plot of main factors for working space @10 m/s in PSD2 profile

The corresponding regression equation is:

$$
\begin{aligned}
&Discomfort = \\
&+0.52493 \\
&+(2.10827e-003) * \boldsymbol{k_3} \\
&-6.82415 * \boldsymbol{Damping} \\
&-7.99580 * \boldsymbol{m_1} \\
&+0.24909 * \boldsymbol{Tire\ Stiffness} \\
&+13.43018 * \boldsymbol{Damping} * \boldsymbol{m_1} \\
&-0.044020 * \boldsymbol{Damping} * \boldsymbol{Tire\ Stiffness} \\
&-0.18571 * \boldsymbol{m_1} * \boldsymbol{Tire\ Stiffness}
\end{aligned}
\tag{5.5}
$$

In Table 5.11, the significant factors are listed.

Performance Metric	v = 1 m/s	v = 10 m/s	v = 50 m/s
		PSD1	
Discomfort	E,F,H,FH (R^2 = 0.8967)	E,F,H,FH (R^2 = 0.8967)	E,F,H,FH (R^2 = 0.9190)
Road Holding	F,H,FH (R^2 = 0.8153)	F,H,FH (R^2 = 0.8153)	F,H,FH (R^2 = 0.8153)
Working Space	D,E,F,G,H,FH (R^2= 0.9995)	D,E,F,G,H,FH (R^2 = 0.9995)	D,E,F,G,H,FH (R^2 = 0.9995)
		PSD2	
Discomfort	E,F,G,H,EF,EH,FH,GH (R^2= 0.9801)	D,E,F,H,EF,EH,FH (R^2 = 0.9960)	D,E,F,H,DH,EF,EH,FH (R^2 = 0.9930)
Road Holding	E,F,G,H,EF,EH,FH,GH (R^2 = 0.9746)	E,F,G,H,EF,EH,FH,GH (R^2= 0.9928)	E,F,G,H,EF,EH,FH,GH (R^2 = 0.9984)
Working Space	E,F,H,FH (R^2= 0.9301)	E,F,H,FH (R^2 = 0.9207)	D,E,F,G,H,FH,GH (R^2= 0.9737)

Table 5.11: Significant Factors for main factors study at all speeds and in all road profiles

The R^2 value of the regression model is important. For example for road holding; in PSD2 and at v=1 m/s configuration, R^2 value is 0.97. That means 97 % of the variability in the response variable can be explained with the regression model. All the R^2 values are listed for the significant design parameters' regression expressions in Table 5.11. If we summarize the results based on the performance metrics, the following observations can be made:

Discomfort (Standard deviation of the vertical body acceleration);

(1) The tire radial stiffness (H) significantly influences $\sigma_{\ddot{x}}$ (the influence is stronger at high speed considering the 2S-PSD),

(2) $\sigma_{\ddot{x}}$ does not depend significantly on the tire mass (G)

(3) $\sigma_{\ddot{x}}$ depends strongly on the vehicle body mass (F)

(4) The suspension damping (E) has influence on the standard deviation $\sigma_{\ddot{x}}$, especially in PSD2 type of road.

Road Holding (Standard deviation of the dynamic wheel load)

(1) σ_{Fz} depends on the tire stiffness (H)

(2) σ_{Fz} increases with speed but almost the opposite occurs at high speed considering the PSD2

(3) σ_{Fz} depends on the tire mass (G) for PSD2

(4) The suspension damping (E) has significant influence on σ_{Fz} for PSD2.

Working Space (Standard deviation of suspension stroke)

(1) σ_{x2-x1} is influenced by suspension springs (D) and tire stiffness (H) for both 1S and 2S PSD excitation

(2) Body mass (F) has a remarkable influence on σ_{x2-x1}

(3) σ_{x2-x1} is influenced by the suspension damping (E)

5.6 ADDITIONAL STUDIES REQUESTED BY TOFAŞ (DIFFERENT PARAMETERS)

Based on the feedback from TOFAS, we realized that in some cases it is not possible to change the vehicle mass and the tire characteristics to improve the vehicle performance. They also mentioned that the suspension damping may not be considered as a design parameter in real life studies. So the designer has to work on the rest of the design parameters if he/she wants to improve the performance of the system. In the following studies, we discarded some of these factors to see if they have dominated the results obtained in the previous studies. We eliminated the following factors from DOE study one by one and observed their effect only on the discomfort metric.

- Vehicle mass (F)
- Vehicle mass and damping element (F, E)
- Vehicle mass, damping element, tire mass and stiffness (F, E, G, H)

In the first step, the vehicle mass (m_1) is excluded from the original design and it is discovered that in this situation the most significant factors are *"tire stiffness, interaction between k_3 and damping, damping, interaction between k_3 and tire mass (m_2), m_2, interaction between k_3 and tire stiffness, k_3, k_2', and interaction between k_3 and tire stiffness".* These results were obtained for all of the speeds in this design.

In the second step, the damping is also omitted from the original design in addition to car mass. In this situation the factors significant are turned out to be *"tire stiffness, interaction*

between k_1 and k_3, tire mass, interaction between k_1 and tire mass, k_2' and interaction between k_2 and k_3".

As a last setup, the tire mass and tire stiffness was also disregarded and only the springs remained in the DOE analysis. It was observed that the significant factors are *"k_2' and k_3"* for all of the speeds.

All of these results are summarized in Table 5.12.

Discomfort	w/out vehicle mass	w/out vehicle mass and damping	w/out vehicle mass, damping, tire mass and stiffness
v= 1 m/s	H,DE,E,DG,G,DH,D,C,DH	H,AD,G,AG,C,BD	C,D
v= 10 m/s	H,DE,E,DG,G,DH,D,C,DH	H,AD,G,AG,C,BD	C,D
v= 50 m/s	H,DE,E,DG,G,DH,D,C,DH	H,AD,G,AG,C,BD	C,D

Table 5.12: Significant factors for discomfort, for three different parameterizations

From this study we can see how body mass has dominated the whole system when altered ±20%. When this parameter is removed from the list, many different factors came out to be important which were unseen in the previous studies.

5.7 MULTI AND SINGLE-OBJECTIVE OPTIMIZATION

The regression models obtained from Section 5.5 are used in the optimization study. Numerical optimization tool of the Design-Expert software is used for minimizing the three performance metrics simultaneously. Equal weight was assigned to every metric and optimization was employed to find the optimal set of the main design factors. The altered parameters for multi-objective optimization are tabulated in Table 5.13. The results are shown in Table 5.14 for the discomfort, road holding and working space; together with the percentage improvement for the relevant metric. As it can be observed from the table, some of the optimum values of the discomfort were worse than the nominal values which was represented by a negative percentage improvement.

Numerical optimization was also performed for each performance metric individually and the results are tabulated in Tables 5.15, 5.16 and 5.17. When the single metric optimization is compared with the multiobjective optimization, it can be easily observed that single metric optimization results are much better than the multi objective optimization results. We believe that the performance metrics are conflicting, i.e. improving one of them implies at least

worsing another one. That explains the negative percentage improvements for the discomfort in the multiobjective optimization.

Note that Stiffnesses are in "N/mm", Damping is in "N.s/m" Discomfort in "mm/s^2", Road Holding in "N", Working Space in "mm", "Masses are in kg".

Case	k_1	k_2	k_2'	k_3	Damping	m_1	m_2	Tire Stiffness
PSD1-v1	1500	2666	0.33	1644	1.2	0.4632	0.0128	144
PSD1-v10	1500	2666	0.33	1644	1.2	0.4632	0.0128	144
PSD1-v50	1500	2666	0.33	1644	1.2	0.4632	0.0128	144
PSD2-v1	1500	2666	0.33	2055	1.2	0.4632	0.0128	144
PSD2-v10	1500	2666	0.33	1644	1.2	0.4754	0.0137	144
PSD2-v50	1500	2666	0.33	1646	1.2	0.47	0.0128	144

Table 5.13: New parameters according to **Multi**-Objective Optimization

Case	Nominal Discomfort	Optimized Discomfort	Improvement (Percentage)	Nominal Road Holding	Optimized Road Holding	Improvement (Percentage)	Nominal Working Space	Optimized Working Space	Improvement (Percentage)
PSD1-v1	22.025	22.184	-0.724	3.666	3.144	14.250	0.0367	0.0294	19.924
PSD1-v10	69.6491	70.153	-0.724	11.595	9.943	14.250	0.1162	0.0931	19.924
PSD1-v50	155.740	160.233	-2.885	25.927	22.232	14.250	0.2599	0.208	19.924
PSD2-v1	12.476	11.228	9.995	2.516	1.898	24.559	0.0037	0.0031	16.817
PSD2-v10	17.957	15.211	15.290	2.156	1.693	21.474	0.0018	0.0014	21.421
PSD2-v50	12.526	10.340	17.451	1.621	1.306	19.451	0.0010	0.0007	25.341

Table 5.14: Nominal and **Multi**-Objective Optimization Results of the objective functions

Case	k_1	k_2	k_2'	k_3	Damping	m_1	m_2	Tire Stiffness	Nominal Values	Optimal Values	Improvement (%)
PSD1-v1	1500	2666	0.33	2055	1.2	0.6948	0.016	144	22.025	20.206	8.256
PSD1-v10	1500	2666	0.33	2055	1.195	0.6929	0.016	144.25	69.649	64.005	8.102
PSD1-v50	1500	2666	0.33	2055	1.2	0.6948	0.016	144	155.740	146.248	6.094
PSD2-v1	1500	2666	0.33	2055	1.2	0.6948	0.0128	144	12.476	10.087	19.148
PSD2-v10	1500	2666	0.33	1660	1.198	0.6941	0.016	144.22	17.957	11.194	37.663
PSD2-v50	1500	2666	0.33	1644	1.2	0.6948	0.016	144	12.526	7.245	42.160

Table 5.15: Nominal and **Single**-Objective Optimization Results of "discomfort"

Case	k_1	k_2	k_2'	k_3	Damping	m_1	m_2	Tire Stiffness	Nominal Values	Optimal Values	Improvement (%)
PSD1-v1	1500	2666	0.33	2055	1	0.4632	0.016	144	3.666	3.144	14.250
PSD1-v10	1500	2666	0.33	2055	1	0.4632	0.016	144	11.595	9.943	14.250
PSD1-v50	1500	2666	0.33	2055	1	0.4632	0.016	144	25.927	22.232	14.250
PSD2-v1	1500	2666	0.33	2055	1.2	0.4632	0.0128	144	2.516	1.898	24.559
PSD2-v10	1500	2666	0.33	2055	1.2	0.4632	0.0128	144	2.156	1.686	21.819
PSD2-v50	1500	2666	0.33	2055	1.2	0.4632	0.0128	144	1.621	1.305	19.497

Table 5.16: Nominal and **Single**-Objective Optimization Results of "road holding"

Case	k_1	k_2	k_2'	k_3	Damping	m_1	m_2	Tire Stiffness	Nominal Values	Optimal Values	Improvement (%)
PSD1-v1	1500	2666	0.33	1644	1.2	0.4632	0.0128	216	0.0367	0.0286	22.020
PSD1-v10	1500	2666	0.33	1644	1.2	0.4632	0.0128	216	0.1162	0.0906	22.020
PSD1-v50	1500	2666	0.33	1644	1.2	0.4632	0.0128	216	0.2599	0.202	22.020
PSD2-v1	1500	2666	0.33	2055	1.2	0.4632	0.016	144	0.0037	0.0031	16.817
PSD2-v10	1500	2666	0.33	2055	1.2	0.4632	0.016	144	0.0018	0.0014	23.791
PSD2-v50	1500	2666	0.33	2466	1.2	0.4632	0.0128	144	0.0010	0.00068	30.887

Table 5.17: Nominal and **Single**-Objective Optimization Results of "working space"

5.8 A STOCHASTIC APPROACH TO OPTIMIZATION

Many mechanical engineering design problems are solved by employing deterministic optimization techniques. However, in fact, actual systems are often subject to variations, uncertainties and unexpected deviations that arise from a variety of sources like manufacturing processes, external disturbances, operating conditions. For this reason almost every engineering design should be performed within a stochastic framework. A stochastic system is described by a mathematical model in which there are some random quantities subject to uncertainty. In this section we are going to describe the stochastic model that we have implemented in our studies.

In the previous optimization studies, we have used the Design-Expert software to find the optimum configurations for the design parameters. However, when the stochastic approach is implemented, this requires further calculations while obtaining the objective functions. For that reason, we decided to perform our optimization studies in MATLAB to be able to integrate those formulations. As a first step, we validated our MATLAB optimization code such that the same results can be obtained before implementing the stochastic approach. Table 5.18 and 5.19 tabulate sample optimization results for PSD1-v1 and PSD2-v10.

PSD1 @ v = 1m/s	Design Expert Results	Hand-Written Code Results
Discomfort	20.2066	20.2069
Damping	1.2	1.2
m_1	0.69	0.6948
Tire Stiffness	144	144

Table 5.18: Discomfort results comparison between the software and the hand-written code (PSD1 @ $v = 1m/s$)

PSD1 @ v = 1m/s	Design Expert Results	Hand-Written Code Results
Discomfort	11.1255	11.1258
k_3	1644	1644
Damping	1.2	1.2
m_1	0.69	0.6948
Tire Stiffness	144	144

Table 5.19: Discomfort results comparison between the software and the hand-written code

$$(\text{PSD2 @ v} = 10\text{m/s})$$

When the results are compared, it can be observed that they are almost equal to each other. Then the stochastic formulations are integrated to the MATLAB optimization code to study the variations and uncertainties that arise from a variety of sources, i.e. manufacturing processes, external disturbances, operating conditions.

The stochastic system is expressed as a mathematical model which includes some random quantities that are subject to uncertainty. These random quantities are not under the designer's control and they are expressed as the "c column" in the model. On the other hand, the design variables are the quantities whose expected values (i.e mean) can comfortably be defined by the designer and these quantities are expressed within the "z column" in the mathematical stochastic model [13]. For our case parameters that take place in the response surface function are the design variables (z) and the remaining ones are the random variables (c).

The mean of the stochastic performance metric function and its variance can be estimated as shown in the following equations (5.6) and (5.7):

$$f_i = f_i(\mu_z, \mu_c) \tag{5.6}$$

$$\sigma_{fi}^2 = \sum_{i=1}^{n} \left(\frac{\partial_{fi}}{\partial_{zi}}\right)^2 \sigma_{zi}^2 + \sum_{i=1}^{n} \left(\frac{\partial_{fi}}{\partial_{ci}}\right)^2 \sigma_{ci}^2 \tag{5.7}$$

First term of the right hand side of equation 5.7 is the ***z*** column and it includes the design parameters. Second term of the right hand side is the ***c*** column which involves the random quantities in the design.

Since the ***z*** column parameters are all included in the response surface function, processing those variables mathematically (i.e. taking their partial derivatives) is straightforward. However, column ***c*** is not included in the response surface function so the related partial derivatives should be taken in some other way. To accomplish this task, we used the formal definition of derivative and considered an infinitesimally small variation around the mean

value of the parameters. The formula applied to find the sensitivity of the random variables for discomfort performance metric function is shown in expression (5.8):

$$\frac{\partial_f}{\partial_c} = \frac{\sigma_{\ddot{x}}(new) - \sigma_{\ddot{x}}(nominal)}{c(new) - c(nominal)} \tag{5.8}$$

With an infinitesimal amount of change in the parameter, what is meant here is actually 1% difference from the nominal parameter values. So, $c(new)$ is actually 1.01 times $c(nominal)$.

On the other hand, variance terms of both "***z***" and "***c***" are calculated by squaring the standard deviations of the parameters, which is roughly calculated by multiplying the expected parameter values (nominal values) with 2 percent (as provided by TOFAŞ feedback).

When these stochastic variations are included in the formulations, the equations obtained from the response surfaces can be modified and the mean of the performance metric can be expressed as:

$$\overline{f_i} = f_i + \alpha_i \sigma_{f_i} \tag{5.9}$$

In this formula, left side is representing the new equation we are looking for. On the right side, first part is the equation obtained from response surfaces and the second part is the additional part added with the stochastic approach. And the α value included in the formula is obtained as below

$$\alpha_i = \phi^{-1}(\beta_i) \tag{5.10}$$

Where ϕ^{-1} is the inverse of the standard normal distribution and (1-β_i) is the failure probability for different cases. At that point β is taken as 0.9 for all of the cases for the calculations.

With the stochastic approach the results of the optimum points change slightly (see Tables 5.18 and 5.19 for optimum configurations). And as a last step, to see the effect of z parameters and c parameters, the discomfort values are calculated with and without the z and c parameters to see their effect. The results are tabulated in Tables 5.20 and 5.21.

PSD1 @ v = 1m/s	Deterministic Approach	Stochastic Approach	Stoc. Approach w/o $\boldsymbol{c}$ column
Discomfort	20.2069	20.4089	20.6397
Damping	1.2	1.2	1.2
m_1	0.6948	0.6948	0.6948
Tire Stiffness	144	144	144

Table 5.20: Comparison of stochastic optimization with deterministic results (PSD1 @v=1m/s)

PSD2 @ v = 10m/s	Deterministic Approach	Stochastic Approach	Stoc. Approach w/o $\boldsymbol{c}$ column
Discomfort	11.1258	12.0160	11.7316
k_3	1644	1644	1644
Damping	1.2	1.2	1.2
m_1	0.6948	0.6948	0.6948
Tire Stiffness	144	144	144

Table 5.21: Comparison of stochastic optimization with deterministic results (PSD2 @v=10m/s)

When the stochastic optimization is finished, we see that the optimum results changed slightly. However the optimum configuration remained unchanged when compared to the deterministic results. In addition to that, it is also obvious that the effect of $\boldsymbol{c}$ parameters (random effects) on this approach was almost negligible compared to the effect of $\boldsymbol{z}$ parameters (design parameters). This result was expected because of the fact that the $\boldsymbol{z}$ parameters are the ones which are included in the response surfaces. This means the sensitivity of the discomfort values is more dependent the response surface parameters.

CHAPTER 6

ANALYSIS AND OPTIMIZATION OF THE FRONT SUSPENSION SYSTEM

ACCORDING TO MATERIAL PROPERTIES AND COMPONENT THICKNESSES

The aim of all the studies done so far was to decrease the magnitudes of discomfort, working space and road holding to give the passengers a more comfortable ride experience. To achieve this, different methods have been presented. In this section, a more realistic approach has been followed to optimize the design parameters. Two major components of the front suspension system, the anti-roll bar (Figure 6.1) and wishbones (Figure 6.2), are taken into consideration in this study. The thicknesses of the components are altered while trying three different materials to find an optimum set of solutions. Instead of the stick finite element model, high fidelity finite element model is used in this study.

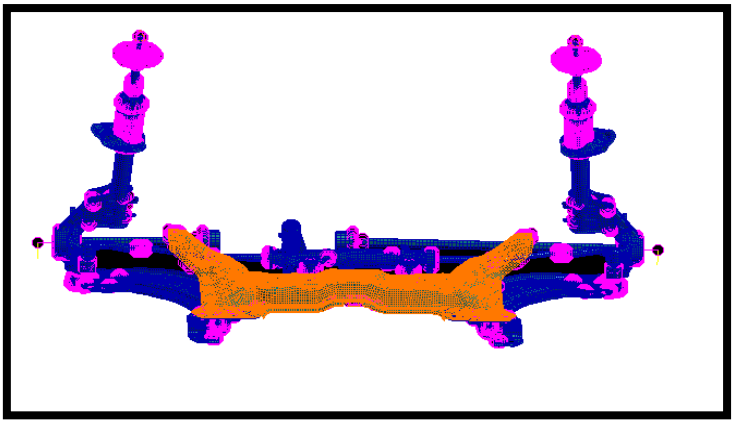

Figure 6.1: Anti-Roll Bar (ARB) component

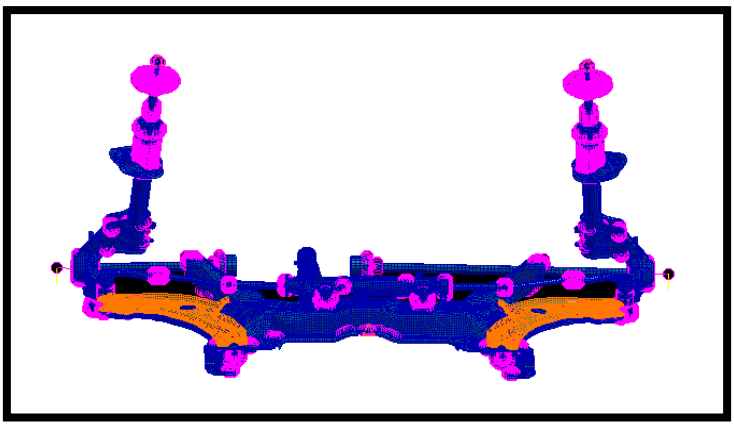

Figure 6.2: Wishbone components

6.1 OBJECTIVE FUNCTIONS AND DESIGN VARIABLES

The optimization objectives in this study are discomfort, working space and road holding. The two design variables are the thickness of the ARB (t_1) and the thickness of the wishbones (t_2). The third one is related to the material property. Since a material has more than one parameter to select as a single design variable, we created a property ratio within a simplistic approach (ratio of elastic modulus to density) for each material and assigned that one as the third parameter (u) [28, 29].

$$u = \frac{E}{\rho} \tag{6.1}$$

In this study three materials are taken into account for wishbone and ARB, i.e. magnesium alloy (Mg), steel, aluminum alloy (Al). Mechanical properties of these materials are listed in Table 6.1.

	E (GPa)	Poisson's Ratio	**ρ**(kg/m^3)	u
Magnesium Alloy	45e9	0.35	1.8e3	2.5e7
Aluminum Alloy	70e9	0.33	2.7e3	2.6e7
Steel	210e9	0.30	7.8e3	2.7e7

Table 6.1: Mechanical properties of component materials

6.2 EXPERIMENTAL DESIGN AND RESPONSE SURFACE MODELING

To find a functional relationship between the design variables and the objective functions, RSM and DOE methodology is employed. Corresponding surface equations are obtained via a regression algorithm implemented into MATLAB. The underlying equation is a second order, multi-variable polynomial and is in the form of Equation 5.3.

The design variables used in DOE study are listed in Table 6.2 at three levels (-20%, Center, +20%).

	t_1 (mm)	t_2 (mm)	u
Level 1	1.6	2.0	2.5e7
Level 2	2.0	2.5	2.6e7
Level 3	2.4	3.0	2.7e7

Table 6.2: Design variables at all three levels

In RSM, these quantities are transformed into coded variables that are dimensionless. The transformations are done according to the following equations:

$$x_1 = \frac{t_1 - 2.0}{0.4} \qquad x_2 = \frac{t_2 - 2.5}{0.5} \qquad x_3 = \frac{t_3 - 2.6x10^7}{10^7} \tag{6.2}$$

After doing the transformations, a new table is formed to see the three levels of design clearly:

	x_1	x_2	x_3
Level 1	-1	-1	-1
Level 2	0	0	0
Level 3	1	1	1

Table 6.3: Transformed design variables at three levels

A three level full factorial design would require 3^n experiments to conduct where n is the number of design variables. As the number of experiments increases, time required for simulations also increases significantly especially for complicated models. So a central composite design approach (CCD) is employed to decrease the number of designed experiments.

According to the CCD design, the experimental design for our case includes 2^n (n=3) full factorial points for two level experiment (-1, +1), 2n star points which are located on axes and m_o=1 center points.

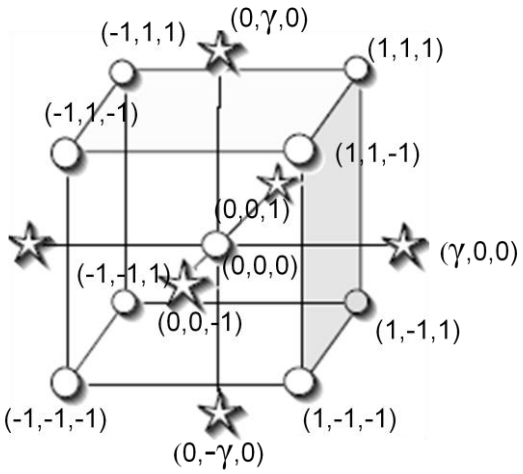

Figure 6.3: Trial points of central composite design

In Figure 6.3 γ is used to determine the position of the star points and it is formulated by:

$$\gamma^2 = \frac{\sqrt{N2^n} - 2^n}{2} \qquad where\ N = 2^n + 2n + m_o \tag{6.3}$$

So; the orthogonal design order and corresponding values are shown in table 6.4 and 6.5:

	x_1	x_2	x_3
1	-1	-1	-1
2	-1	-1	1
3	-1	1	-1
4	-1	1	1
5	1	-1	-1
6	1	-1	1
7	1	1	-1
8	1	1	1
9	0	0	0
10	-1.215	0	0
11	1.215	0	0
12	0	-1.215	0
13	0	1.215	0
14	0	0	-1
15	0	0	1

Table 6.4: Orthogonal design order for DOE

	x_1	x_2	x_3
1	1.6	2.0	Mg
2	1.6	2.0	Steel
3	1.6	3.0	Mg
4	1.6	3.0	Steel
5	2.4	2.0	Mg
6	2.4	2.0	Steel
7	2.4	3.0	Mg
8	2.4	3.0	Steel
9	2.0	2.5	Al
10	1.514	2.5	Al
11	2.486	2.5	Al
12	2.0	1.8925	Al
13	2.0	3.1075	Al
14	2.0	2.5	Mg
15	2.0	2.5	Steel

Table 6.5: Corresponding values of the orthogonal design

According to Table 6.5; discomfort, road holding and working space objective functions are evaluated in PSD1 road profile at 1 and 10 m/s. The results according to these configurations can be seen in Table 6.7.

Run	**PSD1**					
		v =1 m/s			*v =10 m/s*	
	Discomfort	*Road Holding*	*Working Space*	*Discomfort*	*Road Holding*	*Working Space*
1	291,33	35,90	0,15	921,27	113,53	0,48
2	32,64	8,00	0,30	103,22	25,30	0,95
3	98,21	11,60	0,16	310,57	36,69	0,52
4	21,53	6,46	0,22	68,07	20,43	0,69
5	151,73	20,59	0,27	479,82	65,10	0,84
6	22,35	6,21	0,34	70,67	19,63	1,07
7	145,75	29,97	0,84	460,91	94,77	2,66
8	40,06	6,28	0,16	126,69	19,86	0,50
9	72,19	16,68	0,50	228,28	52,75	1,59
10	383,14	64,08	1,06	1211,60	202,64	3,35
11	45,05	11,37	0,42	142,45	35,97	1,33
12	363,12	63,56	1,65	1148,30	201,00	5,22
13	47,32	11,64	0,35	149,64	36,82	1,10
14	132,70	16,33	0,25	419,64	51,63	0,80
15	20,34	6,26	0,32	64,31	19,80	1,02

Table 6.7: DOE Results of the configurations listed in table 6.5.

The corresponding response surface equations are built after this step since we have all the data point required to create regression equations. These equations are listed below

x_1: Thickness of anti-roll bar

x_2: Thickness of wishbone

x_3: Material type

$$Discomfort\ (1\,m/s) = 147.51 - 68.28 * x_3 - 98.8 * {x_3}^2 - 52.6 * x_2 + 25.71 * x_2 * x_3 + 26.3 * {x_2}^2 - 45.16 * x_1 + 12.5 * x_1 * x_3 + 28 * x_1 * x_2 + 32.34 * {x_1}^2 \quad (6.4)$$

$$Discomfort\ (10\,m/s) = 466.48 - 215.92 * x_3 - 312.4 * {x_3}^2 - 166.3 * x_2 + 81.31 * x_2 * x_3 + 83.28 * {x_2}^2 - 142.8 * x_1 + 39.64 * x_1 * x_3 + 85.37 * x_1 * x_2 + 102.28 * {x_1}^2 \quad (6.5)$$

$$Road\ Holding\ (1\,m/s) = 27.86 - 8.11 * x_3 - 20.7 * {x_3}^2 - 7.25 * x_2 + 1.68 * x_2 * x_3 + 4.7 * {x_2}^2 - 5.74 * x_1 - 0.63 * x_1 * x_3 + 4.41 * x_1 * x_2 + 4.78 * {x_1}^2 \quad (6.6)$$

$$Road\ Holding\ (10\,m/s) = 88.11 - 25.67 * x_3 - 65.45 * {x_3}^2 - 22.94 * x_2 + 5.31 * x_2 * x_3 + 14.87 * {x_2}^2 - 18.17 * x_1 - 1.98 * x_1 * x_3 + 13.95 * x_1 * x_2 + 15.14 * {x_1}^2 \quad (6.7)$$

$$Working\ Space\ (1\,m/s) = 0.72 - 0.03 * x_3 - 0.52 * {x_3}^2 - 0.11 * x_2 - 0.105 * x_2 * x_3 + 0.14 * {x_2}^2 - 0.0011 * x_1 - 0.1 * x_1 * x_3 + 0.058 * x_1 * x_2 + 0.028 * {x_1}^2 \quad (6.8)$$

$$Working\ Space\ (10\,m/s) = 2.29 - 0.1 * x_3 - 1.64 * {x_3}^2 - 0.36 * x_2 - 0.33 * x_2 * x_3 + 0.46 * {x_2}^2 - 0.0034 * x_1 - 0.32 * x_1 * x_3 + 0.18 * x_1 * x_2 + 0.088 * {x_1}^2 \quad (6.9)$$

After these equations are obtained, we need to check if these regression equations present the system accurately or not. To do so a variance analysis and an F-Test is performed. $F = S_r/S_e$ is compared with $F(f_r,f_e,\alpha)$ from F distribution tables. When $F > F(f_r,f_e,\alpha)$ we can say that our model is valuable for (1- α) x 100 percent of the data [26,29]. The required information to perform the F-Test is shown in Table 6.8. As an example case, F(Discomfort @1m/s) = 1.74. We can obtain the inequality when α = 0.28. So F>F(9,5,0.28) which tells us our regression equation is valuable for 72 percent of the data. The other equations have F ratios varying between 0.65 and 0.75. These percentages can be increased by increasing the number of experimental data points but this would cost a lot of time which is against the basic idea of design of experiments.

		Degree of Freedom	Variance	Statistical Quantity	F(α)
Fitting Constant	$S_R = \sum_{j=1}^{k} (\hat{y}_j - \bar{y})^2$	f_R=n	V_R=S_R/f_R	F=S_R/S_e	F(n,k-n-1, α)
Residual	$S_e = \sum_{j=1}^{k} (y_j - \hat{y}_j)^2$	f_e=k-n-1	V_e=S_e/f_e		
Sum	$S_T = \sum_{j=1}^{k} (y_j - \bar{y})^2$	f_T=k-1			

Table 6.8: Variance analysis table of RSM

Before moving to the analysis and optimization section; discomfort, road holding and working space expressions are plotted on a surface to determine the relationship between the performance metrics. The case for x_3=-1 (Mg Alloy) is shown in Figure 6.4. Looking at Figure 6.4 and observing the contour plots in Appendix F following conclusions can be reached.

When the figures are examined carefully, we see that as working space gets worse discomfort slightly improves. However the opposite is valid for working space-road holding relationship. Slightly improving road holding performance affects the working space characteristics in a positive manner. Discomfort and road holding on the other hand considerably act in the same way.

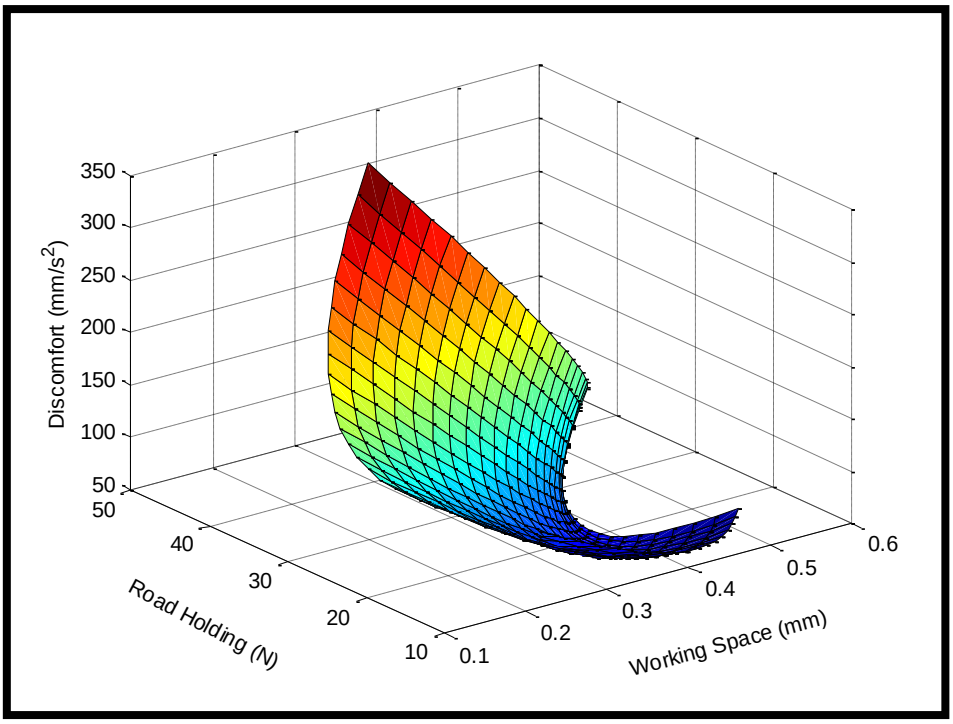

Figure 6.4: Discomfort, road holding and working space plotted together

6.3 ANALYSIS OF THE OBJECTIVE FUNCTIONS WITH DIFFERENT MATERIALS

As the regression polynomials are found out, the RSM of each objective function is created in MATLAB. A total of 18 combinations (2 speeds, 3 objective functions and 3 different materials) are analyzed and plotted in this section. Among these 18, a few samples will be investigated and explained in detail. While investigating the figures, the material parameter is always kept constant since unlike thickness, we cannot pick a material between the present ones. This also reduces the surfaces from 4D to 3D making them visually obtainable.

In Figure 6.5; discomfort is examined when the material property (u) is kept constant at $x_3 = 0$ (Al alloy) Contour lines of this analysis are shown in Figure 6.6.

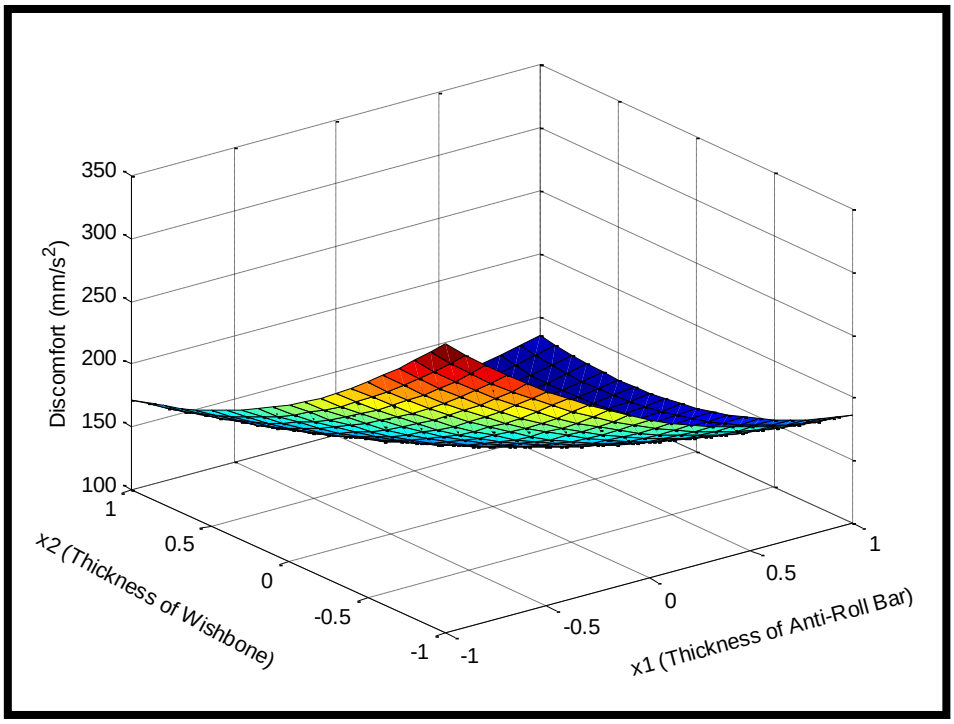

Figure 6.5: The response surface of discomfort @ v=1m/s and $x_3 = 0$

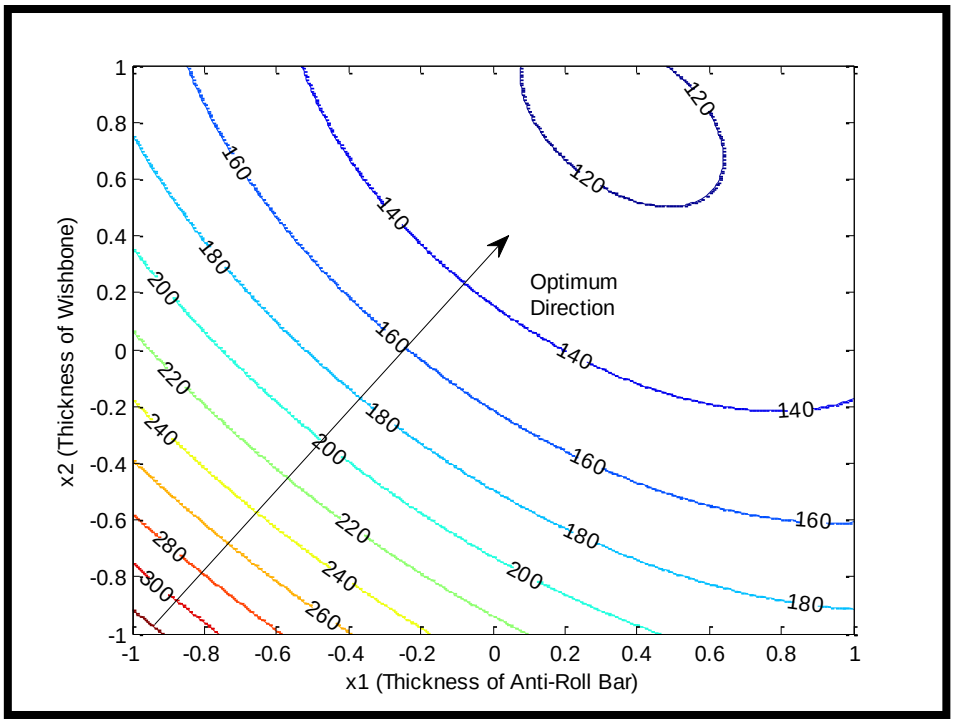

Figure 6.6: The contour lines of discomfort @ v=1m/s and x_3=0 (axes are transformed)

As the thickness of the anti-roll bar increases the discomfort values decreases. The thinner the wishbones are, less discomfort the passengers feel as well. We can conclude that ARB and wish bone thicknesses work in the same way to decrease the discomfort. However when the behavior of the two parameters in the contour plot are investigated, we can see that the wishbone thickness plays a greater role than the thickness of ARB to alter the discomfort values. The optimum direction to follow to efficiently decrease the discomfort is obvious from the contour lines.

Figures 6.7 and 6.8 show the response and contour lines of road holding respectively; at v=1 m/s and material property (u) fixed at x3 = 1 (Steel)

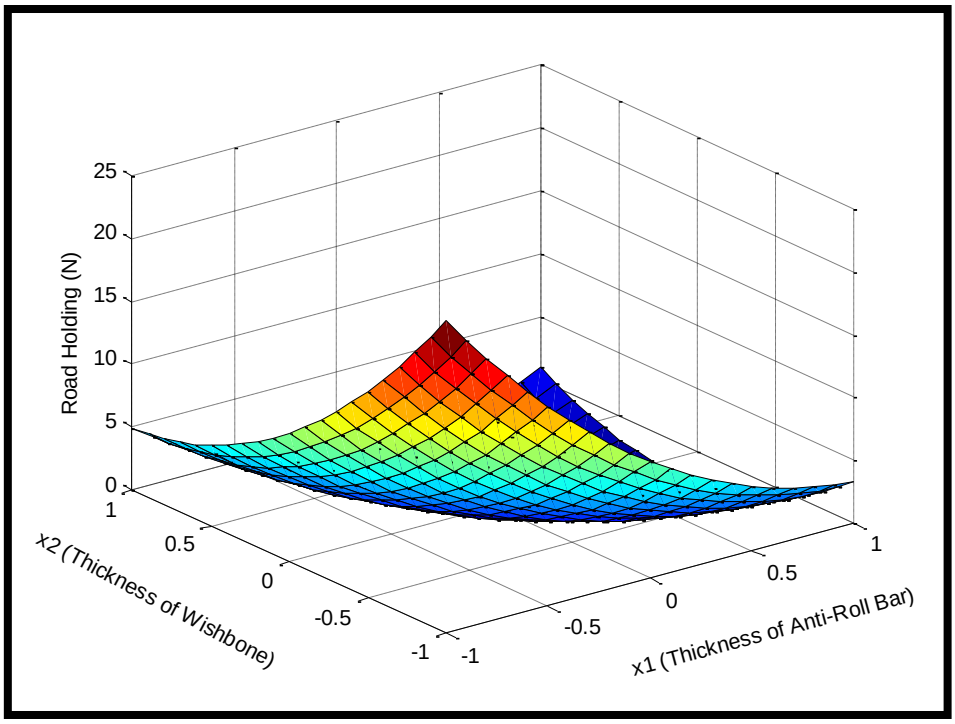

Figure 6.7: The response surface of road holding @ v=1m/s and $x_3 = 1$

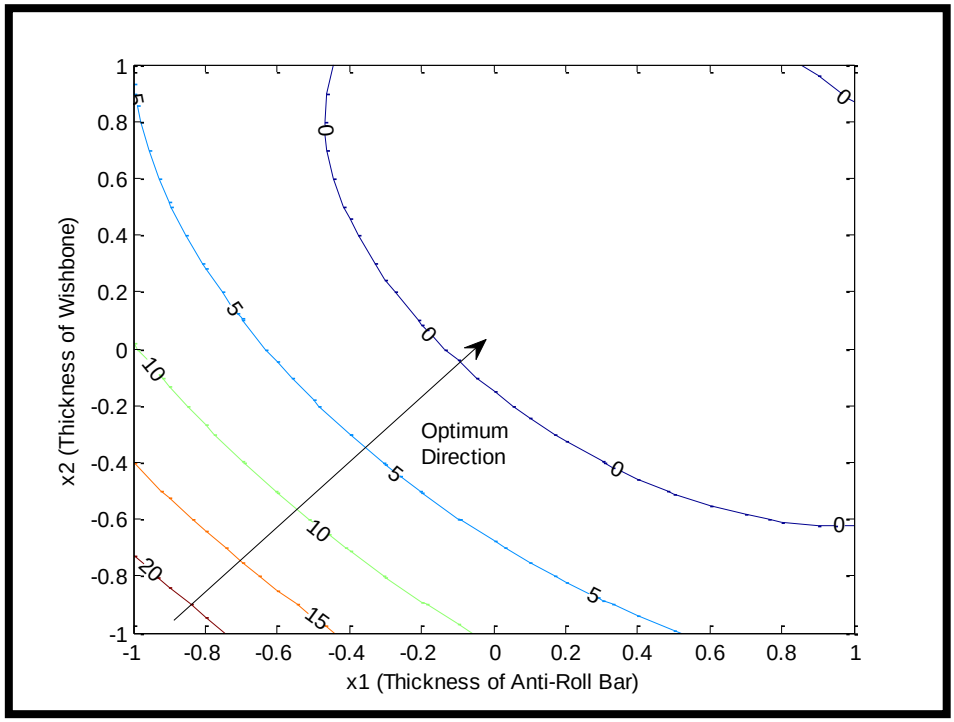

Figure 6.8: The contour lines of road holding @ v=1m/s and $x_3 = 1$ (axes are transformed)

From these plots we obviously see that road holding performance improves with increasing the thickness of the anti-roll bar. Same thing applies to wishbone thickness as well but obviously, same amount of thickness increment is more effective when it is applied to the wishbones since the optimum direction arrow is biased to wishbone axis (x_2).

In Figures 6.9, 6.10, 6.11 and 6.12 response and contour lines of working space objective function are built. The Figures 6.9, 6.10 and 6.11 6.12 in pairs reflect the plots of the cases with two different material properties. (x_3 = -1, Mg Alloy and x_3 = 0, Al Alloy) This is because on the contrary to the other two objective functions, for working space, a major difference is observed between two material choices.

In the case of aluminum (x_3 = 0) it is clear that the effect of anti-roll bar thickness is nearly negligible in our range of interest. The optimum direction lies on a nearly vertical line which makes the only significant parameter wishbone thickness when the material is aluminum alloy.

When the material is picked as Mg alloy, the behavior totally changes. When the contour lines are investigated in Figure 6.12, one can see the drastic effect of anti roll bar thickness on working space. As anti-roll bar thickness decreases, working space performance increases significantly. Wishbone thickness has very little effect on this objective function in the given range.

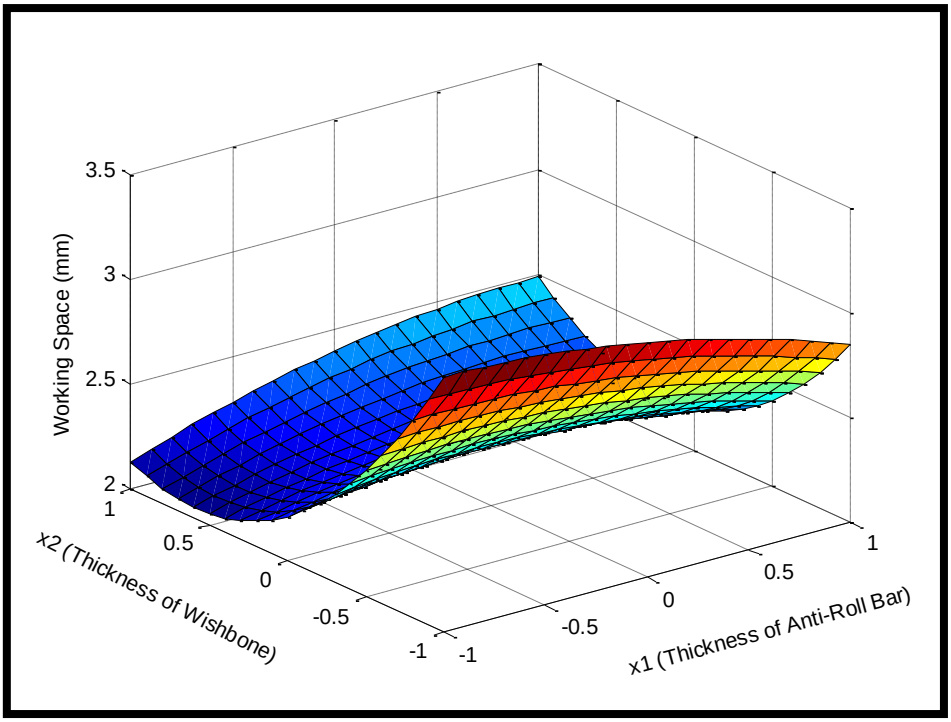

Figure 6.9: The response surface of working space @ v=10m/s and x_3 = 0

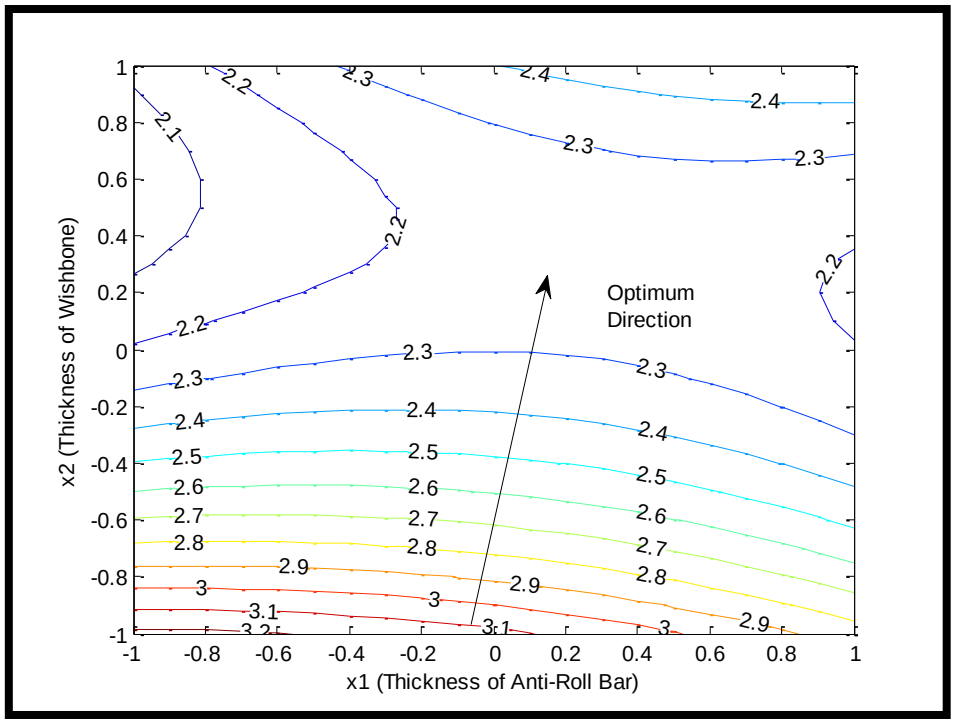

Figure 6.10: The contour lines of working space @ v=10m/s and $x_3 = 0$ (axes are transformed)

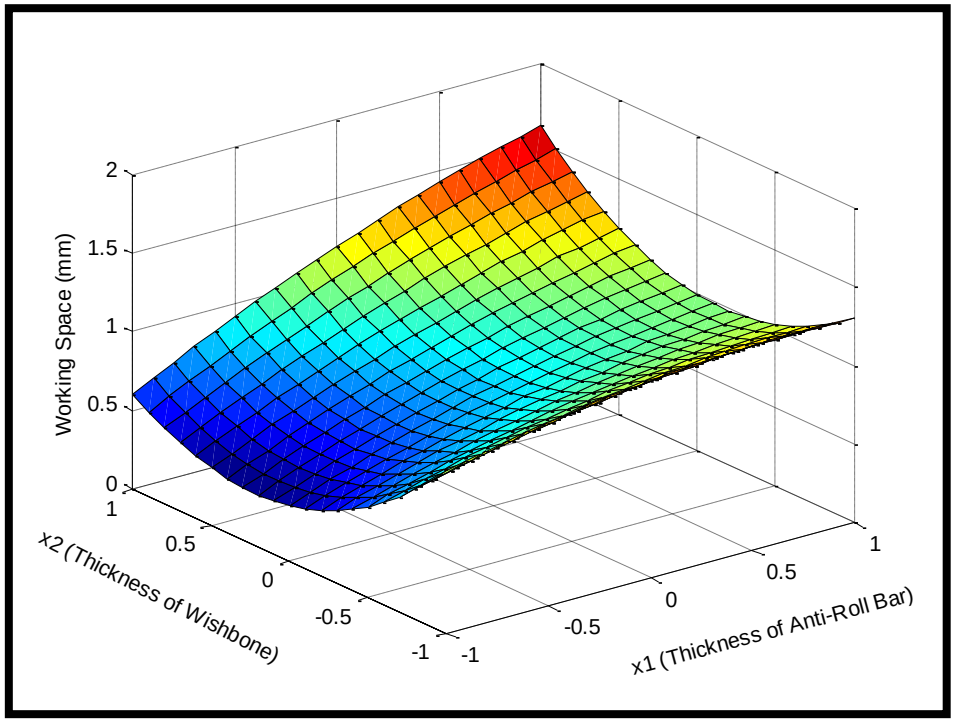

Figure 6.11: The response surface of working space @ v=10m/s and $x_3 = -1$

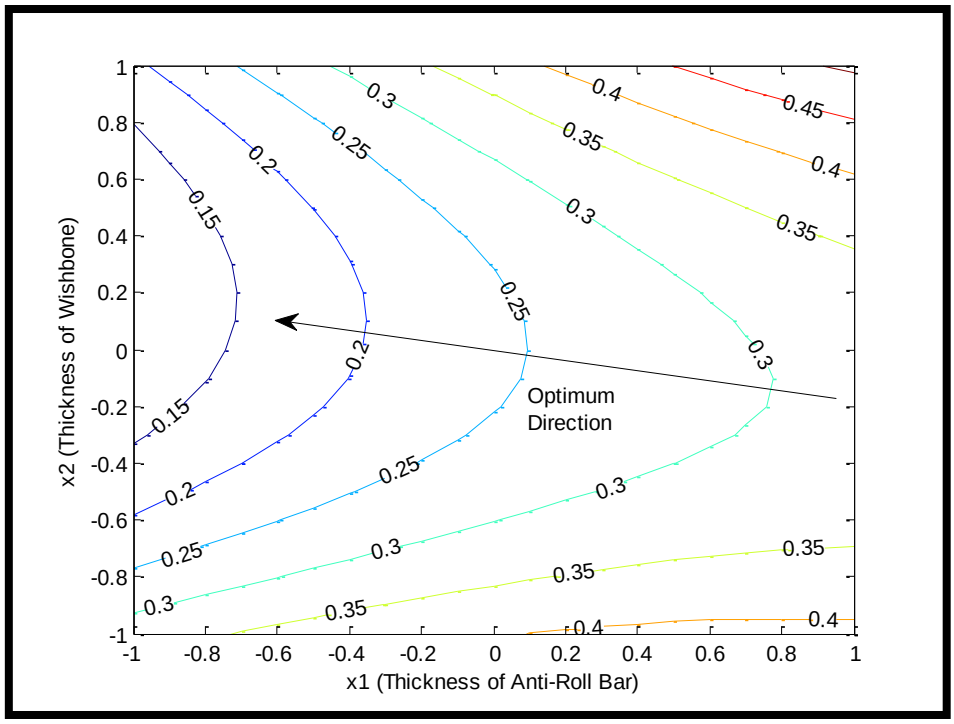

Figure 6.12: The contour lines of working space @ v=10m/s and $x_3 = -1$ (axes are transformed)

This section has a great importance for a designer who wants to try different material types on the components of a product and see the effect of geometrical changes on the behavior of performance metrics. The general flow of the procedure should be the topic of greater interest instead of the values or the components chosen.

6.4 MULTI-OBJECTIVE OPTIMIZATION

For the last part of this section, a multi-optimization approach is applied to minimize the three objective functions. To do this, all performance metrics are normalized to unity to avoid the deviances due to the difference in the order of the magnitudes of the performance metrics. Also the performance metrics are constrained in lower limit to avoid going below a certain level, even zero, which would be practically impossible. Lower limits for discomfort, road holding and working space are defined as 10 mm/s^2, 3 N and 0.10 mm respectively which are about 10 percent of the maximum values seen in the plots. The optimization algorithm used scans all the performance metric arrays on the surface and tries to minimize the maximum of the three metrics. To give a random example, an array of [15, 13, 13] is a better choice than [16,3,4]. In Tables 6.9 and 6.10, the multi-objective optimization results are shown with thicknesses in transformed dimensionless values and in physical domain respectively.

v=1 m/s			
	x_3=-1 (Mg Alloy)	*x_3=0 (Al Alloy)*	*x_3=1 (Steel)*
x_1 (Dimensionless / mm)	0.52 / 2.20	0.46 / 2.18	-0.89 / 1.64
x_2 (Dimensionless / mm)	0.6 / 2.80	0.74 / 2.87	0.92 / 2.96
Discomfort (mm/s^2)	66.65	118.34	10.53
Road Holding (N)	11.62	24.94	3.75
Working Space (mm)	0.36	0.73	0.11

Table 6.9: Multi-Objective optimization results for v=1 m/s

v=10 m/s			
	x_3=-1 (Mg Alloy)	*x_3=0 (Al Alloy)*	*x_3=1 (Steel)*
x_1 (Dimensionless / mm)	0.52 / 2.20	0.46 / 2.18	-0.89 / 1.64
x_2 (Dimensionless / mm)	0.6 / 2.80	0.74 / 2.87	0.92 / 2.96
Discomfort (mm/s^2)	210.78	373.98	33.3
Road Holding (N)	36.75	78.86	11.87
Working Space (mm)	1.08	2.32	0.36

Table 6.10: Multi-Objective optimization results for v=10 m/s

When Tables 6.9 and 6.10 are examined, one can easily realize that the optimum configuration for v=1 m/s or v=10 m/s did not change. The only thing changing is the magnitude of the results which was actually an expected consequence since the corresponding equations (eq. 6.4-6.9) varied with speed in a linear fashion. In the following figures (Figures 6.13, 6.14, 6.15) these optimum locations are pinned to have a better understanding about the optimized results (v = 1 m/s & x=1, steel case).

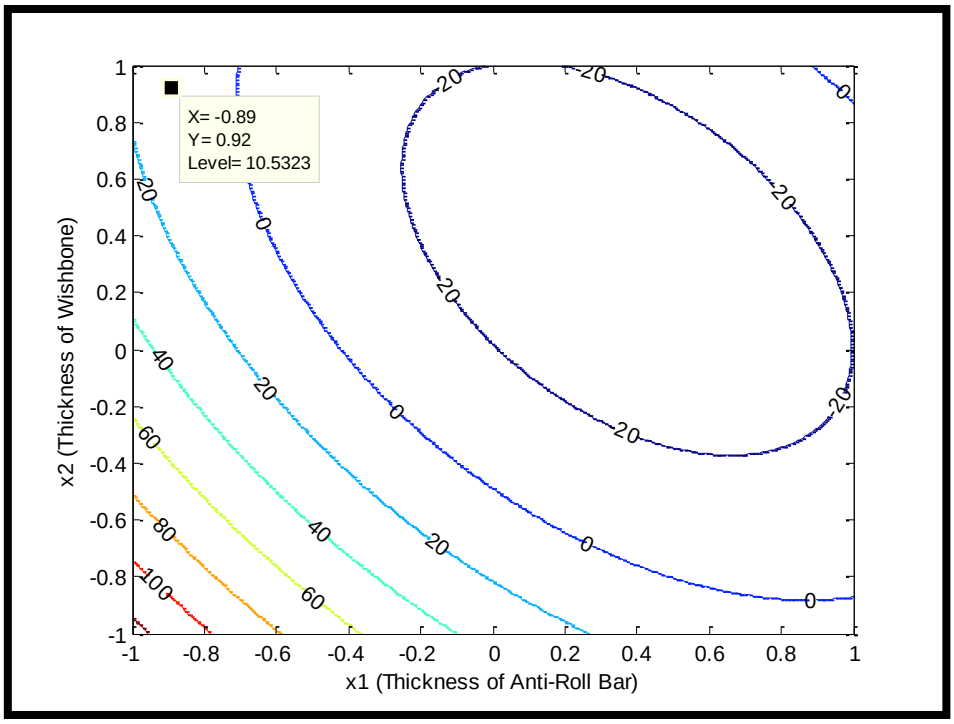

Figure 6.13: Multi-objective optimum point for discomfort @ v=1 m/s and $x_3 = 1$ (axes are transformed)

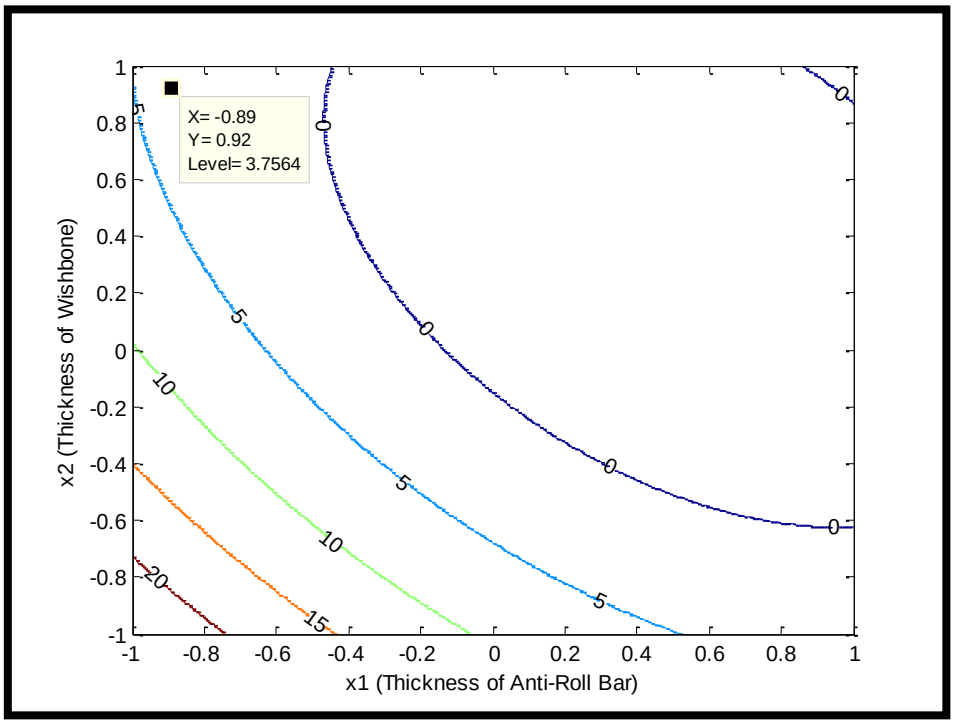

Figure 6.14: Multi-objective optimum point for road holding @ v=1 m/s and $x_3 = 1$ (axes are transformed)

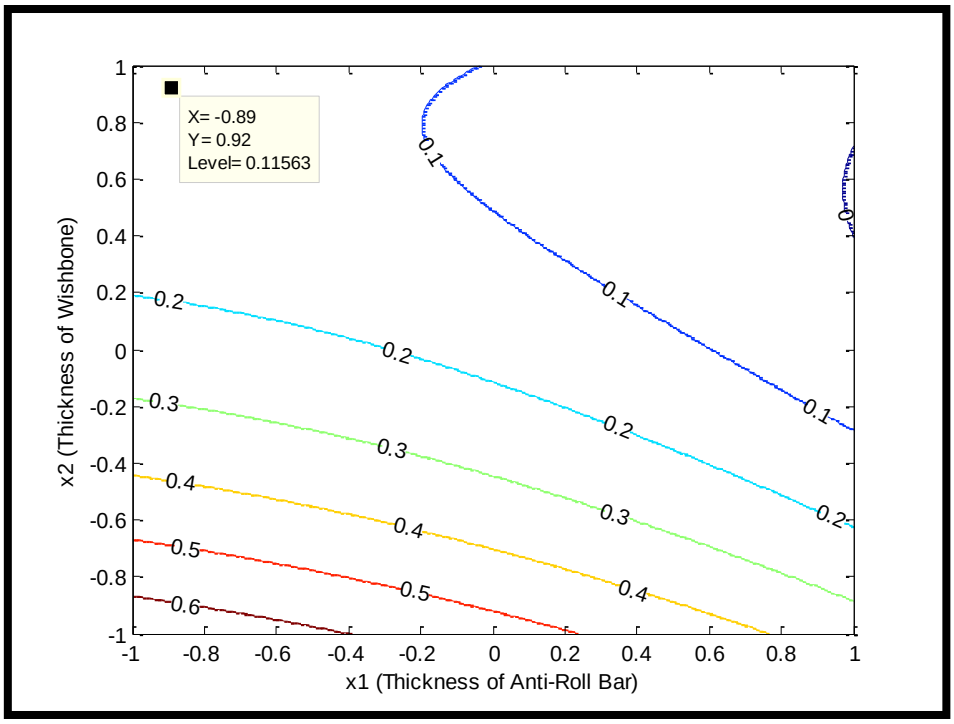

Figure 6.15: Multi-objective optimum point for working space @ v=1 m/s and $x_3 = 1$ (axes are transformed)

6.5 SINGLE-OBJECTIVE OPTIMIZATION

Instead of multi-objective optimization, a single-objective optimization can also be made to observe significant improvement / worsening for each single case. However, this time, since the objective functions can be conflicting; improving one of them may worsen the others which was avoided in multi-objective optimization.

However, our obtained regression equations form surfaces which include contour lines, meaning, we can reach a minimum value at more than one single point. As a consequence, a single-objective optimization will show us a minimum contour line instead of a point like the one in multi-objective optimization. Reaching to that minimum contour line totally depends on the designer which can freely decide according to the cost, availability, feasibility etc. of the component / material to be altered. Moving in the optimum directions shown in contour plots (or moving perpendicularly between contours) gives the most significant improvement in the objective functions.

CHAPTER 7

OPTIMIZATION STUDY FOR THE ACCELERATION FUNCTION OF THE SUSPENSION SYSTEM

The acceleration transfer function is one of the performance measures commonly used in automotive industry. It simply relates the acceleration response of a desired region to a prescribed input force. The location of the excitation and measurement points are shown in Figure 7.1. In this case the transfer function is obtained by exciting the system from the wishbone and measuring the acceleration at the suspension tower. What is simply done is finding out the peaks and trying to lower them by adjusting the contributing parameters. The optimum configuration of the design parameters is calculated in the end. In this study LMS Virtual Lab software is employed.

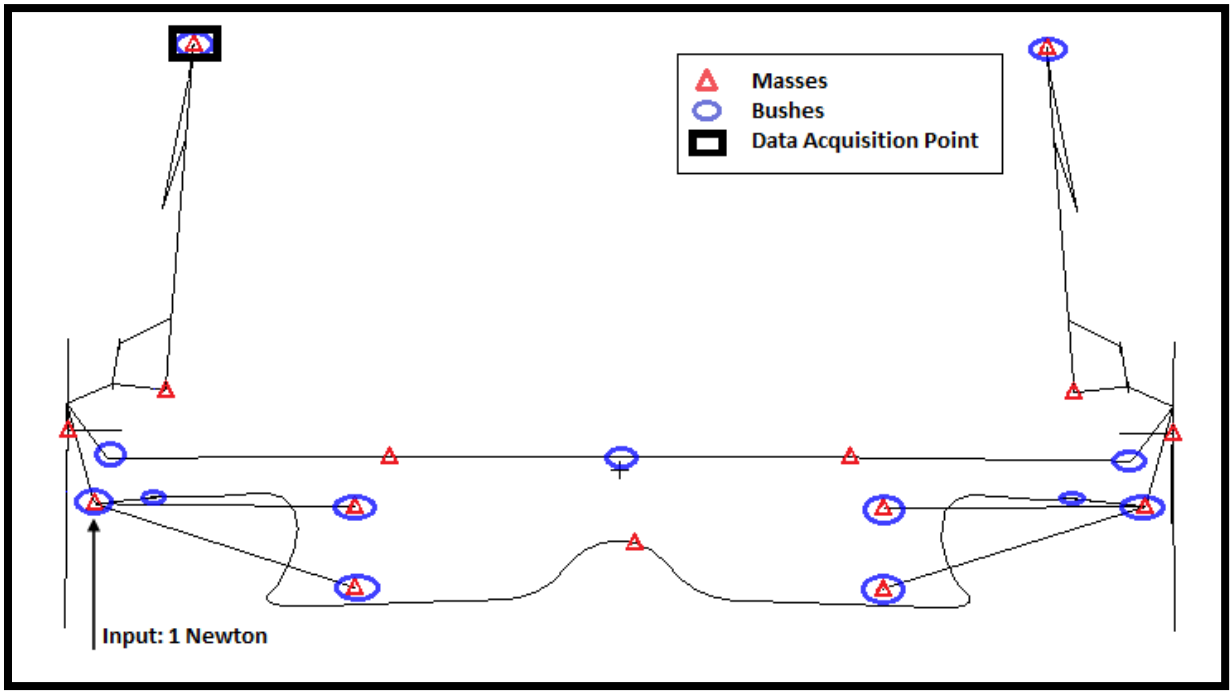

Figure 7.1: The excitation and measurement locations for acceleration transfer function

Spring coefficients of the main components in the suspension system (mostly z components), the body and the tire masses, and the tire stiffness are selected as the design variables. DOE analysis is performed with 7 factors using the amplitude of the highest peak of the acceleration function as the performance metric. The high and low levels for each design

variable were determined by increasing and decreasing the baseline values of the factors by 20%, respectively. A full-factorial experiment is performed 2^7 (=128) runs since the computer sources were enough for this optimization. Obtained transfer function can be found in Figure 7.2. The optimization was performed based on the quadratic regression model.

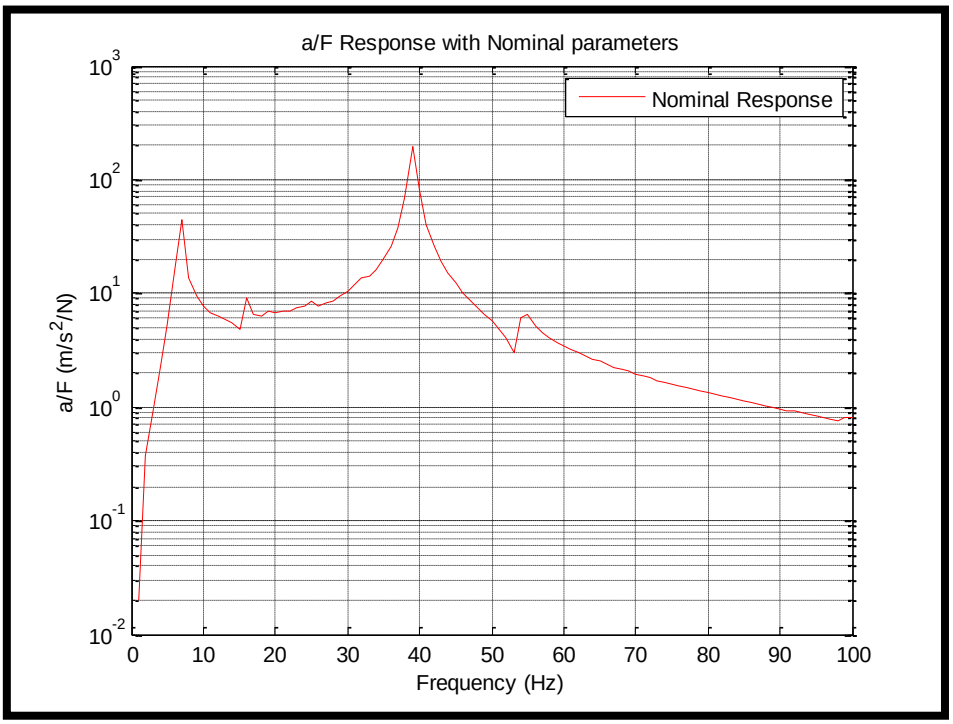

Figure 7.2: a/F Response of the front suspension system

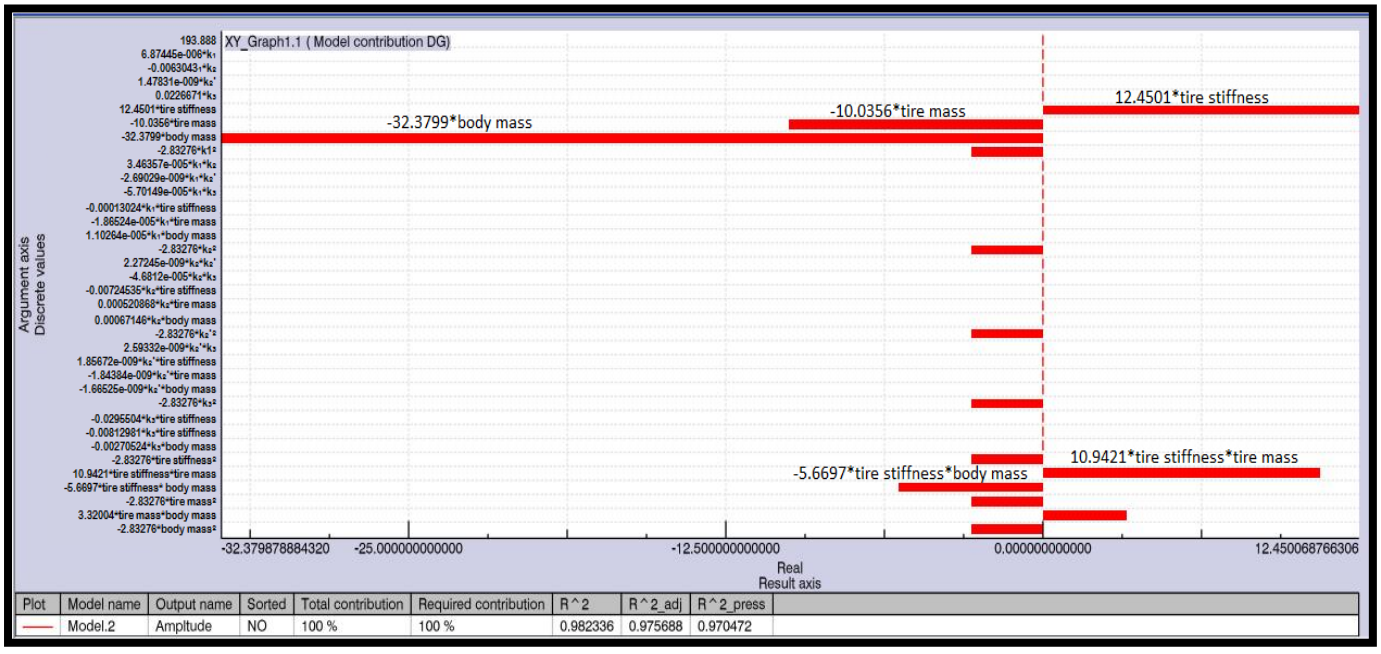

Figure 7.3: Contribution chart of the design variables

The results presented with the bar charts in Figure 7.3 shows the contribution of each design variable to the regression model. It is observed that among the seven parameters considered, body mass is the most significant. Tire mass, tire stiffness, interactions of tire stiffness & tire mass and tire stiffness & body mass are the other significant factors according to the contribution chart. When the regression model parameters are considered, the R^2 value is 0.98. That means 98 % of the variability in the response variable can be explained with the regression model.

After the regression model has appeared, the optimization study to minimize the peak at around 40 Hz is done. LMS Virtual Lab presented a new transfer function like the one in Figure 7.4 after the process, together with the new parameter values listed in Table 7.1.

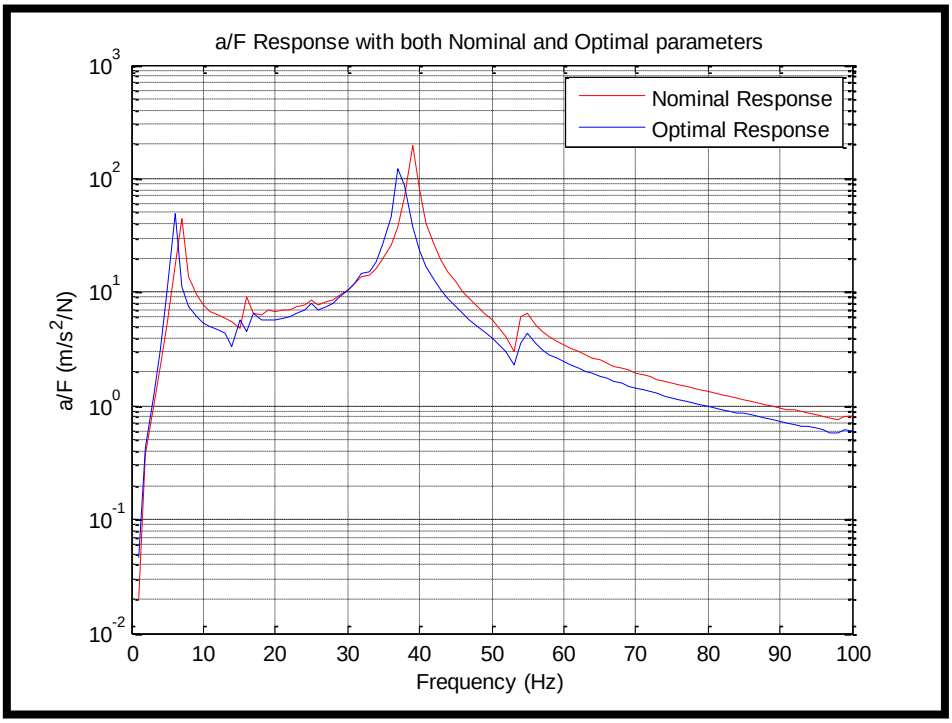

Figure 7.4: (a/F) Response of the front suspension system showing both optimal and nominal curves

The results of the optimization study are tabulated in Table 33. As it can be observed from Figure 7.4 the maximum peak at 40 Hz is reduced significantly by altering the design parameters based on the optimization study. A 37 % reduction is achieved at the max peak by changing the design parameters based on the optimization study.

Case	Nominal Values	Optimal Values
k_1 (N/mm)	2666.5	2656.8
k_2 (N/mm)	2055	1671
k_2' (N/mm)	1500	1796
k_3 (N/mm)	330	281
Tire Stiffness (N/mm)	180	144
Tire Mass (kg)	16	19.2
Body Mass (kg)	144	172.78
Peak Amplitude (a/F)	**194.67**	**122.38**

Table 7.1: Comparison of the nominal and optimal parameters and corresponding results

CHAPTER 8

SUMMARY AND CONCLUSION

In this study, a simplified FE model was built for the front suspension system that can be utilized for the preliminary optimization studies. The simple FE model was validated by comparing it with the results of the high fidelity FE model. Using the simple model instead of the detailed one is very advantageous especially for the DOE analysis which requires long computational times.

A generalized methodology was developed for defining the optimal relationship among the front suspension parameters and the suspension *performance metrics*. Four different metrics were selected to improve the vehicle performance (discomfort, road holding, working space, maximum peak of acceleration function). DOE was used to identify the most significant design parameters that contribute to the performance of the vehicle. Regression models of the performance metrics were built and used for the optimization studies. Optimization was performed both in deterministic and stochastic frameworks and the results were compared.

A more realistic optimization study was also presented using the material properties and dimensional characteristics of the suspension system. This study gives the designer the flexibility to adjust material and dimensional properties independently and find an optimum point in terms of the same performance metrics mentioned above.

In Chapter 2, it was shown that Using DOE methodology significantly improves the time and computer source used for obtaining a relationship between the performance metrics and the design parameters of the suspension system. The significance of the bushes is also studied in this chapter, and it was concluded that for the metrics considered in this study, the bush effect was found to be insignificant. Among the main design factors: body mass, tire stiffness, suspension damping and their interactions have the greatest effect on the performance metrics. For the full list of results, one should refer to section 5.5.2 and table 13.

In the DOE analysis, for the sake of simplicity, all parameters were altered in the ±20% range. However changing the body mass of a vehicle that much is impractical in real life and as mentioned in Section 5.6. In some of the observations made throughout the study, changing these parameters in the ±20% dominated the performance outputs of the vehicle. For that

reason, the developed methodology should be the focus of the reader rather than the quantitative results.

In Chapter 5 and Chapter 6, it was observed that the single objective approach resulted better than the multi-objective approach due to the conflicting nature of the performance metrics. However, in practice, there will always be conflicting parameters and multi-objective optimization should yield more realistic results when compared with the single optimization studies.

We also implemented a "stochastic approach" to the optimization studies to include the variations and uncertainties that arise from a variety of sources, i.e. manufacturing processes, external disturbances, operating conditions. After implementing the stochastic approach the results have slightly changed; however, the optimum configuration remained the same with the deterministic optimization results.

Material and dimension optimization study in Chapter 6 results in many different conclusions, depending on the material choice. If some of the results from Chapter 6 are repeated; for example if the material chosen for anti-roll bar (ARB) and the wishbones is Al-Alloy; as the thickness of the anti-roll bar increases the discomfort values decreases. The thinner the wishbones are, less discomfort the passengers feel as well. We can conclude that ARB and wish bone thicknesses work in the same manner to decrease the discomfort. However when the behavior of the two parameters in the contour plot (Figure 6.6) are investigated, we can see that the wishbone thickness plays a greater role than the thickness of ARB to alter the discomfort values. The optimum direction to follow to efficiently decrease the discomfort is obvious from the contour lines (Figure 6.6).

Similar conclusions can be extracted from Chapter 6 by changing the material type and investigating the contour plots accordingly. However, one of the most beneficial conclusions of this chapter can be obtained from the optimization section. By observing the contour plots, the designer detects that the same outputs can be acquired by inputting different thicknesses for both ARB and wishbones. This gives the designer to alter the thickness inputs and material choices freely so that he/she can find the optimum relationship with the most economical configuration.

In this thesis, a general approach was developed to understand the relationship between the design parameters and the suspension vibration isolation performance. After the relationships are determined, single and multi-objective optimization studies are performed to find the

optimum configurations for the suspension performance. Our results show that the presented approach and techniques can be effectively by the industrial designers to improve the suspension performance by modifying the design parameters of the suspension system.

REFERENCES

[1]: M. GOBBI and G. MASTINU, Analytical description and optimization of the dynamic behavior of passively suspended road vehicles, Journal of Sound and Vibration (2001) 245(3), 457-481

[2]: P. MUELLER and W. SCHIEHLEN, Linear Vibrations Dordrecht: Martinus Nijoff 1985

[3]: D. HROVAT, Transactions of the American Society of Mechanical Engineers, Applications of optimal control to advanced automotive suspension design, Journal of Dynamic Systems, Measurement, and Control 115, 328-342, 1993

[4]: R. CHALASANI, 1983 Internal Report General Motor Research Laboratories. Ride performance potential of active suspension systems.

[5]: A. THOMPSON, Paper 830663. Suspension design for optimum road holding, SAE 1983

[6]: X. LU and AL, A design procedure for optimization of vehicle suspensions, 1984 International Journal of Vehicle Design 5, 129-141.

[7]: G. MASTINU, Technical Report. Politecnico di Milano. Escursione della sospensione dell' autoveicolo: derivazione analitica della risposta in presenza di eccitazione stocastica 1993

[8]: P. VENHOVENS, Optimal Control of Vehicle Suspensions, Ph.D. Thesis, Delft University of Technology, Delft, The Netherlands, 1994.

[9]: J. DIXON, Tires, Suspension and Handling, Cambridge University Press, Cambridge, 1991.

[10]: R. SHARP and D. CROLLA 1987 Vehicle system Dynamics, 16, 167-192. Road vehicle suspension system design - a review.

[11]: M. GOBBI and G. MASTINU, Analytical description and optimization of the dynamic behavior of passively suspended road vehicles, Journal of Sound and Vibration 3 (245) (2001) 457–481.

[12]: M. GOBBI and G. MASTINU, Symbolical multi-objective optimization of the dynamic behavior of actively suspended road vehicles, International Journal of Vehicle Design 28 (1–3) (2002) 189–213.

[13]: M. GOBBI, F. LEVI, G. MASTINU, Multi-objective stochastic optimization of the suspension system of road vehicles, Journal of Sound and Vibration 298 (2006) 1055–1072

[14]: L. BALMER, Signals and Systems; An Introduction (2nd edition) 1997

[15]: K. KAMASH, J.D. ROBSON, The application of isotropy in road surface modeling, Journal of Sound and Vibration 1 (57) (1978) 89–100

[16]: C. DODDS, J. ROBSON, The description of road surface roughness, Journal of Sound and Vibration 2 (31) (1973) 175–183.

[17]: M. MITSCHKE, Dynamik der Kraftfahrzeuge, Springer, Berlin, 1990

[18]: G. E. P. BOX and K. B. WILSON, On the Experimental Attainment of Optimum Conditions, J. Royal Statistical Society, Ser. B, v. 13 (1951), pp. 1-45.

[19]: G. KAMCI, I. BASDOGAN, Vibro - Acoustic Analysis of a Commercial Vehicle Integrated with Design of Experiments Methodology, 8th World Congress on Structural and Multidisciplinary Optimization June 1 - 5, 2009, Lisbon, Portugal

[20]: R. H. MYERS, D. C. MONTGOMERY, G. G. VINING, C. M. BORROR, S. M. KOWALSKI, Response Surface Methodology: A Retrospective and Literature Survey, Journal of Quality Technology, 36(1), 53-77, 2004.

[21]: R. H. MYERS and D. C. MONTGOMERY, Response Surface Methodology, Process and Product Optimization Using Designed Experiments, (2nd Ed.), John Wiley and Sons, New York, NY, 2002.

[22]: Theoretical Background for Optimus Booklet, Noesis Solutions, November 2008

[23]: J. W. SUTHERLAND, Design of Experiments Lecture Notes, Michigan Tech. University Dept. Of Mechanical Engineering

[24]: R. JAIN, Computer Systems Analysis Lecture Notes, Washington University in Saint Louis, Department of Computer Science & Engineering

[25]: D. BANKS, Data Mining Lecture Notes, Duke University, Department of Statistical Science

[26]: D. C. MONTGOMERY, Design and Analysis of Experiments (7th Edition) 2009

[27]: Design Expert StatEase® Software User Manuals

[28]: X. LIANG, Z. LIN and P. ZHU, Acoustic analysis of damping structure with Response Surface Method, Journal of Applied Acoustics 68 (2007) 1036–1053

[29]: Z. LI and X. LIANG, Vibro-acoustic analysis and optimization of damping structure with Response Surface Method, Journal of Materials and Design 28 (2007) 1999–2007

APPENDICES

A) Parameter Set Used For Bush Optimization (Stiffnesses in N / mm)

Run	A	B	C	D	E	F	G	H	I
1	1880	7840	2853.6	400	26400	1200000	7200	120	2400
2	2820	7840	2853.6	400	26400	800000	4800	80	1600
3	1880	11760	2853.6	400	26400	800000	4800	80	2400
4	2820	11760	2853.6	400	26400	1200000	7200	120	1600
5	1880	7840	4280.4	400	26400	800000	4800	120	1600
6	2820	7840	4280.4	400	26400	1200000	7200	80	2400
7	1880	11760	4280.4	400	26400	1200000	7200	80	1600
8	2820	11760	4280.4	400	26400	800000	4800	120	2400
9	1880	7840	2853.6	600	26400	800000	7200	80	1600
10	2820	7840	2853.6	600	26400	1200000	4800	120	2400
11	1880	11760	2853.6	600	26400	1200000	4800	120	1600
12	2820	11760	2853.6	600	26400	800000	7200	80	2400
13	1880	7840	4280.4	600	26400	1200000	4800	80	2400
14	2820	7840	4280.4	600	26400	800000	7200	120	1600
15	1880	11760	4280.4	600	26400	800000	7200	120	2400
16	2820	11760	4280.4	600	26400	1200000	4800	80	1600
17	1880	7840	2853.6	400	39600	1200000	4800	80	1600
18	2820	7840	2853.6	400	39600	800000	7200	120	2400
19	1880	11760	2853.6	400	39600	800000	7200	120	1600
20	2820	11760	2853.6	400	39600	1200000	4800	80	2400
21	1880	7840	4280.4	400	39600	800000	7200	80	2400
22	2820	7840	4280.4	400	39600	1200000	4800	120	1600
23	1880	11760	4280.4	400	39600	1200000	4800	120	2400
24	2820	11760	4280.4	400	39600	800000	7200	80	1600
25	1880	7840	2853.6	600	39600	800000	4800	120	2400
26	2820	7840	2853.6	600	39600	1200000	7200	80	1600
27	1880	11760	2853.6	600	39600	1200000	7200	80	2400
28	2820	11760	2853.6	600	39600	800000	4800	120	1600
29	1880	7840	4280.4	600	39600	1200000	7200	120	1600
30	2820	7840	4280.4	600	39600	800000	4800	80	2400
31	1880	11760	4280.4	600	39600	800000	4800	80	1600
32	2820	11760	4280.4	600	39600	1200000	7200	120	2400
Centroid	2350	9800	3567	500	33000	1000000	6000	100	2000

A. Tassello Superiore DX/SX (Translational Z)

B. Boccola Anteriore Pinna Lato Scocca DX/SX (Translational Z)

C. Boccola Posteiore Pinna Lato Scocca (Translational Z)

D. Attacco Barra-Pinna DX/SX (Translational Z)

E. Attacco Barra-Pinna DX/SX (Rotational Y)

F. Analisi Entita' Delle Forze A DX/SX (Translational Z)

G. Attacco Barra Lato Scocca DX/SX (Translational Z)

H. Analisi Entita' Delle Forze B DX/SX (Translational Z)

I. Interconnessione (Translational Y)

B) Design Resolution

Before specifically defining what a design resolution is a brand new example will be introduced to show things more clearly.

8 experiments will be conducted for 6 parameters.

$$2^{k-p} = 2^{6-3} = (2^m) = 8$$

k = 6 variables to be studied

p = 3 variables to be introduced using interactions from base design

m = 3 number of variables in the base design

If variables 4, 5 and 6 are introduced through the interactions of 12, 13 and 23 respectively, the base design becomes:

Experiment Nr.	I	1	2	3	12	13	23	123
1	+	—	—	—	+	+	+	—
2	+	+	—	—	—	—	+	+
3	+	—	+	—	—	+	—	+
4	+	+	+	—	+	—	—	—
5	+	—	—	+	+	—	—	+
6	+	+	—	+	—	+	—	—
7	+	—	+	+	—	—	+	—
8	+	+	+	+	+	+	+	+

Table B.i: Introduction of parameters 4, 5 and 6 through 12, 13 and 23 respectively

This time, the generators are 4 = 12, 5 = 13, 6 = 23 or in other words I = 124, I = 135 and I = 236. In the end the recipe matrix becomes:

Experiment Nr.	I	1	2	3	4	5	6
1	+	—	—	—	+	+	+
2	+	+	—	—	—	—	+
3	+	—	+	—	—	+	—
4	+	+	+	—	+	—	—
5	+	—	—	+	+	—	—
6	+	+	—	+	—	+	—
7	+	—	+	+	—	—	+
8	+	+	+	+	+	+	+

Table B.ii: The recipe matrix

Before describing some relationships, one should know that according to the confounding algorithm, any term of power 2 is erased.

We have *p* generators

I = 124 = 135 = 236

Consider their products, 2 terms at a time

124 • 135 = 2345

124 • 236 = 1346

135 • 236 = 1256

Products, 3 terms at a time

124 • 135 • 236 = 456

In general, all the way up to “products, p terms at a time”.

So,

I = 124 = 135 = 236 = 2345 = 1346 = 1256 = 456

There are 2^p “words” = 8 (7 + Identity) “Word” is a string, like one of the ones above (236, 2345 etc.)

Now an exact definition to “Design Resolution” can be made [23].

Design Resolution is “The length of the shortest word in the defining relation (excluding I)”. For the example given, the resolution of design is III.

What does Design Resolution mean?

• Design Resolution = II: Main effects confounded with one another. (A very weak and inaccurate approach)

• Design Resolution = III: Main effects are confounded with two factor interactions (1 with 2) and 3 = 1 + 2.

• Design Resolution = IV: Main effects are confounded with three factor interactions (1 with 3) and 4 = 1 + 3. It can also be two factor interactions are confounded with one another (2 with 2) and 4 = 2 + 2.

• Design Resolution = V: Main effects confounded with 4 factor (1 + 4 = 5), or, two-factor interactions are confounded with three factor interactions (2 + 3 = 5)

StatEase® Design Expert software helped us about preparing these experiments according to the logic explained in the related sections.

C) Parameter Set Used For Main Factor Optimization

Run	A	B	C	D	E	F	G	H
1	1200	2132.8	0.264	3288	0.8	463.2	13.496	216
2	1800	2132.8	0.264	3288	0.8	694.8	20.244	216
3	1200	3199.2	0.264	3288	0.8	694.8	20.244	144
4	1800	3199.2	0.264	3288	0.8	463.2	13.496	144
5	1200	2132.8	0.396	3288	0.8	694.8	13.496	144
6	1800	2132.8	0.396	3288	0.8	463.2	20.244	144
7	1200	3199.2	0.396	3288	0.8	463.2	20.244	216
8	1800	3199.2	0.396	3288	0.8	694.8	13.496	216
9	1200	2132.8	0.264	4932	0.8	463.2	20.244	144
10	1800	2132.8	0.264	4932	0.8	694.8	13.496	144
11	1200	3199.2	0.264	4932	0.8	694.8	13.496	216
12	1800	3199.2	0.264	4932	0.8	463.2	20.244	216
13	1200	2132.8	0.396	4932	0.8	694.8	20.244	216
14	1800	2132.8	0.396	4932	0.8	463.2	13.496	216
15	1200	3199.2	0.396	4932	0.8	463.2	13.496	144
16	1800	3199.2	0.396	4932	0.8	694.8	20.244	144
17	1200	2132.8	0.264	3288	1.2	463.2	13.496	144
18	1800	2132.8	0.264	3288	1.2	694.8	20.244	144
19	1200	3199.2	0.264	3288	1.2	694.8	20.244	216
20	1800	3199.2	0.264	3288	1.2	463.2	13.496	216
21	1200	2132.8	0.396	3288	1.2	694.8	13.496	216
22	1800	2132.8	0.396	3288	1.2	463.2	20.244	216
23	1200	3199.2	0.396	3288	1.2	463.2	20.244	144
24	1800	3199.2	0.396	3288	1.2	694.8	13.496	144
25	1200	2132.8	0.264	4932	1.2	463.2	20.244	216
26	1800	2132.8	0.264	4932	1.2	694.8	13.496	216
27	1200	3199.2	0.264	4932	1.2	694.8	13.496	144
28	1800	3199.2	0.264	4932	1.2	463.2	20.244	144
29	1200	2132.8	0.396	4932	1.2	694.8	20.244	144
30	1800	2132.8	0.396	4932	1.2	463.2	13.496	144
31	1200	3199.2	0.396	4932	1.2	463.2	13.496	216
32	1800	3199.2	0.396	4932	1.2	694.8	20.244	216
Centroid	1500	2666	0.33	4110	1	579	16.87	180

A. Molla Primaria (N/mm)

B. Fonda Corsa Ammortizzatore (N/mm)

C. Pressurizzazione (N/mm)

D. Tampone di Tamponamento (N/mm)

E. Damper (N.s/mm)

F. Body Mass (kg)

G. Tire Mass (kg)

H. Tire Stiffness (N/mm)

D) Bush Optimization DOE Set

Run	PSD1								
		v =1 m/s			*v =10 m/s*			*v =50 m/s*	
	Discomfort	*Road Holding*	*Working Space*	*Discomfort*	*Road Holding*	*Working Space*	*Discomfort*	*Road Holding*	*Working Space*
1	2,195E+01	3,544E+00	3,625E-02	6,941E+01	1,121E+01	1,146E-01	1,552E+02	2,506E+01	2,563E-01
2	2,220E+01	3,792E+00	3,715E-02	7,021E+01	1,199E+01	1,175E-01	1,570E+02	2,681E+01	2,627E-01
3	2,195E+01	3,544E+00	3,625E-02	6,941E+01	1,121E+01	1,146E-01	1,552E+02	2,506E+01	2,563E-01
4	2,220E+01	3,792E+00	3,715E-02	7,020E+01	1,199E+01	1,175E-01	1,570E+02	2,681E+01	2,627E-01
5	2,220E+01	3,792E+00	3,715E-02	7,021E+01	1,199E+01	1,175E-01	1,570E+02	2,681E+01	2,627E-01
6	2,195E+01	3,544E+00	3,625E-02	6,941E+01	1,121E+01	1,146E-01	1,552E+02	2,506E+01	2,563E-01
7	2,220E+01	3,792E+00	3,715E-02	7,020E+01	1,199E+01	1,175E-01	1,570E+02	2,681E+01	2,627E-01
8	2,195E+01	3,544E+00	3,625E-02	6,941E+01	1,121E+01	1,146E-01	1,552E+02	2,506E+01	2,563E-01
9	2,219E+01	3,792E+00	3,715E-02	7,019E+01	1,199E+01	1,175E-01	1,569E+02	2,681E+01	2,627E-01
10	2,194E+01	3,544E+00	3,625E-02	6,939E+01	1,121E+01	1,146E-01	1,552E+02	2,506E+01	2,563E-01
11	2,219E+01	3,792E+00	3,715E-02	7,018E+01	1,199E+01	1,175E-01	1,569E+02	2,681E+01	2,627E-01
12	2,194E+01	3,544E+00	3,625E-02	6,939E+01	1,121E+01	1,146E-01	1,552E+02	2,506E+01	2,563E-01
13	2,194E+01	3,544E+00	3,625E-02	6,939E+01	1,121E+01	1,146E-01	1,552E+02	2,506E+01	2,563E-01
14	2,219E+01	3,792E+00	3,715E-02	7,018E+01	1,199E+01	1,175E-01	1,569E+02	2,681E+01	2,627E-01
15	2,194E+01	3,544E+00	3,625E-02	6,939E+01	1,121E+01	1,146E-01	1,552E+02	2,506E+01	2,563E-01
16	2,219E+01	3,792E+00	3,715E-02	7,018E+01	1,199E+01	1,175E-01	1,569E+02	2,681E+01	2,627E-01
17	2,220E+01	3,787E+00	3,713E-02	7,019E+01	1,198E+01	1,174E-01	1,570E+02	2,678E+01	2,626E-01
18	2,195E+01	3,541E+00	3,624E-02	6,940E+01	1,120E+01	1,146E-01	1,552E+02	2,504E+01	2,562E-01
19	2,219E+01	3,787E+00	3,713E-02	7,019E+01	1,198E+01	1,174E-01	1,569E+02	2,678E+01	2,626E-01
20	2,195E+01	3,541E+00	3,624E-02	6,940E+01	1,120E+01	1,146E-01	1,552E+02	2,504E+01	2,562E-01
21	2,195E+01	3,541E+00	3,624E-02	6,940E+01	1,120E+01	1,146E-01	1,552E+02	2,504E+01	2,562E-01
22	2,220E+01	3,787E+00	3,713E-02	7,019E+01	1,198E+01	1,174E-01	1,570E+02	2,678E+01	2,626E-01
23	2,194E+01	3,541E+00	3,624E-02	6,940E+01	1,120E+01	1,146E-01	1,552E+02	2,504E+01	2,562E-01
24	2,219E+01	3,787E+00	3,713E-02	7,019E+01	1,198E+01	1,174E-01	1,569E+02	2,678E+01	2,626E-01
25	2,192E+01	3,544E+00	3,646E-02	6,931E+01	1,121E+01	1,153E-01	1,550E+02	2,506E+01	2,578E-01
26	2,219E+01	3,787E+00	3,713E-02	7,017E+01	1,198E+01	1,174E-01	1,569E+02	2,678E+01	2,626E-01
27	2,194E+01	3,541E+00	3,624E-02	6,937E+01	1,120E+01	1,146E-01	1,551E+02	2,504E+01	2,562E-01
28	2,219E+01	3,787E+00	3,713E-02	7,016E+01	1,198E+01	1,174E-01	1,569E+02	2,678E+01	2,626E-01
29	2,219E+01	3,787E+00	3,713E-02	7,017E+01	1,198E+01	1,174E-01	1,569E+02	2,678E+01	2,626E-01
30	2,194E+01	3,541E+00	3,624E-02	6,938E+01	1,120E+01	1,146E-01	1,551E+02	2,504E+01	2,562E-01
31	2,219E+01	3,787E+00	3,713E-02	7,016E+01	1,198E+01	1,174E-01	1,569E+02	2,678E+01	2,626E-01
32	2,194E+01	3,541E+00	3,624E-02	6,937E+01	1,120E+01	1,146E-01	1,551E+02	2,504E+01	2,562E-01
Centroid	2,206E+01	3,652E+00	3,668E-02	6,975E+01	1,155E+01	1,160E-01	1,560E+02	2,583E+01	2,594E-01

Run	PSD2								
		v =1 m/s			*v =10 m/s*			*v =50 m/s*	
	Discomfort	*Road Holding*	*Working Space*	*Discomfort*	*Road Holding*	*Working Space*	*Discomfort*	*Road Holding*	*Working Space*
1	1,263E+01	2,518E+00	3,668E-03	1,802E+01	2,166E+00	1,836E-03	1,260E+01	1,624E+00	9,898E-04
2	1,252E+01	2,533E+00	3,772E-03	1,797E+01	2,160E+00	1,859E-03	1,259E+01	1,622E+00	9,983E-04
3	1,263E+01	2,518E+00	3,668E-03	1,800E+01	2,166E+00	1,835E-03	1,258E+01	1,624E+00	9,883E-04
4	1,252E+01	2,533E+00	3,772E-03	1,796E+01	2,160E+00	1,858E-03	1,256E+01	1,622E+00	9,968E-04
5	1,252E+01	2,533E+00	3,772E-03	1,797E+01	2,160E+00	1,859E-03	1,258E+01	1,622E+00	9,982E-04
6	1,263E+01	2,518E+00	3,668E-03	1,802E+01	2,166E+00	1,836E-03	1,260E+01	1,624E+00	9,897E-04
7	1,252E+01	2,533E+00	3,772E-03	1,796E+01	2,160E+00	1,858E-03	1,256E+01	1,622E+00	9,967E-04
8	1,263E+01	2,518E+00	3,668E-03	1,800E+01	2,166E+00	1,835E-03	1,258E+01	1,624E+00	9,882E-04
9	1,251E+01	2,533E+00	3,771E-03	1,792E+01	2,161E+00	1,858E-03	1,255E+01	1,622E+00	9,975E-04
10	1,262E+01	2,518E+00	3,668E-03	1,797E+01	2,166E+00	1,835E-03	1,256E+01	1,624E+00	9,890E-04
11	1,250E+01	2,533E+00	3,771E-03	1,791E+01	2,160E+00	1,857E-03	1,253E+01	1,622E+00	9,959E-04
12	1,262E+01	2,518E+00	3,668E-03	1,795E+01	2,166E+00	1,834E-03	1,254E+01	1,624E+00	9,874E-04
13	1,262E+01	2,518E+00	3,668E-03	1,797E+01	2,166E+00	1,835E-03	1,256E+01	1,624E+00	9,888E-04
14	1,251E+01	2,533E+00	3,771E-03	1,792E+01	2,161E+00	1,858E-03	1,255E+01	1,622E+00	9,973E-04
15	1,262E+01	2,518E+00	3,668E-03	1,795E+01	2,166E+00	1,834E-03	1,254E+01	1,624E+00	9,873E-04
16	1,250E+01	2,533E+00	3,771E-03	1,790E+01	2,160E+00	1,857E-03	1,253E+01	1,622E+00	9,958E-04
17	1,252E+01	2,533E+00	3,770E-03	1,797E+01	2,161E+00	1,859E-03	1,259E+01	1,622E+00	9,982E-04
18	1,263E+01	2,518E+00	3,667E-03	1,802E+01	2,166E+00	1,835E-03	1,260E+01	1,624E+00	9,897E-04
19	1,252E+01	2,533E+00	3,770E-03	1,796E+01	2,160E+00	1,858E-03	1,256E+01	1,622E+00	9,966E-04
20	1,263E+01	2,518E+00	3,667E-03	1,801E+01	2,166E+00	1,835E-03	1,258E+01	1,624E+00	9,882E-04
21	1,263E+01	2,518E+00	3,667E-03	1,802E+01	2,166E+00	1,835E-03	1,260E+01	1,624E+00	9,896E-04
22	1,252E+01	2,533E+00	3,770E-03	1,797E+01	2,160E+00	1,858E-03	1,258E+01	1,622E+00	9,981E-04
23	1,263E+01	2,518E+00	3,667E-03	1,800E+01	2,166E+00	1,835E-03	1,258E+01	1,624E+00	9,881E-04
24	1,252E+01	2,533E+00	3,770E-03	1,796E+01	2,160E+00	1,858E-03	1,256E+01	1,622E+00	9,965E-04
25	1,262E+01	2,518E+00	3,673E-03	1,796E+01	2,166E+00	1,836E-03	1,256E+01	1,624E+00	9,892E-04
26	1,251E+01	2,533E+00	3,770E-03	1,792E+01	2,161E+00	1,858E-03	1,255E+01	1,622E+00	9,973E-04
27	1,262E+01	2,518E+00	3,667E-03	1,795E+01	2,166E+00	1,834E-03	1,254E+01	1,624E+00	9,873E-04
28	1,251E+01	2,533E+00	3,770E-03	1,791E+01	2,160E+00	1,857E-03	1,253E+01	1,622E+00	9,958E-04
29	1,251E+01	2,533E+00	3,770E-03	1,792E+01	2,161E+00	1,858E-03	1,255E+01	1,622E+00	9,972E-04
30	1,262E+01	2,518E+00	3,667E-03	1,797E+01	2,166E+00	1,834E-03	1,256E+01	1,624E+00	9,887E-04
31	1,250E+01	2,533E+00	3,770E-03	1,790E+01	2,160E+00	1,857E-03	1,253E+01	1,622E+00	9,957E-04
32	1,262E+01	2,518E+00	3,667E-03	1,795E+01	2,166E+00	1,834E-03	1,254E+01	1,624E+00	9,872E-04
Centroid	1,256E+01	2,524E+00	3,717E-03	1,793E+01	2,163E+00	1,845E-03	1,254E+01	1,623E+00	9,918E-04

E) Main Factors Optimization DOE Set

Run	PSD1								
		v =1 m/s			v =10 m/s			v =50 m/s	
	Discomfort	Road Holding	Working Space	Discomfort	Road Holding	Working Space	Discomfort	Road Holding	Working Space
1	3,201E+01	5,190E+00	3,039E-02	1,012E+02	1,641E+01	9,611E-02	2,263E+02	3,670E+01	2,149E-01
2	2,167E+01	4,252E+00	4,316E-02	6,854E+01	1,344E+01	1,365E-01	1,533E+02	3,006E+01	3,052E-01
3	2,178E+01	4,276E+00	4,484E-02	6,886E+01	1,352E+01	1,418E-01	1,540E+02	3,024E+01	3,171E-01
4	2,275E+01	2,900E+00	3,085E-02	7,193E+01	9,172E+00	9,757E-02	1,608E+02	2,051E+01	2,182E-01
5	2,045E+01	3,605E+00	4,417E-02	6,466E+01	1,140E+01	1,397E-01	1,446E+02	2,549E+01	3,123E-01
6	2,282E+01	3,126E+00	3,165E-02	7,216E+01	9,885E+00	1,001E-01	1,613E+02	2,210E+01	2,238E-01
7	2,831E+01	4,625E+00	3,079E-02	8,953E+01	1,463E+01	9,737E-02	2,002E+02	3,271E+01	2,177E-01
8	2,252E+01	4,331E+00	4,280E-02	7,123E+01	1,370E+01	1,353E-01	1,593E+02	3,062E+01	3,026E-01
9	2,292E+01	3,132E+00	3,177E-02	7,248E+01	9,904E+00	1,005E-01	1,621E+02	2,215E+01	2,246E-01
10	2,041E+01	3,591E+00	4,433E-02	6,453E+01	1,136E+01	1,402E-01	1,443E+02	2,539E+01	3,135E-01
11	2,293E+01	4,483E+00	4,311E-02	7,250E+01	1,418E+01	1,363E-01	1,621E+02	3,170E+01	3,048E-01
12	2,871E+01	4,721E+00	3,107E-02	9,080E+01	1,493E+01	9,824E-02	2,030E+02	3,338E+01	2,197E-01
13	2,176E+01	4,295E+00	4,372E-02	6,881E+01	1,358E+01	1,383E-01	1,539E+02	3,037E+01	3,092E-01
14	3,196E+01	5,242E+00	3,088E-02	1,011E+02	1,658E+01	9,766E-02	2,260E+02	3,706E+01	2,184E-01
15	2,259E+01	2,893E+00	3,140E-02	7,144E+01	9,149E+00	9,930E-02	1,597E+02	2,046E+01	2,220E-01
16	2,114E+01	4,097E+00	4,550E-02	6,686E+01	1,296E+01	1,439E-01	1,495E+02	2,897E+01	3,217E-01
17	2,267E+01	3,133E+00	2,947E-02	7,168E+01	9,909E+00	9,318E-02	1,603E+02	2,216E+01	2,084E-01
18	2,118E+01	4,447E+00	4,344E-02	6,697E+01	1,406E+01	1,374E-01	1,498E+02	3,144E+01	3,071E-01
19	2,138E+01	4,483E+00	4,168E-02	6,760E+01	1,418E+01	1,318E-01	1,512E+02	3,170E+01	2,947E-01
20	2,746E+01	4,322E+00	2,874E-02	8,682E+01	1,367E+01	9,088E-02	1,941E+02	3,056E+01	2,032E-01
21	2,182E+01	4,386E+00	4,118E-02	6,899E+01	1,387E+01	1,302E-01	1,543E+02	3,102E+01	2,912E-01
22	2,594E+01	4,220E+00	2,900E-02	8,202E+01	1,335E+01	9,169E-02	1,834E+02	2,984E+01	2,050E-01
23	2,289E+01	3,429E+00	3,010E-02	7,237E+01	1,084E+01	9,517E-02	1,618E+02	2,425E+01	2,128E-01
24	2,030E+01	3,906E+00	4,276E-02	6,420E+01	1,235E+01	1,352E-01	1,435E+02	2,762E+01	3,024E-01
25	2,604E+01	4,251E+00	2,938E-02	8,234E+01	1,344E+01	9,292E-02	1,841E+02	3,006E+01	2,078E-01
26	2,196E+01	4,460E+00	4,157E-02	6,945E+01	1,410E+01	1,315E-01	1,553E+02	3,154E+01	2,940E-01
27	2,026E+01	3,904E+00	4,299E-02	6,407E+01	1,235E+01	1,359E-01	1,433E+02	2,761E+01	3,040E-01
28	2,290E+01	3,432E+00	3,033E-02	7,241E+01	1,085E+01	9,590E-02	1,619E+02	2,427E+01	2,144E-01
29	2,069E+01	4,309E+00	4,396E-02	6,541E+01	1,363E+01	1,390E-01	1,463E+02	3,047E+01	3,109E-01
30	2,250E+01	3,107E+00	2,982E-02	7,114E+01	9,824E+00	9,429E-02	1,591E+02	2,197E+01	2,108E-01
31	2,729E+01	4,307E+00	2,897E-02	8,630E+01	1,362E+01	9,162E-02	1,930E+02	3,045E+01	2,049E-01
32	2,129E+01	4,472E+00	4,206E-02	6,733E+01	1,414E+01	1,330E-01	1,506E+02	3,162E+01	2,974E-01
Centroid	2,202E+01	3,667E+00	3,675E-02	6,965E+01	1,159E+01	1,162E-01	1,557E+02	2,593E+01	2,599E-01

Run	PSD2								
		v =1 m/s			*v =10 m/s*			*v =50 m/s*	
	Discomfort	*Road Holding*	*Working Space*	*Discomfort*	*Road Holding*	*Working Space*	*Discomfort*	*Road Holding*	*Working Space*
1	2,376E+01	4,288E+00	3,563E-03	2,773E+01	3,220E+00	2,226E-03	1,839E+01	2,121E+00	1,242E-03
2	1,308E+01	3,082E+00	4,239E-03	1,842E+01	2,599E+00	2,341E-03	1,218E+01	1,935E+00	1,319E-03
3	1,116E+01	2,636E+00	5,957E-03	1,324E+01	1,814E+00	2,634E-03	8,709E+00	1,341E+00	1,307E-03
4	1,268E+01	2,051E+00	3,109E-03	1,815E+01	1,754E+00	1,570E-03	1,246E+01	1,327E+00	8,667E-04
5	1,034E+01	2,290E+00	5,267E-03	1,281E+01	1,745E+00	2,397E-03	8,698E+00	1,325E+00	1,239E-03
6	1,232E+01	2,099E+00	3,416E-03	1,795E+01	1,737E+00	1,623E-03	1,204E+01	1,322E+00	8,502E-04
7	1,992E+01	3,724E+00	3,251E-03	2,660E+01	2,944E+00	1,963E-03	1,756E+01	2,034E+00	1,091E-03
8	1,436E+01	3,323E+00	4,275E-03	1,849E+01	2,726E+00	2,464E-03	1,246E+01	1,974E+00	1,418E-03
9	1,257E+01	2,106E+00	3,527E-03	1,990E+01	1,747E+00	1,586E-03	1,461E+01	1,322E+00	8,004E-04
10	1,038E+01	2,280E+00	5,366E-03	1,417E+01	1,753E+00	2,350E-03	1,057E+01	1,323E+00	1,181E-03
11	1,490E+01	3,462E+00	4,636E-03	2,052E+01	2,795E+00	2,484E-03	1,513E+01	1,985E+00	1,351E-03
12	2,047E+01	3,810E+00	3,587E-03	2,939E+01	2,991E+00	1,997E-03	2,121E+01	2,043E+00	1,045E-03
13	1,347E+01	3,170E+00	4,555E-03	2,058E+01	2,655E+00	2,331E-03	1,491E+01	1,947E+00	1,255E-03
14	2,383E+01	4,341E+00	4,106E-03	2,995E+01	3,251E+00	2,375E-03	2,189E+01	2,124E+00	1,232E-03
15	1,273E+01	2,065E+00	3,309E-03	1,980E+01	1,767E+00	1,560E-03	1,499E+01	1,327E+00	8,173E-04
16	1,085E+01	2,543E+00	6,089E-03	1,441E+01	1,804E+00	2,607E-03	1,040E+01	1,337E+00	1,263E-03
17	1,173E+01	2,013E+00	3,014E-03	1,575E+01	1,724E+00	1,447E-03	1,059E+01	1,318E+00	7,692E-04
18	1,009E+01	2,491E+00	5,270E-03	1,149E+01	1,776E+00	2,302E-03	7,424E+00	1,330E+00	1,131E-03
19	1,212E+01	2,942E+00	4,073E-03	1,617E+01	2,532E+00	2,124E-03	1,051E+01	1,914E+00	1,160E-03
20	1,861E+01	3,363E+00	2,985E-03	2,332E+01	2,789E+00	1,777E-03	1,542E+01	1,987E+00	9,976E-04
21	1,298E+01	3,063E+00	4,043E-03	1,616E+01	2,604E+00	2,192E-03	1,069E+01	1,935E+00	1,224E-03
22	1,676E+01	3,155E+00	2,924E-03	2,281E+01	2,684E+00	1,667E-03	1,488E+01	1,956E+00	9,157E-04
23	1,155E+01	2,105E+00	3,299E-03	1,565E+01	1,724E+00	1,515E-03	1,029E+01	1,317E+00	7,704E-04
24	9,616E+00	2,236E+00	4,852E-03	1,121E+01	1,726E+00	2,162E-03	7,449E+00	1,318E+00	1,094E-03
25	1,700E+01	3,181E+00	3,142E-03	2,503E+01	2,706E+00	1,660E-03	1,783E+01	1,958E+00	8,663E-04
26	1,324E+01	3,130E+00	4,311E-03	1,777E+01	2,645E+00	2,206E-03	1,283E+01	1,940E+00	1,172E-03
27	9,629E+00	2,226E+00	4,951E-03	1,230E+01	1,734E+00	2,141E-03	8,955E+00	1,317E+00	1,055E-03
28	1,167E+01	2,105E+00	3,402E-03	1,718E+01	1,732E+00	1,497E-03	1,235E+01	1,317E+00	7,368E-04
29	9,842E+00	2,423E+00	5,428E-03	1,245E+01	1,770E+00	2,308E-03	8,814E+00	1,327E+00	1,108E-03
30	1,174E+01	2,012E+00	3,192E-03	1,716E+01	1,733E+00	1,456E-03	1,266E+01	1,317E+00	7,395E-04
31	1,856E+01	3,362E+00	3,311E-03	2,528E+01	2,800E+00	1,828E-03	1,834E+01	1,985E+00	9,628E-04
32	1,227E+01	2,983E+00	4,334E-03	1,776E+01	2,567E+00	2,127E-03	1,260E+01	1,919E+00	1,111E-03
Centroid	1,248E+01	2,516E+00	3,732E-03	1,796E+01	2,156E+00	1,842E-03	1,253E+01	1,621E+00	9,869E-04

F) Contour Plots of the Surface Containing Discomfort, Road Holding and Working Space

i)

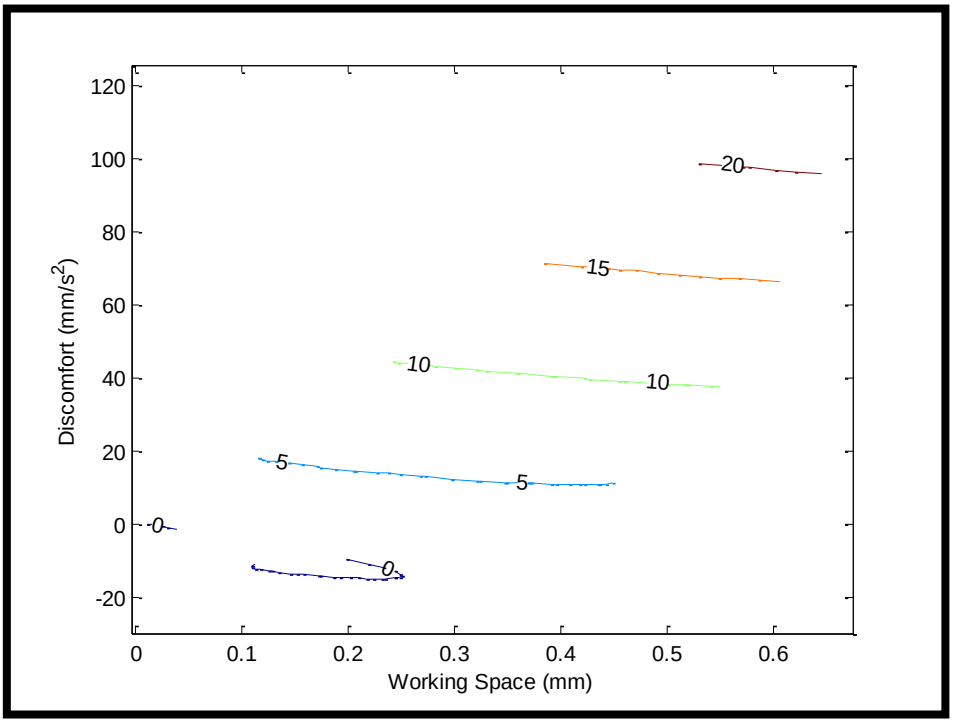

Figure F.i: Contour lines of road holding

ii)

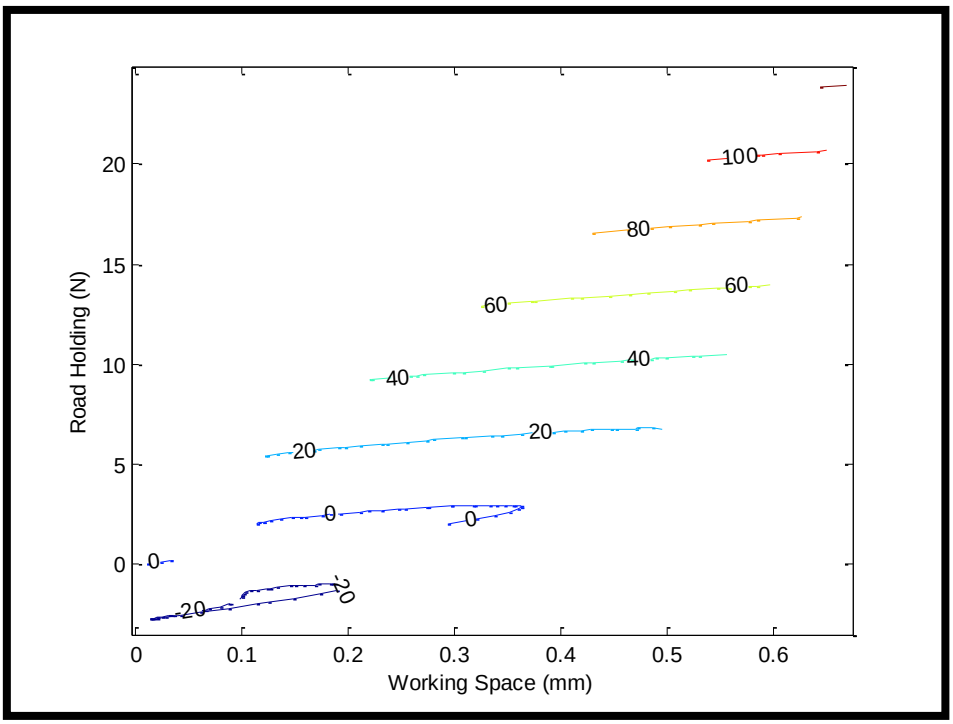

Figure F.ii: Contour lines of discomfort

iii)

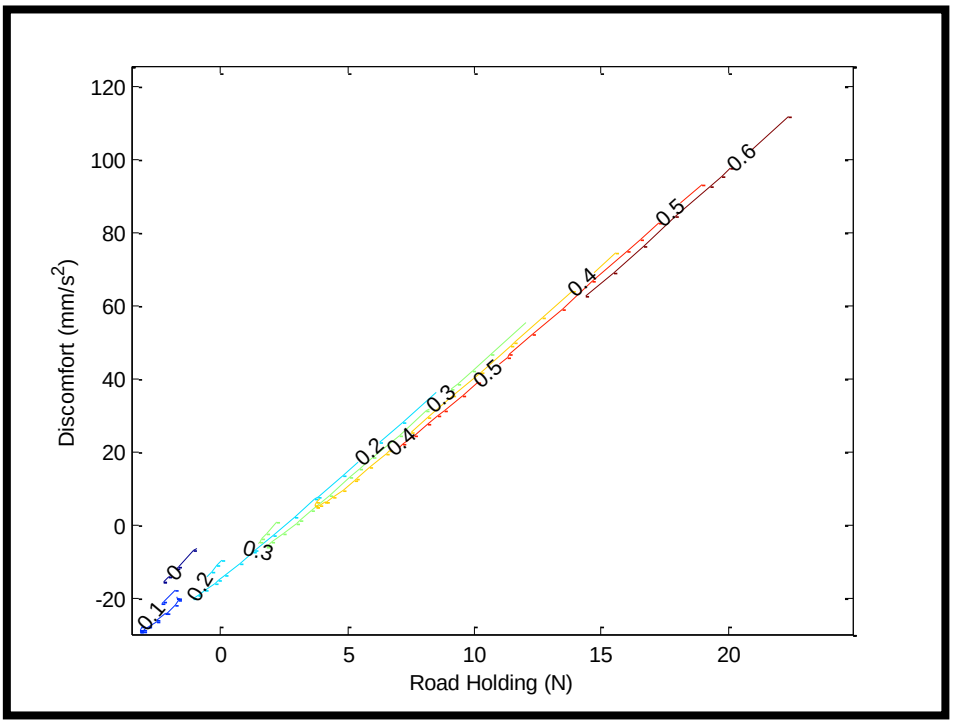

Figure F.iii: Contour lines of working space